Catarina Alexandra Catanas Madeira

Bachelor degree in Biochemistry

Activity of the major autolysin of *Staphylococcus aureus* Atl in the presence of extracellular DNA

Dissertation to obtain the Master Degree in Biochemistry for Health

Supervisor: Rita Gonçalves Sobral, Professora Auxiliar, DCV, FCT-UNL
Co-supervisor: Inês Ramos Grilo, Postdoctoral researcher, DCV, FCT-UNL

September 2018

Catarina Alexandra Catanas Madeira

Bachelor degree in Biochemistry

Activity of the major autolysin of *Staphylococcus aureus* Atl in the presence of extracellular DNA

Dissertation to obtain the Master's Degree in Biochemistry for Health

Supervisor: Rita Gonçalves Sobral, Professora Auxiliar, DCV, FCT-UNL
Co-supervisor: Inês Ramos Grilo, Postdoctoral researcher, DCV, FCT-UNL

Jury:

Chairman: Prof. Doutora Maria Teresa Nunes Mangas Catarino
Examiner: Doutor Pedro Matos Pereira
Vogal: Prof. Doutora Rita Gonçalves Sobral

Faculdade de Ciências e Tecnologia da Universidade Nova de Lisboa

September 2018

Activity of the major autolysin of *Staphylococcus aureus* Atl in the presence of extracellular DNA

Acknowledgments

The work developed throughout this period had the contribution of a large group of excellent professionals and friends. Here I have the opportunity to acknowledge for everything I have learned with them.

First, I would like to express my gratitude to my supervisors, Professor Rita Sobral and Inês Grilo, for accepted me in the laboratory and for all the support I received from them since the first day of work. The knowledge they shared, all the guidance and advice they gave me, their availability and understanding, and their endless patience in teaching me and all the time spend with me was essential during this journey. Without my supervisors, all I accomplished during this year would not be possible.

To all my colleagues in the Laboratory of Molecular Microbiology of Bacterial Pathogens, especially Bárbara Gonçalves, Gonçalo Cavaco and Raquel Portela, for the good environment in the laboratory, for making me feel welcome and integrated since the first day, for always helping me whenever I needed and for all the good moments shared inside and outside the laboratory.

To Cláudia Fernandes and Rafael Marques, the undergraduate trainees that were a precious help during the last working month and that had kept their enthusiasm even on the hardest days. Without them, it would have been so much harder.

To all the people from the Infection Biology Lab and to Ana Pina from the Biomolecular Engineering Lab, for facilitating my access to their laboratories and equipment, being always available for all the help that I needed. Also, to the Tomás Calmeiro from the Nanofabrication Laboratory - Atomic Force Microscopy of CENIMAT/I3N for all the help and availability during the AFM imaging process.

To the staff of Departamento de Ciências da Vida da Faculdade de Ciências e Tecnologia da Universidade Nova de Lisboa for their availability and technical support, essential to develop this work.

This journey would not be possible without all the support that my family and friends gave me. All the patience, advices and strength helped me believe I could do this work and give my best to it. They never stopped encouraging me to continue and they were always available to hear my thoughts and ideas, even when they did not understand a single word. Both family and friends were always available for making me feel good in the toughest days and were always there for me, even when I was only physically with them, but the thoughts were left on the lab bench. They have all the patience in the world, and I will never be able to return everything they have done for me.

Abstract

Staphylococcus aureus, a successful opportunistic pathogen, causes life-threatening disease through mechanisms of survival and proliferation, as antibiotic resistance and virulence factors. The major *S. aureus* murein hydrolase Atl, a bifunctional autolysin, is involved in crucial physiological processes as cell separation, cell wall turnover and biofilm development.

The glucosaminidase (GL) domain of Atl has DNA-binding capacity, already demonstrated as important for biofilm development. In this work, we explored the molecular features of GL-DNA interaction using mobility shift assays and atomic force microscopy, in an *in vitro* approach. Going one step ahead, we aimed to unravel how the GL-DNA interaction interferes with Atl roles, namely peptidoglycan hydrolytic activity.

Our study revealed that a low pH environment enhances the DNA-binding capacity of GL although the interaction does not seem to be purely electrostatic, and that specific divalent cations prevent the interaction *in vitro*. Furthermore, GL was observed to interact with linear DNA molecules and plasmid DNA from different bacteria, in a molar ratio proportional to the DNA length. The interaction of DNA with GL seems to not promote protein oligomerization. The GL hydrolytic activity, tested against several microorganisms, was inhibited *in vitro* by DNA, but the *S. aureus* growth rate was not affected by the addition of DNA to the medium or by different growing temperatures. The activity of the *atl* promoter was not altered at different temperatures or for different added DNA concentrations in strain WIS.

These results provided insights on the molecular mechanism of GL-DNA binding and contributed to unveiling physiological consequences of this association, namely an eventual role in bacterial interspecies interactions.

Key words: *S. aureus*; Atl murein hydrolase; protein-DNA interaction; hydrolysis;

Resumo

Staphylococcus aureus é um agente patogénico oportunista com capacidade de causar doenças fatais através de mecanismos de sobrevivência e proliferação, como resistência a antibióticos e fatores de virulência. A principal hidrolase do peptidoglicano de *S. aureus*, Atl, é uma proteína autolítica bifuncional e está envolvida em processos fisiológicos fundamentais como a separação celular, a renovação da parede celular e o desenvolvimento de biofilmes.

Um dos domínios da Atl, o domínio glicosaminidase (GL), possui capacidade de ligação ao DNA, característica importante para o desenvolvimento de biofilmes. Neste trabalho, exploramos as características moleculares da interação GL-DNA através de ensaios de diferença de mobilidade (EMSA) e microscopia de força atómica, de forma a compreender como esta interação pode interferir com a principal função do Atl, a hidrólise do peptidoglicano.

O nosso estudo revelou que valores de pH baixos favorecem a ligação GL-DNA, embora esta não seja puramente eletrostática, e que catiões divalentes específicos interferem negativamente na interação. Além disso, a GL tem capacidade para interagir tanto com moléculas de DNA linear como de DNA plasmídico, proveniente de bactérias diferentes, em razões molares concordantes com comprimento da molécula de DNA. A interação com DNA parece não promover a oligomerização do domínio GL. A atividade hidrolítica do GL, testada i*n vitro*, para vários microrganismos diferentes, foi inibida pela presença de DNA, contrariamente ao crescimento bacteriano, que não foi afetado pela adição de DNA ao meio, nem por diferentes temperaturas de crescimento. A atividade do promotor do *atl* não foi alterada a diferentes temperaturas bem como com diferentes concentrações de DNA na linhagem WIS.

Esses resultados forneceram informações importantes sobre o mecanismo molecular da interação GL-DNA e contribuíram para desvendar algumas das consequências fisiológicas dessa associação.

Palavras-chave: *S. aureus*; Proteína hidrolítica Atl; Interação proteína-DNA; hidrólise;

Index

Index of figures

Index of tables

Acronyms

AFM	Atomic Force Microscopy
AM	amidase domain of Atl protein
A. U.	Arbitrary Unit
bp	Base pair
BHI	Brain Heart Infusion
CA-MRSA	Community-associated methicillin resistant *Staphylococcus aureus*
$CaCl_2$	Calcium chloride
$CdCl_2$	Cadmium Chloride
CI 95%	Confidence Interval of 95%
$CoCl_2$	Cobalt Chloride
$CuCl_2$	Copper Chloride
DNA	Deoxyribonucleic acid
ECM	Extracellular Matrix
ECP	Excretion of cytosolic proteins
eDNA	extracellular DNA
EDTA	Ethylenediaminetetra-acetic acid
EMSA	Electrophoretic mobility shift assay
EPS	Extracellular polymeric substance
$FeCl_2$	Iron Chloride
FnBP	Fibronectin-binding protein
GL	Endo-β-N-acetylglucosaminidase domain of Atl protein
GlcNAc	N-acetyl glucosamine
HA-MRSA	Hospital-associated methicillin resistant *Staphylococcus aureus*
Kb	Kilo bases
KCl	Potassium Chloride
KD	Dissociation constant
kDa	Kilodalton
KH_2PO_4	Potassium phosphate
LA	Lysogeny Agar
LB	Lysogeny Broth
LTA	Lipoteichoic Acid
M	Molar
MB	Marine Broth
MES	2-(N-morpholino)ethanesulfonic acid
mg	Milligrams
$MgCl_2$	Magnesium chloride
min	Minutes
ml	Millilitre
mM	Millimolar
$MnSO_4$	Manganese Sulphate
MOPS	(3-(N-morpholino)propanesulfonic acid
MRSA	Methicillin resistant *Staphylococcus aureus*
MSCRAMM	Microbial surface components recognizing adhesive matrix Molecule
MurNAc	N-acetyl muramic acid
NaCl	Sodium chloride
Na_2HPO_4	Sodium phosphate di-basic
NaH_2PO_4	Sodium phosphate mono -basic
Na_2MoO_4	Sodium molybdate
NaN_3	Sodium azide
ng	Nanograms
$(NH_4)_2SO_4$	Ammonium sulphate
$NiCl_2$	Nickel chloride
Ni-NTA	Nickel-nitrilotriacetic acid
nm	Nanometre
nM	Nanomolar
OD_{600nm}	Optical density at 600 nm
PAGE	Polyacrylamide gel electrophoresis
PBP	Penicillin Binding Proteins
PBS	Phosphate buffered saline
PCR	Polymerase chain reaction
pI	Isoelectric point
PIA	Polysaccharide intercellular adhesin
pM	Picomolar
PNAG	Polymeric N-acetyl-glucosamine
PSM	Phenol Soluble Modulins
RMS	Root mean square
rpm	rotations per minute
RT	Room temperature
SDS	Sodium dodecyl sulphate
SDS-PAGE	Sodium dodecyl sulphate polyacrylamide gel electrophoresis
SEM	Standard error of the mean
ssDNA	low molecular salmon sperm DNA
SSSTI	Serious skin and soft tissue infections
TA	Teichoic acid
TAE	Tris-acetate-EDTA buffer
TSA	Tryptic soy agar
TSB	Tryptic soy broth
w/v	Weight/volume
WTA	Wall teichoic acids
X-Gal	5-bromo-4-chloro-3-indolyl-β-D-galactopyranoside
$ZnCl_2$	Zinc chloride
µg	Microgram
µl	Microliter
µM	Micromolar
µm	Micrometre

1- Introduction

1.1 - *Staphylococcus aureus*

1.1.1- *S. aureus* - the microorganism

Staphylococcus aureus from the Greek *staphyle* (bunch of grapes) and *kokkos* (berry), was first described in 1880 by Alexander Ogston, found in pus from abscesses[1]. The species was named later, from the Latin *aurum* due to its colonies' goldish colour as other species from this genus[2]. Most of the members of this genus are harmless commensals for humans and other animals, found in the skin and mucous membranes[3]. However, some of them can cause a wide range of infections and *S. aureus* is the most relevant species of this group.

S. aureus is a gram-positive bacterium with spherical shape and a diameter of 1.0 µm, approximately. Its yellowish colour is due to the production of carotenoids, more pronounced in some strains than in others[4,5]. This bacterium can grow in a varied type of conditions, as temperatures from 15 to 45 ºC, pH from 4.8 up to 9.4 and at sodium chloride (NaCl) concentrations as high as 10%[5]. In terms of metabolism, *S. aureus* is an aerobic and facultative anaerobic microorganism, able to respire as well as to ferment yielding, in this case, mainly lactic acid. Its susceptibility to suffer lysis through lysostaphin action, a metalloendopeptidase that targets specifically the pentaglycine bridge of peptidoglycan, can help distinguish staphylococci from micrococcus[5]. *S. aureus* can be distinguished in the staphylococci genus through its capacity to produce coagulase, an enzyme responsible for fibrinogen clotting in human blood[6]. Like all the other staphylococci, *S. aureus* produces catalase, in a much higher level than the coagulase negative species[7].

1.1.2 - *S. aureus*, commensal and opportunistic pathogen

S. aureus is a frequent cause of infections, becoming a relevant pathogen when the host is in an immunocompromised state.

1.1.2.1 – *S. aureus* as a commensal pathogen

Humans are a natural reservoir of *S. aureus*, that acts as a permanent colonizer in approximately 30% of the human population[8]. The skin, mucous membranes, axillae, groins and intestinal tract are the most frequently colonized body parts[3,9]. Despite being a human commensal, *S. aureus* is also a frequent cause of infections from minor skin infections to wound infections in post-operative situations. Other diseases that can be caused by *S. aureus* include endocarditis, pneumonia, meningitis, osteomyelitis, infections associated with foreign bodies, septicaemia, toxic shock syndrome and food poisoning, being some of them life-threatening

conditions[10]. Over the years, many antimicrobials were used to overcome *S. aureus* infections, but the bacteria continuously acquired mechanisms to resist and proliferate to the adopted strategies.

1.1.2.2 – Antibiotic Resistance

β-lactam antibiotics, such as penicillin, target the bacterial cell wall due to their similarity with the substrate of penicillin binding proteins (PBPs), responsible for the transpeptidation and transglycosylation terminal steps of the peptidoglycan synthesis, inhibiting the cross-links formation[11,12]. In the presence of β-lactams, PBPs no longer bind to their natural substrate in the peptidoglycan subunits, interrupting the cross-link formation leading to cell lysis[11]. Despite the introduction of penicillin in the clinical practice in the 1940s and its effectiveness against *S. aureus* infections, in a few years, the bacteria acquired resistance due to the acquisition of penicillinase, a β-lactamase enzyme that can hydrolyse penicillin, encoded by the *blaZ* gene[13]. This gene is plasmid-encoded, acquired by *S. aureus* through lateral gene transfer[13,14].

S. aureus can be not only resistant to penicillin but also to other variants of β-lactams, being the methicillin-resistant *S. aureus* (MRSA) the clinically most relevant strains. One year after the introduction of methicillin, *S. aureus* acquired resistance to this semi-synthetic penicillin, due to the expression of exogenous penicillin binding protein 2A (PBP2a), a transpeptidase with lower binding affinity for β-lactams than the native PBPs[15]. This extra PBP is encoded by *mecA*, a heterologous gene located on the mobile staphylococcal cassette chromosome *mec* (SCC*mec*)[16]. SCC*mec* includes regulatory genes, insertion sequences and recombinase genes that, along with many housekeeping genes designated as factors essential for methicillin resistance (fem) or auxiliary genes (aux), are responsible for the heterogeneity of the MRSA phenotype[17,18]. MRSA strains are virtually resistant to all classes of antibiotics used in the clinical practice, even if their target is the synthesis of proteins or nucleic acids[19].

Along the years, multiple MRSA strains emerged, becoming a severe nosocomial problem around the world, with high mortality rates. These strains, associated with the hospital environment (HA-MRSA), became extremely worrying since the population in these environments are usually immunocompromised and more susceptible to cross-infections between individuals[20]. In the late 1990s, MRSA strains were no longer restricted to hospital environments, but emerged also in the healthy community causing serious skin and soft tissue infections (SSSTI)[21,22].

These two variants of MRSA have different ways of action due to the environment where they proliferate. HA-MRSA strains have higher levels of antibiotic resistance but less virulence factors in comparison with the community-associated strains (CA-MRSA) that have more and stronger virulence factors that are crucial to infect healthy individuals[23], and have shown potential to become the dominant strain in the healthcare setting[24].

1.1.2.3 – Virulence factors

Despite the antibiotic resistance capacity of *S. aureus* that makes it a dangerous pathogen, virulence factors play an essential role for infection to occur. They contribute to the process of infection and for bacteria to proliferate in the environment, facilitating the adhesion to host's tissue or other biotic and abiotic surfaces, immune evasion and suppression to block the host's immune response and cell injury through toxins[21]. Several different molecules are contributors, such as antigens, proteins and toxins that participate differently, depending on the infection stage and the surrounding environment[25,26].

S. aureus is a strong adhesin producer, an important feature for successful infection, mainly for biofilm formation. Adhesins are proteins or other type of molecules that help the cellular attachment in multiple situations, especially in the early stages of a successful infection. They include fibronectin binding proteins (FnBPs)[27], *S. aureus* surface protein G (SasG)[28] among other proteins, polysaccharide intercellular adhesin (PIA)[29] and teichoic acids[30].

1.1.2.4- Biofilms

One important virulence factor is the capacity to produce biofilms. A biofilm is a bacterial community involved in a self-produced extracellular matrix (ECM) that can be composed by proteins, polysaccharides and extracellular DNA (eDNA)[31–33]. These elements are designated extracellular polymeric components (EPS) and help the bacterial community to adhere and stay cohesive to the surface to which they are attached, despite a large number of other functions[33]. Biofilm formation is divided in several steps, attachment, maturation and dispersion (Figure 1.1) and all require different processes and components. Biofilms are a major burden in healthcare because they result in chronic infections, by providing a protection shield for bacteria against treatments and the immune system defences and increasing the mortality rate[34].

For the initial attachment, adherence properties are very significant, and depend on the bacterial surface characteristics, but also on the surface, that can be virtually any kind of abiotic or biotic surface. This first stage of biofilm development is fundamentally mediated by extracellular proteins. When the attachment is made in a biotic surface, a large number of surface proteins, known as Microbial Surface Components Recognizing Adhesive Matrix Molecules (MSCRAMMs), can attach to host proteins, such as fibrinogen, fibronectin and collagen[31,35]. These proteins include Bap[36], Spa[37], FnBPs[27] and SasG[28]. When the surface is inert, proteins together with teichoic acids are important for the attachment to virtually any kind of surface[34]. One of these proteins is Atl, the major *S. aureus* autolysin protein, significant to biofilm formation, due to its adhesive properties along with its primary function of autolysis[38,39].

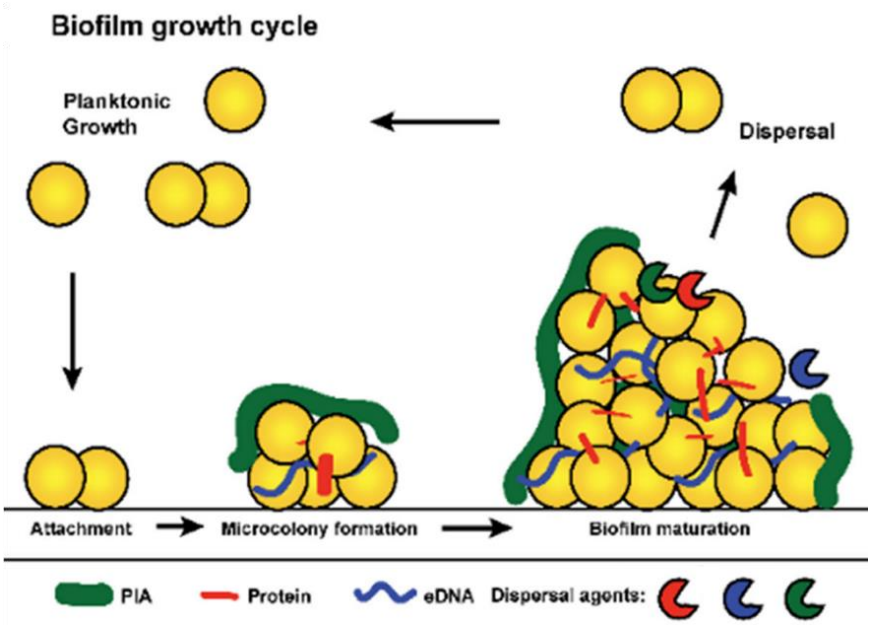

Figure 1.1: Biofilm growth cycle. Different stages of biofilm formation from planktonic growth to initial attachment, accumulation, maturation and finally dispersion of the biofilm. Biofilm constituents and dispersal agents colour correspond to the schematic colours for each different molecule. (adapted from [40])

Cell multiplication starts after the attachment is established and sufficient amounts of nutrients are available for cell division[34]. Proteins remain an important component, but other molecules, such as polysaccharides and eDNA, start to contribute to the biofilm development.

The proteins involved in the attachment stage are still necessary to keep the adhesion, but other proteins become important to establish intercellular interactions. Most them are cell wall-anchored proteins that promote biofilm accumulation and mediate cell-cell interactions as the fibronectin binding proteins (FnbPs)[27,41,42] or the serine-rich repeat glycoprotein (SraP)[43–45]. Also, other secreted proteins are involved in biofilm maturation, such as the β-toxin (Hlb)[46] that is present in some *S. aureus* strains and despite its primary role as a toxin, it can also create covalent crosslinks with itself when eDNA is present, being an important structural feature in biofilm maturation. Some cytoplasmic proteins are found in the ECM as well, and their secretion can be related with the autolysin Atl that can mediate their excretion[47] through a selective nonclassical pathway[48–50], not depending on known signals or secretion motifs[50]. This suggests different moonlight functions for these cytoplasmic proteins in the biofilm development[51,52].

Polysaccharides are another important component of ECM in biofilms, particularly polysaccharide intercellular adhesin (PIA), also named polymeric N-acetyl-glucosamine (PNAG)[53] since it is a polymer composed by β-1,6-linked N-acetylglucosamine monomers[29]. This polysaccharide is synthesized by enzymes encoded by the *icaADBC* operon, that is present in numerous *S. aureus* strains capable to produce biofilms[54]. This molecule has a positive net charge, an important characteristic for the electrostatic interactions that can occur with the cell surface and the negative charges of molecules like teichoic acids[55]. However, PIA is not indispensable for biofilm production, as some strains can develop *ica*-independent biofilms, with different proteins and eDNA performing the intercellular adhesion function of PIA[32,36,37,56,57].

eDNA plays a major role in this stage of biofilm formation, not only due to its function as a nutrient source but also promoting colony spreading and structuring of the biofilm matrix, being an important feature in *S. aureus* biofilms[32,58,59]. The cellular organization, traffic flow and biofilm expansion can also be controlled by the presence of eDNA in specific areas of the ECM[59]. This happens particularly in strains where the polysaccharide's contribution is lower, so eDNA contributes to cell-surface adhesion and to cell-cell interactions[32,60,61]. The eDNA adherence to cells requires the presence of extracellular proteins. Together they create an electrostatic net, forming large clumps that hold cells together[62]. CA-MRSA strains are more likely to develop PIA-independent biofilms, having proteins and eDNA as major components[63].

The biofilm growth cycle ends in the dispersal stage, with some parts of the ECM detaching from the rest of the biofilm essentially through the action of exoenzymes or surfactants[34,64]. This is a way to colonize other areas and start the process again, making a more effective infection. Proteases and nucleases are some of the exoenzymes that act more effectively in biofilms composed of proteins and eDNA. Phenol soluble modulins (PSMs) are surfactant-like peptides that contribute to dispersion of biofilms in a non-specific manner[65,66]. PSMs can form amyloid fibrils that can contribute to the biofilm structure, especially if associated to eDNA[67,68]. These molecules are also very aggressive toxins, being themselves virulence factors.

1.1.3- *S. aureus* cell wall

As all gram-positive bacteria, *S. aureus* possesses a cell wall with a thick layer of peptidoglycan, teichoic acids, surface proteins and other molecules that directly contact with the external environment, since it does not have outer membrane as gram-negative bacteria (Figure 1.2). The cell wall functions as a protective barrier and contributes to the attachment of surface proteins required for cellular processes such as cell division and pathogenesis[69–71].

The structure, biosynthesis and degradation of peptidoglycan, the major compound of the cell wall, will be described in section 1.1.3.1.

S. aureus teichoic acids can be divided in two groups: lipoteichoic acids (LTAs) and wall teichoic acids (WTAs). LTAs are composed of 18 to 50 repeating units of glycerol phosphate that are bound to the cytoplasmic membrane by a glycolipid and WTAs are composed of 40 units of ribitol phosphate linked to peptidoglycan N-acetylmuramic acid (MurNAc) through a disaccharide followed by two units of glycerol phosphate[72]. Both types of teichoic acids can suffer D-alanylation after biosynthesis, altering its properties by reducing the negative charge of the TA backbone[73], which is important for the contact with the external environment. Teichoic acids also play a role in cell division, since their lower presence in specific regions of the cell mark the area where the next cell division will occur[74].

Besides these major compounds, the cell wall also contains proteins and polysaccharides, as for example the already referred MSCRAMMs[31] and PIA[53] respectively, that help bacteria to survive and communicate with the surrounding environment[31,75]. These molecules contribute to virulence, attachment capacity, biofilm formation and other interactions with the host,

becoming factors that contribute to all varieties of infections that *S. aureus* can cause. Many staphylococcal surface proteins have structural features in common. The majority is synthetized in the cytosol and then directed to the cell surface through the general protein secretion pathway (Sec)[76]. This mechanism directs proteins that possess an N-terminal signal peptide and that remain unfolded until reaching the cell membrane to be translocated and processed in the exterior[77]. Then, the signal peptide is cleaved, the protein suffers folding and it is covalently bound to the cell wall or is released in the surrounding medium and directed to the place where it should perform its function. In the case of peptidoglycan hydrolases, as the major autolysin Atl, the attachment to the cell wall is not done covalently but through specific repeat structures that flank the enzymatic domains of the proteins.

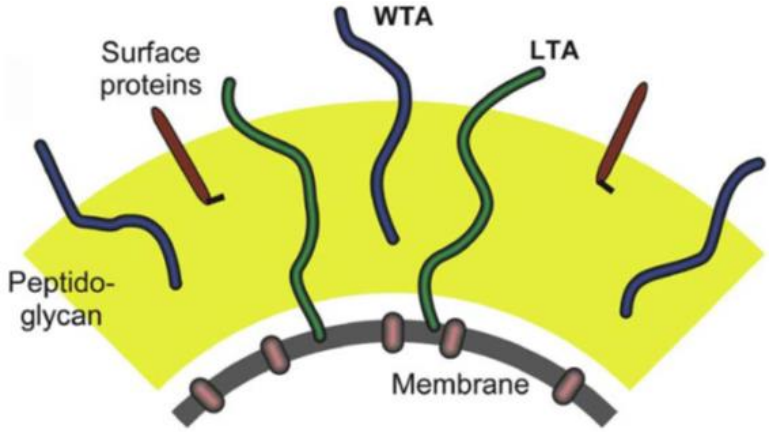

Figure 1.2: gram-positive cell wall schematic representation. Peptidoglycan is represented in yellow and attached to its structure are the other components of the cell wall: surface proteins, wall teichoic acid (WTA) and lipoteichoic acid (LTA) that attach to the cell membrane. (adapted from [72])

1.1.3.1 – Peptidoglycan structure, biosynthesis and degradation

Peptidoglycan is the major cell wall component of *S. aureus*, representing about 50% of the cellular weight[5,78]. Peptidoglycan, also called murein, is a macromolecule composed by two polysaccharide subunits of N-acetylglucosamine (GlcNAc) and N-acetylmuramic acid (MurNAc) linked by β-1,4-glycosidic bonds. The N-acetylmuramic acid unit is linked to a stem peptide, composed by L-alanine-D-iso-glutamine-L-lysine-D-alanine-D-alanine[79]. To create a three-dimensional structure, *S. aureus* has a characteristic pentaglycine bridge, that binds the L-lysine of one stem peptide to the fourth amino acid, D-alanine, of a neighbouring pentapeptide. When the cross-linking reaction occurs, the terminal D-alanine residue is lost[79]. This pentaglycine bridge is long and flexible enough to ensure the strength of *S. aureus* peptidoglycan[80].

Peptidoglycan biosynthesis is a complex process that occurs in three stages (Figure 1.3) and starts in the cytoplasm with the formation of the nucleotide precursors of GlcNAc and MurNAc, followed by the sequential attachment of the five amino acids to MurNAc through the action of Mur ligases (MurC to MurF)[81]. In the next stage, the MurNAc-stem peptide is bound to the membrane acceptor bactoprenol, by MraY protein, forming Lipid I. The GlcNAc precursor is linked to MurNAc on Lipid I, leading to the formation of Lipid II, where the pentaglycine bridge is

added through the activity of specific peptidyltransferases[82]. This structure is translocated through the membrane through the action of a flippase, MurJ[83]. At the outer side of the cell membrane, Lipid II suffers transglycosylation (glycan chain extension) and transpeptidation (cross-linking of stem peptides via the glycine bridge) by the action of PBPs[84] (Figure 1.3). Peptidoglycan can suffer modifications that confer different characteristics in different bacterial microorganisms. Some of these modifications in *S. aureus* are the O-acetylation of MurNAc and amidation of the stem peptide, among others[85].

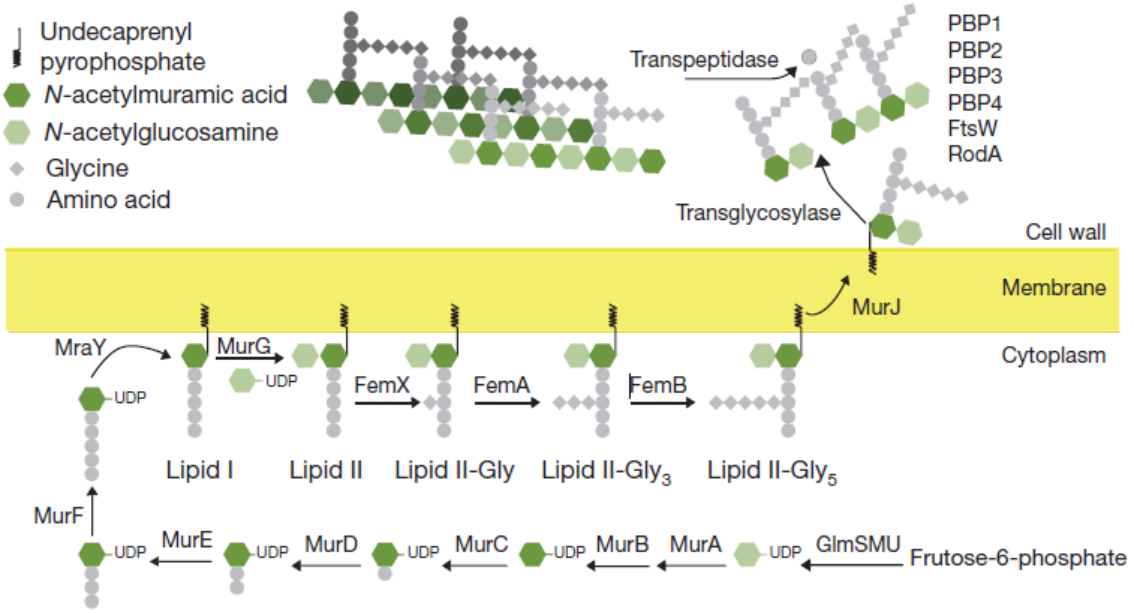

Figure 1.3: Peptidoglycan biosynthesis in *S. aureus*. Peptidoglycan biosynthesis occurs in three stages: assembly of the nucleotide precursors and sequential attachment of the amino acids that form the stem peptide in the cytoplasm; association of the MurNAc-stem peptide precursor to the membrane, forming Lipid I and subsequently Lipid II by the addition of GlcNAc, that is translocated to the outer side of the cell membrane; where will suffer transglycosylation and transpeptidation reactions resulting in the peptidoglycan polymerization. (Adapted from [83])

Several antimicrobials act on steps of peptidoglycan biosynthesis in order to interrupt this process, disrupting the cell wall and consequently leading to cell death, as for example the β-lactams mentioned before[86].

Both synthesis and degradation of peptidoglycan are necessary for proper cell growth and division: while it is necessary to cleave the peptidoglycan structure to incorporate new peptidoglycan monomers, peptidoglycan hydrolysis is also necessary to allow cells to divide and separate. Peptidoglycan hydrolases are the enzymes responsible for cleaving the covalent bonds in peptidoglycan at specific cleavage sites[87], being involved in several bacterial processes as cellular growth, cell separation and cell division, cell wall turnover, autolysis and also immune evasion.

1.2 - *S. aureus* extracellular protein Atl

1.2.1 Atl protein - the major autolysin and its domains

Among other peptidoglycan hydrolases in *S. aureus*, Atl is the major and most important of the group. Atl is a bifunctional autolysin with two catalytic domains, N-acetylmuramoyl-L-alanine amidase (AM) and endo-β-N-acetylglucosaminidase (GL)[88]. It is fundamentally involved in cell separation during cell division, cell wall turnover and in lysis induced by antibiotics[88,89].

The open reading frame for *atl* is 3768 bp in length, encoding a protein of 1256 amino acids with a theoretical molecular size of 137.381 kDa[90]. Atl protein is translated as a single unit and is directed to the Sec pathway to be translocated to the exterior[90]. After secretion, the protein is proteolytically processed: the signal peptide and the propeptide are cleaved and the separation of its two catalytic domains occurs by an unidentified mechanism[91] (Figure 1.4). As with other peptidoglycan hydrolases, Atl is non-covalently attached to the cell wall through its repeat regions. The repeat regions are differently associated with the two catalytic domains: repeats 1 and 2 (R_1R_2) are associated with the AM domain, and repeat 3 (R_3) is associated with the GL domain. In both cases, the repeat regions do not show lytic activity, being responsible for cell wall attachment[39,92] among other functions as in biofilm formation[93,94]. The binding of AM and GL to the cell wall is localized at the septum of dividing cells, marking the equatorial plane of cell division[91,95] and is targeted by the lower amount of WTA in this cell wall region[74].

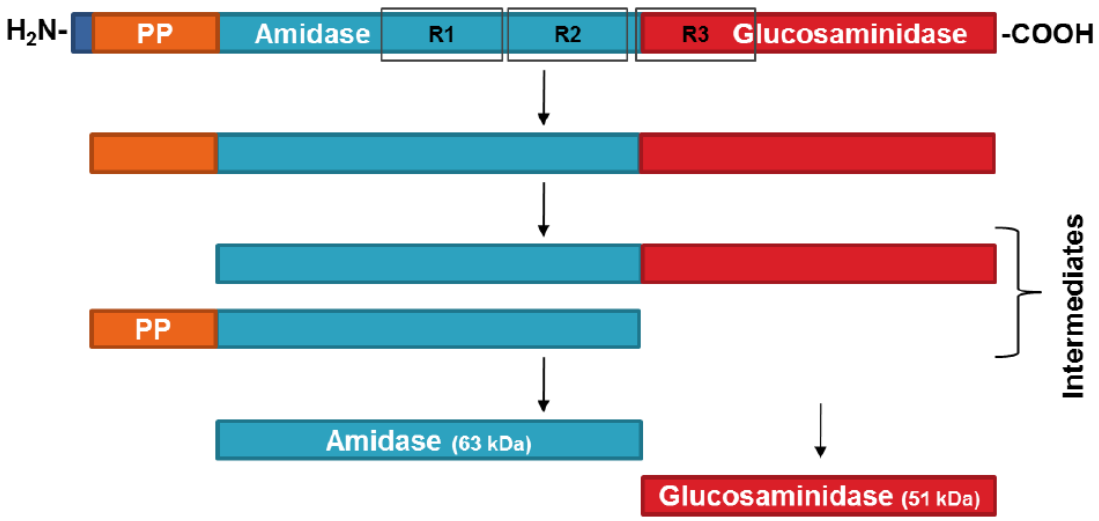

Figure 1.4: Atl protein processing and organization. Signal peptide (SP-dark blue), propeptide (PP-orange) and the catalytic domains amidase (AM-light blue) and glucosaminidase (GL-red) are exported to the extracellular milieu where Atl is proteolytically processed, generating the two mature proteins AM and GL, coupled to R_1R_2 and R_3 repeat regions, respectively. (adapted from [96])

1.2.2- Physiological roles and activity of Atl

Atl protein, as the major autolysin, is essentially involved in cell separation during cell division, and cell wall turnover. Deletion mutants of *atl* form large cell clusters with an unclear

separation between cells[39], despite the growth capacity not being affected, demonstrating the importance of a functional autolysin. Atl not only has the capacity to hydrolyse *S. aureus* peptidoglycan but also peptidoglycan from other microorganisms, as it was verified in the case of *Micrococcus luteus*[90].

Furthermore, as it was previously mentioned, Atl is also involved in biofilm formation, not only due to its lytic activity that leads to cell lysis and consequent release of genomic DNA to the ECM, but also because of its adhesive properties to host's proteins and abiotic surfaces. Furthermore, the secretion of cytoplasmic proteins through a specific secretion process (ECP) that Atl seems to be involved with[47], also contributes to biofilm formation. These roles will be discussed in later sections.

1.2.2.1- Regulation of Atl activity

As it is involved in many different and important physiological functions, the regulation of *atl* expression must be highly controlled to ensure it does not compromise cell survival. Several regulatory systems are involved, from gene transcription to protein localization.

The gene *atl* is negatively regulated by AtlR transcriptional repressor[97], that is located immediately downstream of *atl* and binds to its promoter region, preventing *atl* expression. This leads to evident cellular alterations, especially in the development of biofilm[97]. Positive transcriptional regulation is controlled by two different systems: the WalKR two-component system and the GraSR (glycopeptide resistance-associated) two-component system[98,99]. The first one is highly conserved in low-G+C gram-positive bacteria and its transcriptional regulation of *atl* can lead to a decrease in autolysis activity, defects in cell organization and in cell wall structure and composition[100]. The GraSR system seems to be essential in *S. aureus* and *S. epidermidis* to resist cationic antimicrobial peptides. It is associated with *atl* in a similar way as the WalKR system, since both systems are also involved in the regulation of *S. aureus* virulence factors by influencing regulatory virulence expression systems[99].

Another regulatory system, LytSR, is a two-component system that regulates autolysis in *S. aureus* through the *cidABC* and *lrgAB* operons involved in programmed cell death and lysis[101,102]. LrgA and CidA proteins have a role in peptidoglycan hydrolysis in an opposite way, and both have characteristics similar to the bacteriophage holin family of proteins[101]. LrgA may function as an inhibitor of peptidoglycan hydrolase activity, while CidA seems to enhance their activity[101,103,104]. The expression of the *lrgAB* operon seems to be influenced by changes in the proton motive force of the cytoplasmic membrane[105] and other environmental conditions, such as pH, glucose concentration and metabolism by-products[103]. Moreover, the LytSR system is also involved in *S. aureus* biofilm development due to its role in the induction of autolysis and DNA release[61,106,107].

Protein localization in the cell is important for its correct function. In the case of the Atl proteins, their localization is regulated by D-alanylated wall teichoic acids, since a lower amount of WTA is indispensable for Atl attachment at the equatorial division plane of the cell wall[74]. When

WTAs are in lower amounts along the entire cell surface, Atl can localize everywhere at the bacterial cell surface, leading to uncontrolled autolysis[74,108].

1.2.2.2- N-acetylmuramoyl-L-alanine amidase (AM)

The N-acetylmuramoyl-L-alanine amidase (AM) domain of *atl* gene ranges from bp 614 to bp 2325, with the corresponding polypeptide extending from Ala199 to Lys775[90]. After proteolytic processing, the AM domain has a molecular mass of 63 kDa and cleaves peptidoglycan between the N-acetylmuramic acid moiety and the L-alanine of the stem peptide[39]. Along with the catalytic domain, the AM domain encompasses two repeat regions (R_1R_2) that are involved in the attachment of the protein to the *S. aureus* cell wall. These repeat regions have more affinity for peptidoglycan than the AM catalytic domain[39].

The function of the AM domain has been more frequently described and studied, since it is very similar with amidases from other Staphylococci[109]. The AM catalytic domain structure of *S. epidermidis* was determined by Zoll *et al*.[110]. The AmiE protein has a globular fold, with a six-stranded central β-sheet surrounded by seven α-helices. It has a zinc ion coordinated by three amino acids (His-265, His-370, and Asp-384) and a water molecule, creating a typical active site of zinc-dependent metalloenzymes[110]. Also, the AM-associated repeats R_1R_2 have its structure characterized[92]. The repeats are able to bind LTA, suggesting that the AM domain is bound to the cell wall through this interaction[39,92]. The repeat units R_1R_2 can be individually divided into two subunits a and b, and both carry a highly conserved glycine-tryptophan (GW)-motif that can play a role in host ligands binding[93], as for example vitronectin and fibronectin.

1.2.2.3- endo-β-N-acetylglucosaminidase (GL)

The endo-β-N-acetylglucosaminidase (GL) catalytic domain begins at bp 2326 and ends at bp 3768 of *atl* gene, with the corresponding polypeptide extending from Ala776 to Lys1256[90]. This 51 kDa domain cleaves the bond between the two polysaccharide subunits N-acetylglucosamine and N-acetylmuramic acid of peptidoglycan. The GL domain is associated with repeat region R_3, that binds to the *S. aureus* cell wall in its proper localization[90]. Contrarily to the AM domain, the structure of GL domain has not been resolved yet. The repeat region R_3 is more divergent from the other two repeat regions (R_1R_2) that are more similar to each other[109]. An evidence that supports this is the inability of R_3 to bind to host plasma proteins, contrary to R_1R_2 repeat regions[111].

The GL domain does not show lytic activity against *S. aureus* heat-inactivated cells, despite its primarily role of hydrolysing the bond between the two polysaccharide subunits of peptidoglycan, but it is capable to lyse *M. luteus* cells[94]. The degree of peptidoglycan cross-linking, the presence of other components of the cell wall besides peptidoglycan and the chemical properties of the peptidoglycan itself, are factors that can influence the capacity of hydrolases to perform their functions[112], which may occur with the GL domain. The structural differences between *S. aureus* and *M. luteus* peptidoglycan, as they belong to different peptidoglycan sub-groups[79], suggests that *S. aureus* peptidoglycan may have to be pre-digested by the AM domain

or other peptidoglycan hydrolases so that the GL domain can reach the bond between N-acetylglucosamine and N-acetylmuramic acid for hydrolysis[113].

1.2.3- DNA-binding activity of Atl at cell surface

eDNA is present in several environmental locations, most of them of microbial origin[114]. In this way it is normal for cells to interact with DNA molecules present on the extracellular surrounding. The role of eDNA in biofilm formation has been largely discussed and what kind of interactions it can perform.

Among its many functions, the Atl protein can also bind DNA molecules at the cell surface (Grilo, I.R., unpublished). The GL catalytic domain, the repeat regions and the whole pre-processed Atl protein are able to bind to DNA with no sequence specificity, in contrast to the AM catalytic domain, that does not show DNA binding capacity[96]. The repeat regions are known to bind to a variety of molecules such as LTA and peptidoglycan[92], and its properties and structural similarities with other SH3-like proteins, able them to also bind to RNA and DNA[93,115]. The AM domain only can bind eDNA due to the adhesive properties of R_1R_2 repeat regions[96].

In the case of the GL catalytic domain, no specific function for this interaction has been assigned. Since GL and eDNA are present in the biofilm structure, the GL-DNA interaction can have some importance during the biofilm development and it is also possible that the DNA binding capacity of GL domain may be involved with the cellular uptake of DNA. DNA-mediated genetic transformation was reported in *S. aureus*[116], and the GL domain could be an important factor for this process. Also, the presence of eDNA seems to not affect the hydrolytic activity of the GL domain[96]. The DNA binding ability of GL opens a whole new range of interactions and roles in the already known functions of Atl.

The complete Atl protein can also bind DNA, strengthening the hypothesis of Atl being able to bind DNA not only in the extracellular milieu but also intracellularly[96].

1.2.4- Biofilms: the role of Atl

The Atl protein has a vital role in biofilm development. It is involved in the initial stage of attachment and both AM and GL domains are essential in this process[38,97]. The repeat regions R_1R_2 are also important, since they can bind to several host proteins as vitronectin and fibronectin[93] and abiotic surfaces[94]. In *atl* mutants, biofilm development is highly decreased[39,94], especially in strains that produce PIA-independent biofilm comparing with strains that produce PIA-dependent biofilm[97]. When *atl* mutant strains are complemented with AM and GL, a normal biofilm formation can be restored, but not entirely if only one of the Atl domains is added[38], confirming the importance of the two catalytic domains of Atl for biofilm development.

The controlled autolysis activity of Atl is directly involved with biofilm formation and with the release of genomic DNA to the ECM[38,97,107]. *S. aureus* biofilms have a high contribution of eDNA, and the DNA availability is crucial for proper biofilm development[60], as well as the interactions of eDNA with other biofilm components, particularly with proteins that possibly protect

eDNA from the action of nucleases[62]. The interaction of eDNA with proteins and peptides such as PSM[68], β-toxin [46] or LytC in pneumococcal species[117] were already described.

Besides the autolysis and release of all cell components, the possible involvement of Atl in the cytoplasmic proteins secretion to the ECM can be another role for the protein during biofilm development. It was thought that the presence of these cytoplasmic proteins was due to cell lysis, but the most abundant cytoplasmic proteins are not found in the exoproteome of *S. aureus*, suggesting that this excretion happens through non-classical secretion pathways[47,49]. Atl protein can be involved in this process since the secretome pattern of the *atl* mutant was different compared with the wild type, being also suggested that the cytoplasmic protein excretion occurs at the septum region, the Atl binding site[47].

1.2.4.1- GL-DNA interaction in biofilm formation

Grilo et al.[96] demonstrated that the GL domain has the capacity to bind DNA with no sequence specificity, with or without the presence of the R_3 repeat region. This interaction between the GL domain and DNA can reveal a whole new gathering of functions that involves both molecules. During biofilm development, the association between proteins and eDNA is important for the maintenance of the biofilm structure, as mentioned in the previous sections. Atl has many roles during biofilm formation, and the GL-DNA interaction could be an additional function, although the mechanism behind the GL-DNA interaction is still unknown. In this way, the interactions between DNA and other proteins also involved in biofilm formation[46,117] can provide clues on the binding mechanism between eDNA and the GL catalytic domain.

2- Materials and Methods

2.1 - Bacterial strains, plasmids and growth conditions

Bacterial strains used in this work (Table 2.1) were grown at 37ºC with aeration except for *S. pyogenes* cells that were grown statically, *M. luteus* at 30ºC and *C. marina* and *M. hydrocarbonoclasticus* that were grown at 28ºC, in the following media: Tryptic Soy Broth (TSB) or Tryptic Soy Agar (TSA) (Biokar, Odivelas, Portugal or BD, New Jersey, USA) for *S. aureus* and *S. epidermidis* strains, Lysogeny Broth (LB) or Lysogeny Agar (LA) (Liofilchem, Roseto degli Abruzzi, TE, Italy) for *E. coli*, *S. agalactiae* and *S. pyogenes* strains, Brain Heart Infusion (BHI) (Oxoid, Thermo Fisher Scientific, Waltham, MA, USA) for *M. luteus* and *E. faecalis* strains and Marine Broth (MB) (Carl Roth, Karlsruhe, Germany) for *C. marina* and *M. hydrocarbonoclasticus* strains. Antibiotics kanamycin (Km, 30 µg/ml), chloramphenicol (Cm, 10 µg/ml), erythromycin (Em, 10 µg/ml) and ampicillin (Amp, 100 µg/ml) were used as needed (Sigma-Aldrich, St. Louis, MO).

Table 2.1: Strains and plasmids used in this study.

Strains	Description	Source
Staphylococcus aureus		
COL	Homogenous Mcr (MIC, 1,600 µg/ml); Em^s	Rockefeller University Collection
WIS	Biofilm producing CA-MRSA strain, from Taiwan clone, Em^s	[118]
WISΔ*atl*	WIS strain with an *atl* deletion. Em^s	This study
Escherichia coli		
DH5α	*recA endA1 gyrA96 thi-1 hsdR17 supE44 relA1 ϕ80 ΔlacZΔM15*	Thermo Fisher Scientific
BL21 (DE3)	*F⁻ompT gal dcm lon hsdS$_B$* ($r_B^- m_B^-$) λ(DE3 [*lacI lacUV5-T7 gene 1 ind1 sam7 nin5*])	Thermo Fisher Scientific
K12 (MG1655)	*F⁻ λ⁻ rph-1*	[119]
Micrococcus luteus	High G+C content gram-positive actinobacteria	Laboratory collection
***Cobetia marina* DSMZ 4741**	Marine bacterium isolated from coastal seawater	Leibniz Institute DSMZ – Collection of Microorganisms and Cell Cultures
***Marinobacter hydrocarbonoclasticus* DSMZ 8798**	Isolated from sediments at the mouth of a petroleum refinery	Leibniz Institute DSMZ – Collection of Microorganisms and Cell Cultures
***Staphylococcus epidermidis* RP62A**	Methicillin resistant *S. epidermidis* (MRSE) biofilm-producing clinical isolate	[120]
***Streptococcus agalactiae* NEM316**	Group B Streptococcus serotype III isolate (NEM316)	[121]

***Streptococcus pyogenes* GAP58**	Clinical clone from invasive infection. Tetracycline^r	[122]
***Enterococcus faecalis* ATCC19433**	Control strain for Group D Streptococcus	American Type Culture Collection (ATCC)
Plasmids	**Description**	**Source**
pET28a(+)	*E. coli* expression vector	Novagen
pET-AM	pET28a(+) expressing AM as an N-terminal His6-tag fusion	[96]
pET-R_3GL	pET28a(+) expressing R_3GL as an N-terminal His6-tag fusion	[96]
pET-GL	pET28a(+) expressing GL as an N-terminal His6-tag fusion	[96]
pIG4	*atl* promoter::sGFP, Cm^r	I.R. Grilo (unpublished)
pGC1	Shuttle vector for gene regulation studies. *pta* promoter controlling GFP expression; Amp^r, Cm^r	G. Cavaco (unpublished)
pMAD-Atl	pMAD vector carrying downstream and upstream regions of *atl* gene. Em^r	[123]

2.2 - DNA methods

2.2.1 – DNA extraction and manipulation

For extraction of the plasmids described in Table 2.1, ZR Plasmid Miniprep – Classic Kit (Zymo Research, Irvine, CA, USA) was used. For *S. aureus* plasmids, an additional initial lysis step was performed: lysostaphin was added to a final concentration of 50 ng/µl (AMBI PRODUCTS LLC, Lawrence, NY, USA) to the initial kit buffer, and samples were incubated at 37ºC for 45 min, before continuing the extraction process as described by the manufacturer.

For genomic DNA extraction from *S. aureus* strain COL to use as PCR template, Wizard Genomic DNA Purification Kit (Promega, Madison, WI, USA) was used. Overnight culture was centrifuged and resuspended in 50 mM EDTA and 250 ng/µl lysostaphin. The samples were incubated at 37ºC for 45 min and centrifuged again before continuing the extraction process as described by the manufacturer.

For genomic DNA extraction to perform *S. aureus* colony screening, 2 colonies from the desired strain were resuspended in TE (10 mM Tris, 1 mM EDTA, pH 8) enriched with lysostaphin at a final concentration of 250 ng/µl and incubated in a water bath at 37ºC for 15 minutes. A denaturation is performed at 95ºC for 15 minutes followed by the addition of 180 µl of dH_2O and a centrifugation of 16 060 g for 5 minutes recovering the supernatant.

2.2.2 – PCR amplification

Routine PCR amplification was performed with NZYTaq DNA polymerase (NZYTech, Lisboa, Portugal), to amplify Fragment A with primers pddlalow3 and pmurFGS4 (Table 2.2) using DNA from *S. aureus* strain COL as a template. The PCR product was purified with NZYGelpure Kit (NZYTech).

Table 2.2: Primers used in this study.

Primer	Nucleotide Sequence (5' – 3')	Source
PmurFGS4	CACAGTGATATCAGCTATAG	[96]
PddlAlow3	CCTCCAATGATATATCAGGG	[96]
pGLSH3fwBamHI	CCAGGATCCGCAATGGATACGAAGCGTTTAGC	I.R. Grilo (unpublished)
pAMR2rvSalI	CCAGTCGACTTAGGTAGTTGTAGATTGCG	I.R. Grilo (unpublished)
pMADrv	CGTCATCTACCTGCCTGGAC	I.R. Grilo (unpublished)
pMADfw	CTCCTCCGTAACAAATTGAGG	I.R. Grilo (unpublished)
pGLR3fwBamHI	CGTGGATCCGCACCAACTGCTGTGAAACC	I.R. Grilo (unpublished)
pMADatlupfwBglII	CCTGCAGATCTTTGTTAGGATGTGGAGG	I.R. Grilo (unpublished)
pMADatldownrvBamHI	CGGCAGGATCCAATTGCTGTTGCGTTGTC	I.R. Grilo (unpublished)
pGLrvSalI	CCAGTCGACTTATTTATATTGTGGGATGTCG	I.R. Grilo (unpublished)

2.3 – Expression and purification of recombinant proteins

To purify recombinant Atl proteins, the respective plasmids (Table 2.1) were expressed in *E. coli* BL21 (DE3) through an auto-induction expression method described by Studier, 2005[123]. The auto-induction medium composition was 0.1% 1M $MgSO_4$, 2% 50X 5052 (25% glycerol, 2.5% glucose and 10% α-lactose monohydrate), 5% 20X NPS (1M Na_2HPO_4, 1M KH_2PO_4, and 0.5 M $(NH_4)_2SO_4$) and 100 µg/mL of Km in LB medium. The culture was incubated at 37°C with high aeration and shaking (180 rpm) for 18 hours. Cells were centrifuged at 8 421 g for 10 min at RT and the pellets obtained were resuspended in Lysis Buffer (50 mM Na_2HPO_4, 300 mM NaCl, 10 mM Imidazole, pH 8), enriched with benzonase nuclease (Novagen, Merck Millipore) to remove nucleic acids and with Pierce Protease Inhibitor Mini Tablets, EDTA Free (Thermo Fisher Scientific) to protect proteins from degradation during the purification process.

After mechanical cell disruption, that was done using a sonicator (UP200S Ultrasonic Processor, Hielscher Ultrasonics) at an 80% amplitude, 0.5 of pulse mode cycles to perform 5 cycles of 1 minute with pauses, proteins were present in the soluble fraction. The lysates were cleared by centrifugation at 8 421 g for 60 min at 4°C. Purification was achieved using Ni-NTA agarose columns (Thermo Fisher Scientific) under native conditions, according to the manufacturer's instructions. The lysate supernatant was placed in the pre-prepared column equilibrated with Lysis Buffer. The column was washed with Lysis buffer and with Wash buffer (50 mM NaH_2PO, 30 mM imidazole, 300 mM NaCl, pH 8.0). To recover the His-tagged protein, Elution buffer (50 mM NaH_2PO_4, 300 mM imidazole, 300 mM NaCl, pH 8.0) was used.

SDS-PAGE was performed for all fractions collected to identify the most concentrated elution fractions. PD10 desalting columns (GE Healthcare Life Sciences, Buckinghamshire, UK) were used following the manufacturer's instructions and loaded with PBS, pH 7.4 (phosphate buffered saline: 137 mM NaCl, 2.7 mM KCl, 10 mM Na_2HPO_4, 1.8 mM KH_2PO_4). The concentrations of each protein were determined with the Nanodrop Spectrophotometer ND-1000 using its respective theoretical molar extinction coefficient (ε). The protein samples were aliquoted and maintained at -20°C.

2.4 - Electrophoretic Mobility Shift Assay (EMSA)

2.4.1 – EMSA in agarose electrophoresis

EMSAs were performed using recombinant protein GL and purified DNA fragment A, amplified by PCR. The binding reaction was performed with recombinant GL protein at different final concentrations from 0 to 1 µM, in PBS pH 7.4. All EMSA reactions were performed with DNA fragment A (16 nM) or with pGC1 plasmid DNA extracted from *E. coli* or from *S. aureus* cells (Table 2.1), at a final concentration of 1.1 nM. After a 30 min incubation step at RT, each binding reaction was separated by 1% agarose gel electrophoresis (Tris-Acetate-EDTA buffer, TAE: 40 mM Tris-base, 20 mM Glacial Acetic Acid, 1 mM EDTA). Visualization was performed in Universal Hood II Gel Doc System, using ethidium bromide (Bio-Rad, Hercules, CA, EUA) as DNA intercalator.

EMSA reactions were performed for different pH values as described above using PBS and TAE buffers with altered pH values in a 5 to 10 range. Sequential concentrations in the range of 0 – 200 mM of NaCl, KCl, $CaCl_2$, $CdCl_2$, $CoCl_2$, $CuSO_4$, $FeCl_2$, $MgCl_2$, $MnSO_4$, Na_2MoO_4, $NiCl_2$ and $ZnSO_4$ salts were used for three different protein concentrations (0, 50 and 1000 nM).

The gel images of every different EMSAs performed at different pH values were analysed using FIJI (https://imagej.net/Fiji/Downloads), by calculating the intensity of each band. The bands were plotted, and the generated areas corresponded to the intensities of each band. The bands without protein were used as controls, corresponding to 100% of DNA, i.e. no binding, and as a comparison to all the other bands. The results were analysed using non-linear regression curve fit using GraphPad Prism 6.

2.4.2 – EMSA in polyacrylamide electrophoresis

To perform Protein-DNA binding reactions, GL was used in a 2.5 to 12.6 µM range, 3.85 nM of pCG1 plasmid in PBS pH 7.4 as binding buffer. After 4 hours of binding reaction at RT, each reaction was separated in 12% SDS-PAGE (Tris-Glycine-SDS buffer). Visualization was performed using Coomassie Brilliant Blue R-250 (AppliChem, Darmstadt, Germany).

Acidic native-PAGE gels were assembled using buffers for native gels at various pH values as described previously[125]. The chosen buffer had a pH of 6.1, composed by 25 mM Histidine and 30 mM MES, and it was used subsequently as sample buffer and running buffer.

Protein-DNA binding reactions were performed as for SDS-PAGE. GL protein was used in a 2.5 to 12.6 µM range, pCG1 plasmid in a 0.55 to 55.03 nM range and PBS pH 7.4 was used as binding buffer. After 4 hours of binding reaction at RT, each reaction was separated in 6% acidic native-PAGE at 140V for 55 minutes and the electrophoretic cell poles were changed for a positive to negative migration. Visualization was done with Coomassie Brilliant Blue R-250.

2.5 – Atomic Force Microscopy (AFM) measurements of Protein-DNA interaction

To perform AFM measurements, 220 pM of pGC1 plasmid DNA were placed in a muscovite mica together with 2.5 mM of $NiSO_4$ and left to be adsorbed for 5 minutes. The solution was rinsed off using MilliQ water and dried using pressurized air. In case of Protein-DNA interaction samples, the protein was added after DNA adsorption, incubated for 10 minutes and then washed and dried. Two recombinant proteins were used separately, GL (505 nM) and AM (690 nM).

The operation of the AFM was performed in intermittent contact mode in air, using Nanosensors SSS-NCHR (Nanosensors, Switzerland) rectangular silicon probes with aluminium reflex coating. These have advertised resonant frequency of 330 kHz, spring constant of 42 N/m and average tip radius of 2 nm with an aluminium coat.

Experiments were done in the Nanofabrication Laboratory - Atomic Force Microscopy of CENIMAT/I3N at Faculdade de Ciências e Tecnologia of Universidade Nova de Lisboa (FCT-UNL). The AFM operated was an Asylum Research MFP-3D Stand Alone. 2D AFM images and analysis were generated with Gwyddion (gwyddion.net). In order to increase contrast between elements of study and the background, images were plane fitted and had its scalebar range limited to at least ±4 RMS.

2.6 – Hydrolytic activity assays

2.6.1 – Preparation of heat-inactivated cells

Heat-inactivated cells of several different microorganisms, listed in Table 2.1, were used as substrate for the hydrolytic activity assay. Heat inactivated cells were prepared following a previously described procedure[126]. Briefly, cultures were incubated until an OD_{600nm} of 0.7. Cells were recovered by centrifugation at 8 421 g, 4ºC for 10 min and washed twice in 200 ml ice-cold ultrapure water. After resuspension, cells were heat-inactivated by autoclaving at 121ºC for 15 minutes. Once again, heat-inactivated cells were washed twice in the same amount of ice-cold ultrapure water. Cells were finally resuspended in the minimum amount of water with 0.05% NaN_3 and stored.

2.6.2 - Hydrolytic activity assays in the presence of extracellular DNA

The hydrolytic activity of the GL domain, with and without R_3, in presence of extracellular DNA (eDNA) was performed through optical density monitorization. First, the pH for hydrolytic activity was optimized using several 50 mM sodium phosphate buffers with different pH values (5.85 to 8.07). Heat-inactivated cells of *M. luteus* were resuspended in 50 mM sodium phosphate buffer to an initial OD_{600nm} of 0.7. Purified GL or R_3GL proteins were added at a 10 µg/ml concentration. OD_{600nm} was measured immediately and at several subsequent timepoints up to 120 minutes. During the assay, the samples were maintained at 37ºC with shaking.

The hydrolytic activity of each protein for heat-inactivated cells of the different microorganisms was determined using the previously optimized buffer pH. These assays were repeated in the presence of low-molecular weight salmon sperm DNA (Sigma-Aldrich) at different concentrations (0.1 to 10 mg/ml), using the same conditions as before. The hydrolytic activity was determined by comparing, for each sample, the OD_{600nm} of each timepoint with the respective initial OD_{600nm} in percentage. Each assay was performed in triplicate and the results are shown as Mean and SEM (standard error of the mean) of each assay.

Hydrolysis assays data were analysed by performing a two-way ANOVA with Tukey multiple comparison tests, using GraphPad Prism 6.

2.7 – Monitoring *S. aureus* growth

2.7.1 - WISΔ*atl* mutant construction using pMAD plasmid

WISΔ*atl* strain was obtained through an allelic replacement strategy using the pMAD vector, essentially as described[127]. The previously constructed pMAD-Atl plasmid in WIS strain (I.R. Grilo, unpublished) was integrated into the chromosome through homologous recombination at a non-permissive temperature (43ºC) in TSA with X-Gal (100 µg/ml) and Em (10 µg/ml). Genomic DNA extraction from several clones and screening for pMAD integration was done using primers pairs pGLSH3fwBamHI/pMADrv and pAMR2rvSalI/pMADfw, listed in Table 2.2. Positive clones were inoculated in TSB at a permissive temperature (30ºC) and then plated in TSA with X-Gal (100 µg/ml) at the same temperature. White colonies were chosen, and the efficiency of the allelic replacement event was confirmed through PCR screening using primers pairs pMad_atl_up_fw/pMad_atl_down_rv and pGLrvSalI/pGLR3fwBamHI, listed in Table 2.2.

The pIG4 plasmid was later transduced to the chosen WISΔ*atl* clone using phage Φ11[128]. An overnight culture from WISΔ*atl* was diluted in TSB media and incubated at 37ºC for 1 hour. Cells were recovered by centrifugation at 1747 g for 10 min and the resulting pellet resuspended in 500 µl of TSB, enriched with 400 ng/µl $CaCl_2$. Φ11 phage containing pIG4 was added to the media followed by two incubations, at the room temperature for 10 minutes and at 30ºC for 35 minutes. Without mixing, 2.5 ml of TSB were added and then centrifuged in same conditions as above. The pellet was resuspended in 5 ml of TSB and incubated at 37ºC for 90 minutes with agitation (250 rpm). The cells were then recovered in 500 µl TSB and plated with Cm (10 µg/ml).

2.7.2- Monitoring *S. aureus* growth

Overnight cultures were diluted to an initial OD_{600nm} of 0.05 in 50 ml TSB and were grown with shaking (180 rpm) for 24 hours. Several growth conditions were altered, including different growth temperatures (25ºC, 30ºC, 37ºC and 42ºC) and presence of low molecular weight salmon sperm DNA (at 0.1%, 0.5% and 1% (w/v)). Also, the pH of the culture was stabilized by preparing the growth medium with 100 mM 3-(N-morpholino)propanesulfonic acid (MOPS) pH 7.4. Growth was assessed by measuring OD_{600nm} hourly for 10 hours, and then at 24 hours. For the non-buffered growth assays performed in the presence of DNA, the pH was assessed the end of the assay, to confirm that the pH did not change during the 24-hour growth. Biological replicates were performed in triplicate and the results are shown as Mean and SEM of each assay.

2.8- Determination of gene expression by promoter fusion assays

atl expression was determined for strains WIS with plasmid pIG4 (Table 2.1). Several expression conditions were tested, at different temperatures (25ºC and 37ºC), presence of low molecular weight salmon sperm DNA at final concentrations of 0.1%, 0.5% and 1% (w/v) and pH 7.4 buffered growth medium. Cultures were grown for 24 hours at 180 rpm with aeration. An aliquot of culture was collected at hourly timepoints until 10 hours, and then at 24 hours. The cells were harvested by centrifugation, 1 min at 16 060 g, washed in PBS pH 7.4, resuspended in 500 µl of fresh buffer and introduced into 96-wells Black Polystyrene Microplates (BrandTech Scientific, Essex, CT, USA). The fluorescence was measured using a Tecan i-control infinite 200 apparatus (Tecan, Männedorf, Switzerland) and normalized using the respective value of OD_{600nm}. The excitation and emission wavelengths were 485 nm and 535 nm respectively. Each assay with the different conditions, was only performed once.

3 – Results and Discussion

Previous studies suggested that Atl protein is essential in different stages of the *S. aureus* life cycle, participates in several physiological processes and interacts with different molecules, which have essential roles for the bacterial survival and proliferation[38,39,97]. One of these molecules is DNA, which was shown to associate with the Atl protein, namely with the GL domain[96]. In this study, our aim was to explore the molecular features of the interaction between the GL domain and DNA, and to determine how it interferes with other functions of the protein, namely the primary physiological role of Atl, peptidoglycan hydrolysis.

3.1 – Molecular characterization of GL-DNA association

The DNA-GL interaction was studied using electrophoretic mobility shift assays (EMSA) with the purpose to understand some of the interaction features, since different parameters can affect the DNA-GL binding, such as pH, ion concentration or the nature of the nucleic acid molecules. At the same time, the Atl peptidoglycan hydrolytic activity in the presence of DNA was studied to understand the role of this interaction and if it can interfere with the Atl primary function of hydrolysis.

3.1.1 – DNA-binding capacity of GL at different pH values

GL polypeptide sequence includes many basic amino acids such as Lysine and Arginine[90], with positively charged side chains at biological pH, that are responsible for the high theoretical pI value of the protein (9.58). Therefore, the GL-DNA interaction could be of electrostatic nature and if so, different pH values could affect the DNA-binding capacity of GL domain.

To test this hypothesis, a 5-10 pH value range was tested by EMSA and compared to the physiological pH (7.4) (Figure 3.1). At the tested pH values, the DNA molecules are predominantly negatively charged, and the recombinant GL protein has both positive and negative charges. Phosphate buffer saline (PBS) at the different pH values was used as binding reaction buffer, and TAE electrophoresis buffer was also used at the same pH values, to guarantee that the pH was not altered during electrophoresis (TAE used in agarose electrophoresis has a pH of 8.3).

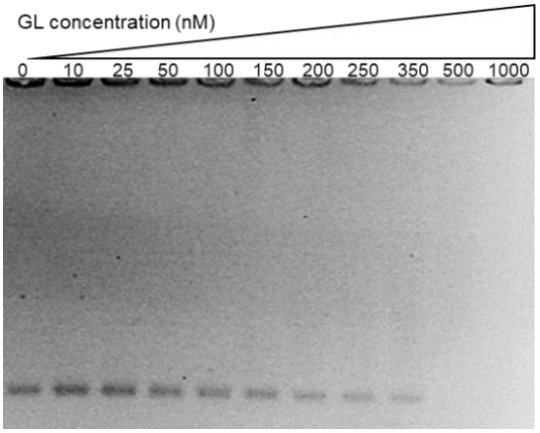

Figure 3.1: EMSA with recombinant GL protein at pH 7.4. 16 nM of DNA fragment A (238bp) were incubated with increasing concentrations of GL (0 to 1000 nM) for 30 minutes in PBS buffer at pH 7.4, and agarose gels were used to visualize the GL-DNA interaction. The gels were stained with ethidium bromide.

The interaction was more efficient at lower pH values, when the net charge of the protein is increasingly positive (Figure 3.2). At pH 5, 100 nM of the GL protein were sufficient to retain 16 nM of the DNA fragment on the gel well (Figure 3.2-A). This concentration is five times lower than the GL concentration needed to retain 16 nM of DNA fragment at pH 7.4 (500 nM). At pH 6 and 7, the GL concentrations needed to retain all the DNA molecules were 200 nM and 250 nM respectively (Figure 3.2-B and C). At pH 8 and 9, the concentration of GL capable of retaining the DNA fragment was the same as at pH 7.4 (Figure 3.2-D and E) and at pH 10, above the theoretical pI value of GL of 9.58, the protein lost the capacity to bind DNA, at the concentrations tested (Figure 3.2-F). From the concentration of GL necessary to retain 16 nM of the DNA fragment, we were able to calculate the GL:DNA molar ratio (Table 3.1), and indicate how many protein molecules can interact with each DNA molecule at the different pH values. At the lowest pH value tested (pH 5), the number of GL molecules that bound to DNA was lower (molar ratio 6.25:1), while at the highest pH value tested that still allowed GL-DNA interaction (pH 9), the molar ratio was five times higher (molar ratio 31.25:1). These results indicate that the apparent binding affinity of GL-DNA association is higher at lower pH values.

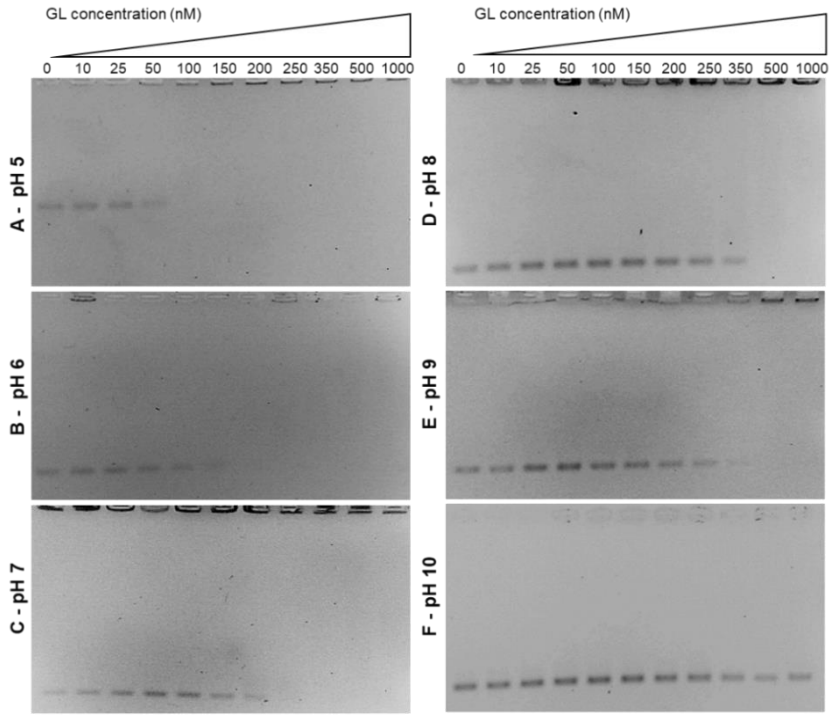

Figure 3.2: EMSA with recombinant GL protein at different pH values. 16 nM of DNA fragment A was incubated with increasing concentrations of GL (0 to 1000 nM) for 30 minutes in PBS buffer at different pH values, and agarose gels were used to visualize the GL-DNA interaction. The pH of the TAE electrophoresis buffer was modified according to the binding reaction. The gels were stained with ethidium bromide.

The performed EMSAs showed that the pH value influences the GL-DNA interaction. At pH 5, the estimated charge of the protein is highly positive, +33.5 (Table 3.1). However, the DNA molecule has a negative net charge at physiological pH, but at pH 5, its net charge is close to zero, as the pI value of DNA is reported to be 4-5, depending on the characteristics of the DNA molecule[129] due to the ionization of the phosphate groups[130]. This stronger interaction between GL and DNA at pH 5 can be explained by the conformational changes that occur on DNA molecules when their net charge is close to zero. In fact, it has been reported that at low pH values, DNA molecules are reported to condensate[131]. It is possible that a more condensed DNA conformation facilitates protein binding due to a lower surface area of DNA molecule available for interaction resulting in a low molar ratio.

As the pH value increased, the GL:DNA molar ratio also increases. The results obtained at pH 8 and 9 indicated that the influence of the net charge was less evident at higher pH, when the charge is above +18, the estimated charge at pH 7.4. At pH 10, GL has negative net charge, -13.1, and no retention of the DNA fragment was observed. In this case, the capacity to interact with the DNA fragment was lost.

These results revealed that the DNA-binding capacity of GL is not totally dependent of the electrostatic forces between the opposite charges of the two molecules.

Table 3.1: Estimated net charge of the recombinant GL domain at different pH values and respective GL:DNA molar ratio needed to retain all DNA fragment on the gel well. Protein charges were estimated using Protein Calculator v3.4, last update at May 13th, 2013; *http://protcalc.sourceforge.net/* (Last visit at September 10th, 2018).

pH value	Estimated charge	GL: DNA ratio
5.0	+ 33.5	6.25
6.0	+ 26.7	12.5
7.0	+ 19.8	15.6
7.4	+ 18.0	31.25
8.0	+ 16.3	31.25
9.0	+ 10.8	31.25
10.0	- 13.1	No binding

To obtain quantitative parameters of the GL-DNA binding, an attempt to calculate the dissociation constant (KD) of the interactions between GL and DNA at different pH values was performed. The KD corresponds to the concentration of GL protein at which half of the DNA is bound to the protein, meaning that a lower KD value corresponds to a higher affinity between the two molecules[132]. The results obtained from the plots of the band intensities of the EMSAs, had too wide confidence intervals (CI 95%) to validate the generated data or the software was incapable to generate a KD value or a non-linear fitting curve (Annex 1 – Figure A.1). This inability to obtain equilibrium data can be explained by the differences between the GL concentrations tested. A higher number of different GL concentrations within the tested range could had given a more adequate curve to retrieve such data. Having a non-proportional stoichiometry between GL and DNA had also difficulted the generation of a KD value or a non-linear fitting curve as well as the lower intensity of the band without protein, used as the control, due to a low quality of the image.

3.1.2 – Effect of different cations on GL-DNA binding

The effect of the presence of different monovalent and divalent cations for the GL-DNA interaction was tested at pH 7.4. Since the pH value can alter the DNA-binding capacity of GL domain, different charges and ion concentrations could also play a role in the interaction. To test this hypothesis, different salts with monovalent and divalent cations with biological relevance were used. Different GL concentrations were tested, above and below 500 nM, the concentration at which GL retains all the DNA molecules on the gel wells at pH 7.4. The influence of the cations on the GL-DNA interaction was tested for two different effects: the ability to benefit the interaction by increasing the binding affinity of GL for DNA, using 50 nM of recombinant GL (Figures 3.3, 3.4 and 3.5 middle panels), and the ability to prevent the interaction by disrupting or inhibiting it using 1000 nM of recombinant GL (Figures 3.3, 3.4 and 3.5 right panels). As a control, the influence of these cations on DNA migration was also tested in the absence of GL protein (Figure 3.3, 3.4 and 3.5 left panels). All shown EMSAs were performed at least two times to confirm the reproducibility of the results.

Sodium (Na^+) and potassium (K^+) monovalent ions did not affect the DNA migration (Figure 3.3-A and D) and the GL-DNA interaction was not affected at the tested NaCl and KCl concentrations. The presence of these cations did not increase the DNA-binding capacity of GL

(Figures 3.3-B and E), neither did it disrupt the interaction when 1000 nM of GL protein were used (Figure 3.3-C and F), a concentration at which GL retains all DNA molecules at the gel well.

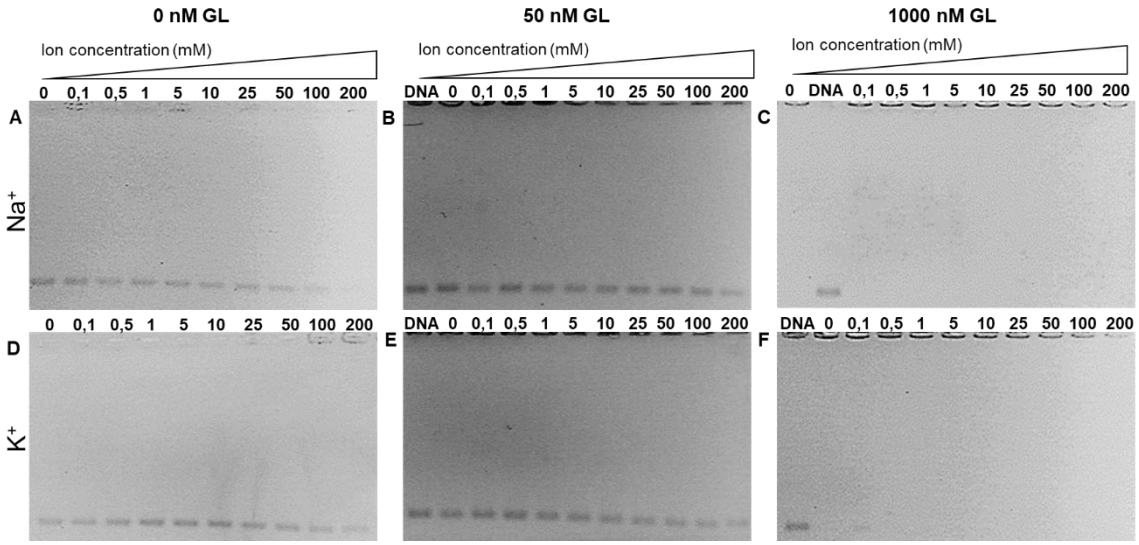

Figure 3.3: Effect of monovalent cations on the DNA migration and GL-DNA binding. 16 nM of DNA fragment A (238bp) was incubated in PBS buffer at pH 7.4 with different concentrations of recombinant GL protein and increasing concentrations of several cations for 30 minutes, and agarose gels were used to visualize the DNA molecules. The gels were stained with ethidium bromide. Left panels (A and D): Effect of Na^+ and K^+ on DNA migration; Middle panels (B and E): Effect of Na^+ and K^+ on the GL-DNA using 50 nM of GL; Right panels (C and F): Effect of Na^+ and K^+ on the GL-DNA using 1000 nM of GL.

For divalent cations, different results were obtained depending on the ion used. Most of the divalent cations studied were shown to influence the migration of free DNA at some concentration (Calcium, Ca^{2+}, Cadmium, Cd^{2+}, Cobalt, Co^{2+}, Cupper, Cu^{2+}, Iron, Fe^{2+}, Molibdenium oxide, MoO_4^{2+}, Manganese, Mn^{2+}, Nickel, Ni^{2+} and Zinc, Zn^{2+}) (Figure 3.4 – left panels and Figure 3.5 – A). The cation concentrations tested were adjusted for the EMSAs with 50 nM of GL to avoid the influence of the cations on the DNA migration itself and so determine the specific effect on the binding affinity of GL for DNA. This adjustment was not needed for the EMSA with 1000 nM of GL since the aim was to verify the ability to inhibit the interaction.

For Ca^{2+}, Cd^{2+}, Co^{2+}, Cu^{2+}, MoO_4^{2+}, Mn^{2+}, Ni^{2+} and Zn^{2+} the results were essentially the same, regarding the GL-DNA interaction. Through the assays performed with a GL concentration of 50 nM (Figure 3.4-middle panels), a concentration at which GL does not bind to all the DNA molecules, it was possible to determine that none of these cations assisted the GL-DNA interaction. In the same way, the assays performed with a GL concentration of 1000 nM (Figure 3.4-right panels), a concentration at which GL binds to all the DNA molecules, allowed to determine that none of the presented cations, Ca^{2+}, Cd^{2+}, Co^{2+}, Cu^{2+}, MoO_4^{2+}, Mn^{2+}, Ni^{2+} and Zn^{2+} had the capacity to inhibit the GL-DNA interaction.

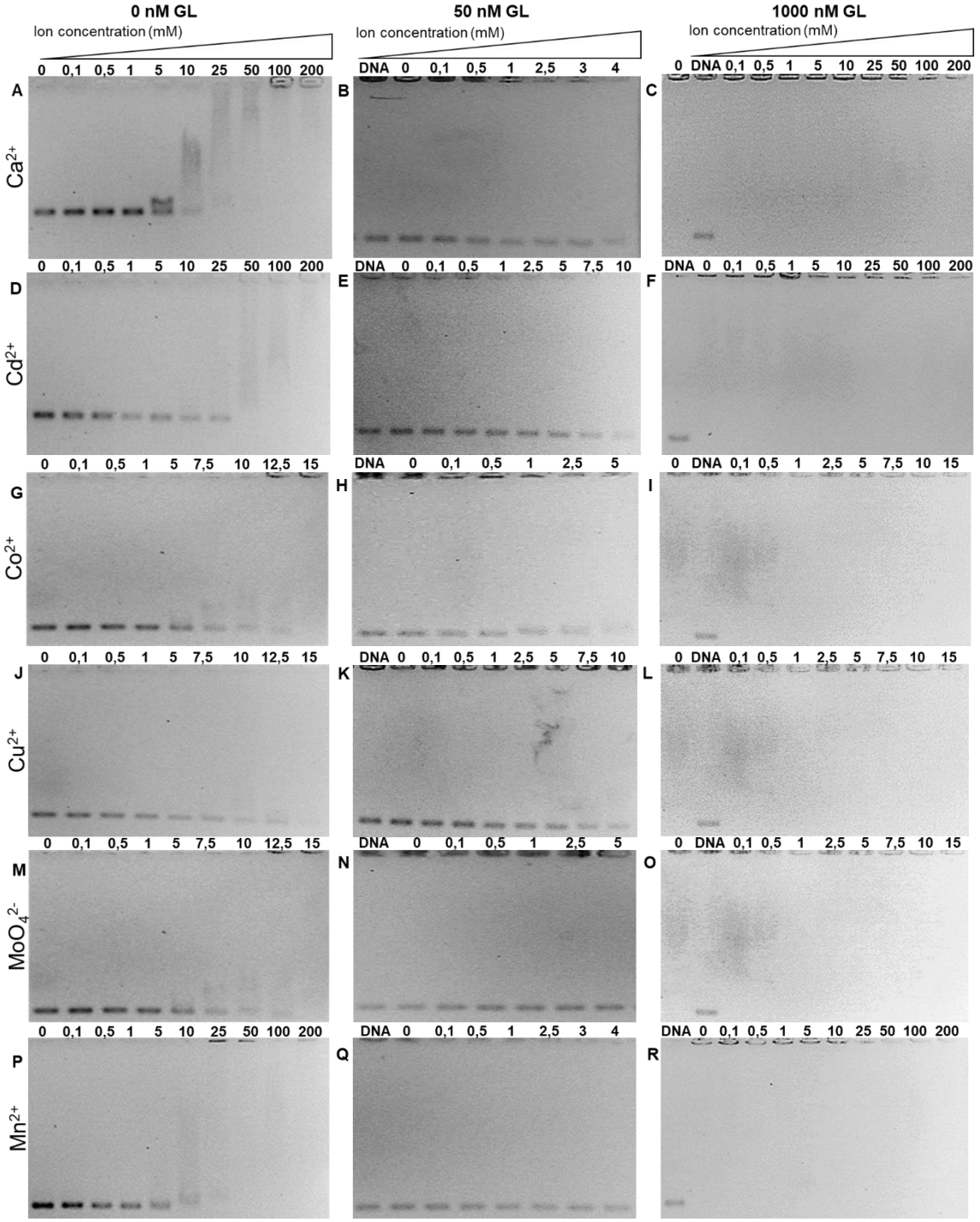

Figure 3.4: Divalent cations without effect on GL-DNA binding. 16 nM of DNA fragment A (238bp) was incubated in PBS buffer at pH 7.4 with different concentrations of recombinant GL protein and increasing concentrations of several cations for 30 minutes, and agarose gels were used to visualize the DNA molecules. The gels were stained with ethidium bromide. Left panels (A, D, G, J, M, P, S and V): Effect of Ca^{2+}, Cd^{2+}, Co^{2+}, Cu^{2+}, MoO_4^{2+}, Mn^{2+}, Ni^{2+} and Zn^{2+} on DNA migration; Middle panels (B, E, H, K, N, Q, T and W): Effect of Ca^{2+}, Cd^{2+}, Co^{2+}, Cu^{2+}, MoO_4^{2+}, Mn^{2+}, Ni^{2+} and Zn^{2+} on the GL-DNA using 50 nM of GL; Right panels (C, F, I, L, O, R, U and X): Effect of Ca^{2+}, Cd^{2+}, Co^{2+}, Cu^{2+}, MoO_4^{2+}, Mn^{2+}, Ni^{2+} and Zn^{2+} on the GL-DNA using 1000 nM of GL.

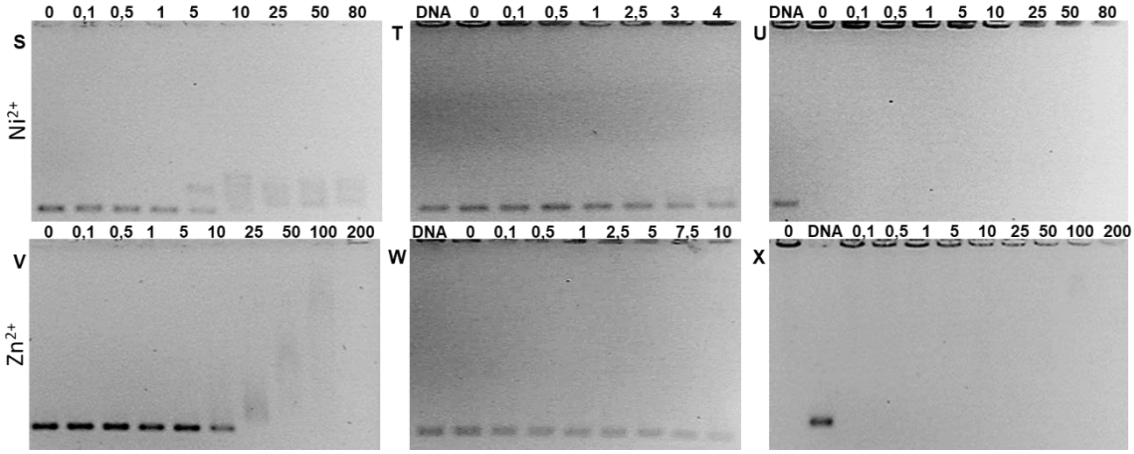

Figure 3.4 (cont.): Divalent cations without effect on GL-DNA binding. 16 nM of DNA fragment A (238bp) was incubated in PBS buffer at pH 7.4 with different concentrations of recombinant GL protein and increasing concentrations of several cations, for 30 minutes, and agarose gels were used to visualize the DNA molecules. The gels were stained with ethidium bromide. Left panels (A, D, G, J, M, P, S and V): Effect of Ca^{2+}, Cd^{2+}, Co^{2+}, Cu^{2+}, MoO_4^{2+}, Mn^{2+}, Ni^{2+} and Zn^{2+} on DNA migration; Middle panels (B, E, H, K, N, Q, T and W): Effect of Ca^{2+}, Cd^{2+}, Co^{2+}, Cu^{2+}, MoO_4^{2+}, Mn^{2+}, Ni^{2+} and Zn^{2+} on the GL-DNA using 50 nM of GL; Right panels (C, F, I, L, O, R, U and X): Effect of Ca^{2+}, Cd^{2+}, Co^{2+}, Cu^{2+}, MoO_4^{2+}, Mn^{2+}, Ni^{2+} and Zn^{2+} on the GL-DNA using 1000 nM of GL.

On the other hand, Fe^{2+} and Mg^{2+} cations were found to disrupt the GL-DNA interaction (Figure 3.5-right panel). In the EMSAs performed with 1000 nM of GL, a concentration at which GL retains all the DNA molecules on the gel wells at pH 7.4, the ferrous ion (Fe^{2+}) destabilized the interaction at concentrations above 5 mM and a Mg^{2+} ion concentration above 0.1 mM was sufficient to unable GL to interact with the DNA fragment.

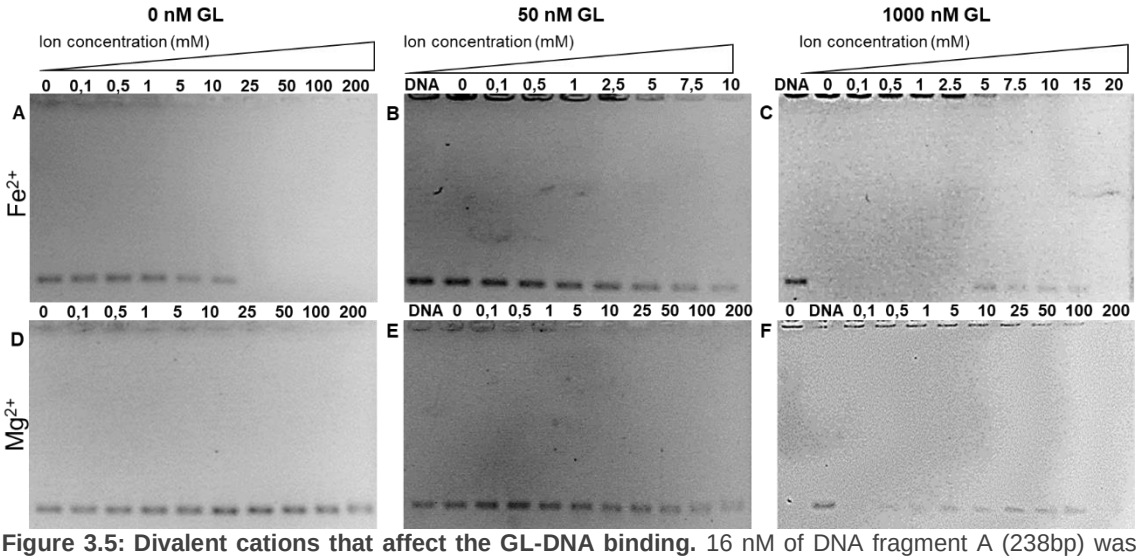

Figure 3.5: Divalent cations that affect the GL-DNA binding. 16 nM of DNA fragment A (238bp) was incubated in PBS 1X buffer at pH 7.4 with 1000 nM of recombinant GL protein and increasing concentrations of several ions, for 30 minutes, and agarose gels stained with ethidium bromide were used to visualize the GL-DNA interaction. Left panels (A and D): Effect of Fe^{2+} and Mg^{2+} on DNA migration; Middle panels (B and E): Effect of Fe^{2+} and Mg^{2+} on the GL-DNA using 50 nM of GL; Right panels (C and F): Effect of Fe^{2+} and Mg^{2+} on the GL-DNA using 1000 nM of GL.

The different effects observed for the different cations with the DNA molecules should be related with their affinity for the DNA molecules and also with their interaction within the DNA structure. The alkali metal cations, Na^+ and K^+, interact exclusively with the phosphate groups of

DNA[133], alkaline earth metals, Ca^{2+} and Mg^{2+}, have higher affinity for the phosphate groups than for the nitrogenous bases[133,134], while transition metals, all the other divalent cations studied, have higher affinity for the nitrogenous bases[134]. Also, the transition metals disturb the DNA molecules more than the alkaline earth metals, due to their higher affinity to the nitrogenous bases, being the double helix structure more affected comparing with the interaction with the phosphate groups[134].

The disruption of the DNA-GL interaction, caused by cations Fe^{2+} and Mg^{2+} is most probably due to the interaction of the cations with the GL protein, since at the concentrations at which the disruption was observed, the cation has no effect on the free DNA molecule migration. How these cations interact with the GL protein was not previously reported and remains to be understood. One hypothesis is that the Fe^{2+} and Mg^{2+} cations interact with the negative amino acids of the protein at pH 7.4, altering its tertiary structure as happens with other proteins[135]. This protein-cation interaction can unable a proper interaction between GL protein and DNA molecules, by conformational change or by occupying interaction spots.

3.1.3 - GL interaction with different nucleic acid molecules

The ability of GL to bind non-specifically to different DNA fragments with different sizes has already been described[96], but its capacity to bind to different nucleic acid molecules had not been tested before. The interaction of GL with plasmid DNA was thus tested, since plasmids can adopt different conformations that could influence the GL binding capacity. Furthermore, plasmid DNA from different bacterial species, namely *S. aureus* and *E. coli,* was used to assess if the GL-DNA binding is altered by different methylation patterns.

The recombinant GL protein showed the capacity to bind to the 7 Kb pGC1 plasmid DNA extracted from *E. coli*, and over than 600 nM of GL protein were necessary for the complete retention of all the DNA molecules (1.1 nM) in the gel well at pH 7.4 (Figure 3.6-A). Using this protein concentration, the molar ratio of GL association to *E. coli* plasmid DNA was determined to be 545:1 (GL:DNA), which means that 545 GL molecules were necessary to retain each plasmid DNA molecule on the well.

The binding of GL to pGC1 plasmid DNA extracted from *S. aureus* was tested by EMSA using the same conditions as for *E. coli* (Figure 3.6-B). The GL-binding capacity was approximately the same as for *E. coli*, with more than 550 nM of GL being necessary to completely retain the *S. aureus* plasmid DNA in the gel well. In this case, the determined molar ratio of the GL association to *S. aureus* plasmid DNA was determined to be 500:1 (GL:DNA).

The electrophoresis migration pattern of the same plasmid, extracted from different microorganisms, was different. Four bands with different intensities were visualized for each sample, corresponding to different plasmid conformations. The plasmid conformation that presented a lower migration rate probably corresponds to the nicked circular conformation, followed by circular, linear and supercoiled conformations, being this last the fastest. For the *E. coli* plasmid (Figure 3.6.A), the band corresponding to the supercoiled conformation was more intense, followed by the circular conformation. The intensity of all bands progressively decreased

with GL concentration, until a 600 mM GL concentration. For the *S. aureus* plasmid (Figure 3.6.B), the band corresponding to the supercoiled conformation was the most intense, followed by the nicked conformation. The intensity of the bands decreased faster for the slowest conformations, but all conformations were still visible for a GL concentration of 550 nM.

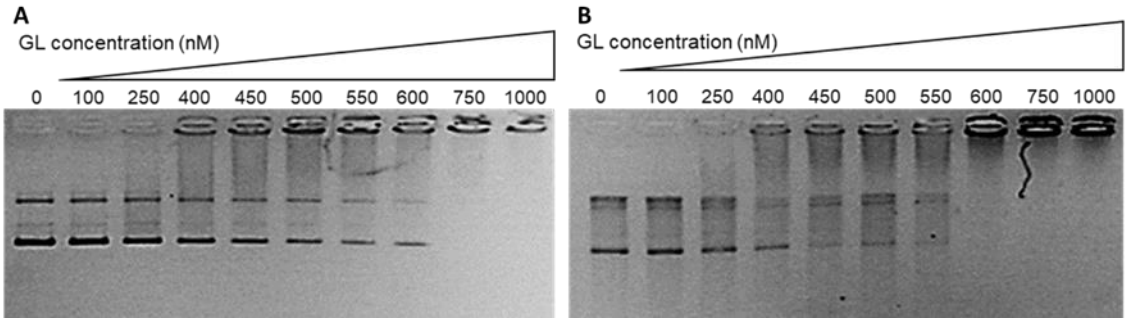

Figure 3.6: EMSA of plasmid DNA with recombinant GL protein. 1.1 nM of pGC1 plasmid DNA (7 Kb) extracted either from A) *E. coli* or B) *S. aureus* were incubated with increasing concentrations of GL, from 0 to 1000 nM, for 30 minutes in PBS buffer at pH 7.4, and agarose gels were used to visualize the GL-DNA interaction. The gels were stained with ethidium bromide.

Despite the differences in the methylation patterns of the plasmid DNA from *E. coli* and from *S. aureus* due to the restriction-modification systems[136], these did not seem to play a major role on the GL-DNA interaction, since the protein concentrations needed to retain all plasmid DNA on the well are very similar, differing only in 50 nM.

In comparison with the EMSA results obtained for the linear DNA fragment (Figure 3.1), the molar ratio of the GL-DNA binding was much higher in case of plasmid DNA, which was expected due to the different number of base-pairs of the two DNA molecules tested. According to the lengths of the different DNA molecules, it is possible to accommodate one GL protein for each 8 base pairs of linear DNA fragment and one GL protein for each 13 base pairs of plasmid DNA, which can indicate a slightly higher binding affinity for GL protein and fragment DNA. Also, the spatial conformation of the different molecules may result in a different manner of GL association with the DNA molecule, parallel with the effect of the pH on the GL-DNA binding, already described (Section 3.1.1). If the alterations in spatial arrangement of DNA, creating a more condensed structure, can enhance the DNA-binding capacity of GL protein, the same could happen with the different conformations that the plasmid DNA can adopt.

Similarly to what occurred with the EMSA performed at different pH values, it was not possible to calculate the KD of the interactions (Annex 1 - Figure A.2).

This assay was performed in triplicate and the concentration of GL needed to retain all plasmid DNA was determined to be between 500 nM and 600 nM for the plasmids extracted from both microorganisms. The presented gels, with protein concentrations ranging from 400 to 600 nM were performed once. More replicates should be done to confirm the difference in the binding affinity of GL to plasmid DNA from *E. coli* or *S. aureus* to ensure these results.

3.1.4 – GL does not oligomerize in the presence of DNA

3.1.4.1 - GL-DNA interaction in SDS-PAGE

The presence of DNA can induce the oligomerization of *S. aureus* proteins involved in biofilm formation, as the case of β-toxin[46] that also has a high pI value, similarly to the GL domain (β-toxin pI >10, GL domain pI 9.58). Since the GL domain is important for biofilm development[38,(I.R. Grilo, unpublished)] and is capable to bind DNA, the oligomerization of GL in the presence of DNA could also occur. To test this hypothesis, EMSA were performed in polyacrylamide gel electrophoresis (PAGE) to monitor the GL protein instead of the DNA molecules. Denaturant conditions (SDS-PAGE) were used to verify if covalent bonds were established between the GL molecules, in the presence of DNA. Bands of higher molecular mass should appear on the gel, if the presence of DNA promoted covalent association of the protein. High concentrations of protein were used to guarantee a good visualization.

No high molecular mass bands were visualized by SDS-PAGE for any of the protein concentrations tested (Figure 3.7), comparing with the control sample without DNA, indicating that the presence of plasmid DNA did not promote covalent association of the GL domain.

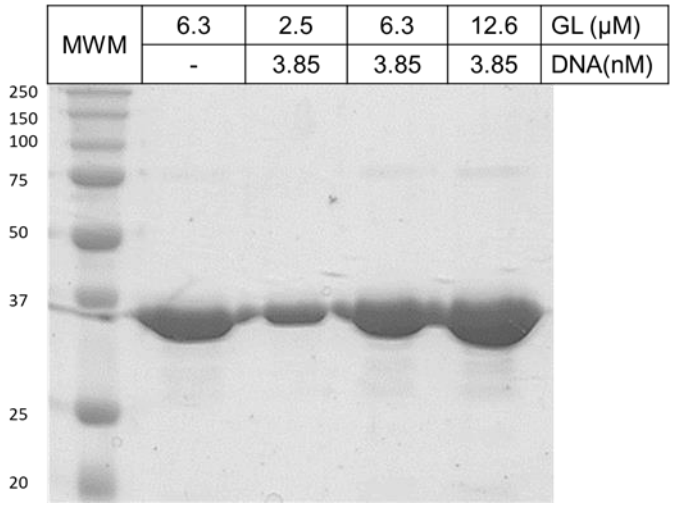

Figure 3.7: SDS-PAGE of GL-DNA interaction showed no covalent binding between different GL molecules. Different concentrations of recombinant GL protein, from 2.5 to 12.6 μM, were incubated with 3.85 nM of pGC1 plasmid DNA (7 Kb) in PBS, pH 7.4. 6.3 μM of GL protein was used for comparison. MWM: Molecular weight marker. The gel was stained with Coomassie Brilliant Blue R-250.

3.1.4.2 - GL-DNA interaction in Acidic native-PAGE

Although the presence of DNA did not promote the oligomerization of the GL domain, another hypothesis was considered. Since the interaction between the two molecules seems to have some electrostatic nature, as suggested through the EMSA at different pH values, non-covalent bonds could also contribute to the binding, affecting the GL protein in its native structure. SDS-PAGE could not be used due to its denaturant properties, so polyacrylamide gels in native conditions were performed. As the assays were performed in non-denaturant conditions, factors such as the pI of the protein and the gel pH were considered. Since the estimated pI of the GL domain is approximately 9.58, an acidic native-PAGE was used to guarantee that the pH of the

gel was sufficiently different from the pI value, ensuring that the GL protein was positively charged. A pH 6.1 McLellan's buffer[125] was used to guarantee the pH-pI separation.

In the absence of DNA, the GL protein migrated at the same rate for all protein concentrations in only one band (Figure 3.8, lanes 1, 2 and 3), suggesting that GL does not oligomerize. Also, size-exclusion chromatography was performed (in collaboration with S. Pauleta, UCIBIO) and only the GL domain corresponding fraction was obtained (30.7± 2 kDa), confirming that the free GL domain does not oligomerize. In the presence of DNA, differences in the migration rate can be observed (Figure 3.8, lanes 4, 5 and 6). For the reaction in which 2.5 µM of GL protein was incubated with 3.85 nM of plasmid DNA, corresponding to a molar ratio of 650:1 (GL:DNA), the mobility of the protein in the gel was lower. This observation indicates a difference in the charge/mass ratio of the protein conditioned by the presence of DNA. However, the number of bands did not change, suggesting that protein oligomerization did not occur in the presence of DNA.

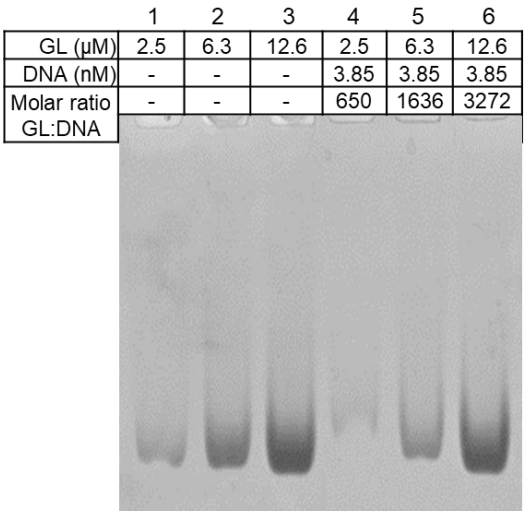

Figure 3.8: EMSA in acidic Native PAGE for different GL concentrations. 3.85 nM of pGC1 plasmid DNA (7 Kb) was incubated with different concentrations of GL in PBS, pH 7.4 (lanes 4, 5, and 6). The same concentrations of purified GL were used for comparison (lanes 1, 2, and 3). The gel was stained with Coomassie Brilliant Blue R-250.

With the evidence that DNA interacts with the GL protein interfering with its migration in a native PAGE, a wide range of pGC1 plasmid DNA concentrations were used for the same protein concentration in acidic native PAGE, to determine at which protein:DNA ratio the interaction delays the migration of GL in the gel (Figure 3.9). Using the same conditions as before, this assay showed that a 1636:1 (GL:DNA) molar ratio was sufficient to delay the migration of the protein in the gel (Figure 3.9, lane 5). Furthermore, for GL:DNA molar ratios below 573:1, no protein bands were detected in the gel.

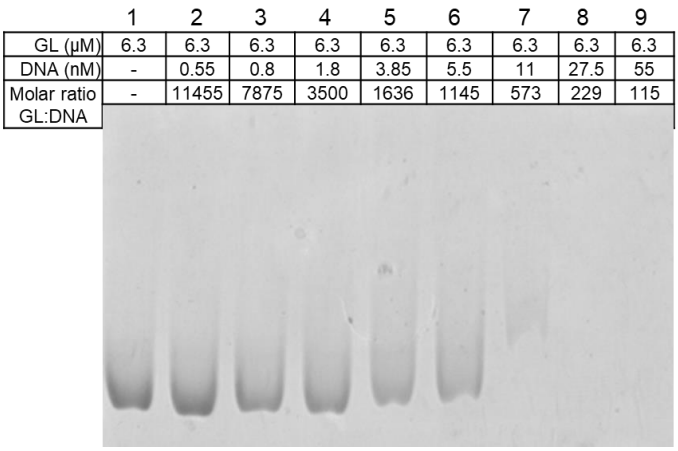

Figure 3.9: EMSA in Acidic Native PAGE for different DNA concentrations. Different amounts of pGC1 plasmid DNA (7 Kb) extracted from *E. coli*, were incubated with 6.3 µM of GL in PBS, pH 7.4 (Lanes 2-9). 6.3 µM of purified GL was used for comparison (Lane 1). The gel was stained with Coomassie Brilliant Blue R-250.

Considering the electrophoresis conditions of the acidic native PAGE performed, the alterations on the protein migration rate could be due to the interaction of GL with the 7 Kb pGC1 plasmid DNA molecules, forming a transient complex with a high molecular weight which does not enter the gel. Furthermore, the electrical current on the native PAGE electrophoresis runs from positive to negative poles, enabling the positively charged protein to enter the gel, but at the same time acting in the opposite way towards the DNA molecules that in this manner are likely not to enter the gel. An additional acidic native PAGE was performed and stained with ethidium bromide to confirm if the DNA was able to enter the gel. In fact, no band was identified, confirming that the DNA was unable to enter in the acidic native PAGE (data not showed). The fact that the GL protein migrates slower in the gel when the GL:DNA ratio is below 1636:1 (GL:DNA) (Figure 3.9, lanes 5, 6 and 7) could be due to the electrostatic forces of the negative charges of the DNA molecule that overlap the electrostatic forces of the electric current, disturbing the normal migration of the protein molecules. When all the protein molecules interact with the DNA, the protein band is no longer visible as presumably the protein does not enter the gel due to its binding to the DNA molecules (Figure 3.9 lanes 8 and 9).

The results obtained in these assays show a molar binding ratio of 573:1 (GL:DNA), which is in agreement with the those obtained in the EMSA with plasmid DNA in agarose gels (Figure 3.6), where the number of GL molecules calculated to retain all *E. coli* plasmid DNA was 545:1.

3.1.5 - Imaging of GL-DNA interaction by atomic force microscopy

The GL-DNA interaction has been previously demonstrated[96] and further characterized in this study, mainly using EMSA. Atomic force microscopy (AFM) has been described as a useful technique to characterize biological interactions, namely protein-DNA interactions[137]. Images of GL incubated with pGC1 plasmid DNA were obtained using AFM and were compared with negative controls, namely images of free pGC1 plasmid DNA and the same plasmid DNA incubated with the catalytic AM domain of Atl, a protein without the capacity to bind DNA[96].

For these assays, the molar ratio of the protein:DNA interaction was 2295:1 (GL:DNA), approximately four times higher than the 573:1 (GL:DNA) molar ratio corresponding to the total interaction obtained in the EMSAs to plasmid DNA. This ratio was chosen to ensure that all DNA molecules deposited on the mica interacted with the GL protein, so that images could reflect the GL-DNA interaction.

In the AFM images of free DNA (Figure 3.10-A), the plasmid molecules deposited on the solid support were observed to be in supercoiled topology, as they were similar to already described images of supercoiled DNA[138,139]. In the close-up image, DNA strings are visible as well as areas with more intense signal, due to higher degree of supercoiling (Figure 3.10-B). Circle-shaped particles appear, likely corresponding to proteins naturally associated with the plasmid molecules or to non-biological material contaminations, which are not related to the sample and were not removed by the washing step. This image is essential to compare with the assay of the GL-DNA interaction, in order to understand how the interaction occurs and discard artefacts that could happen during the imaging process, as well as molecular interactions independent from GL.

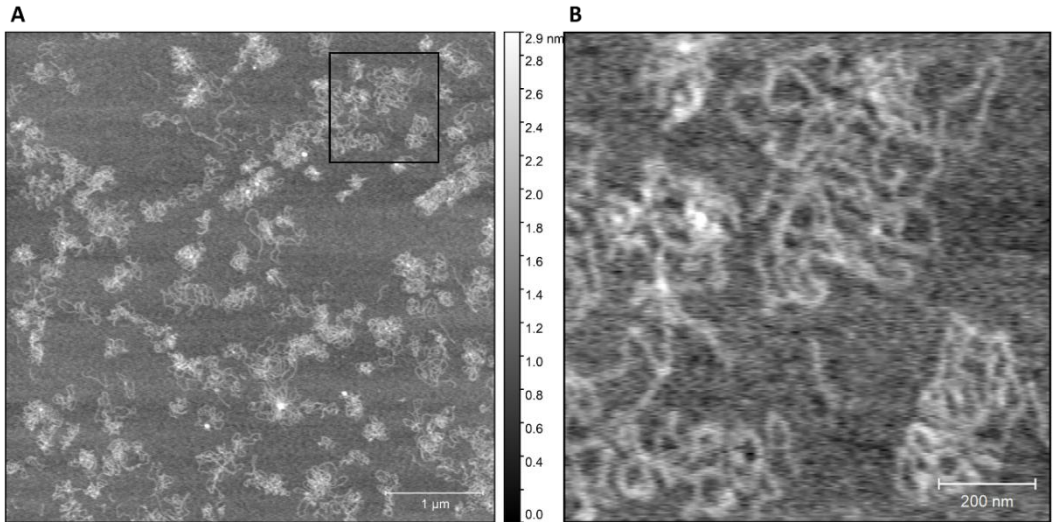

Figure 3.10: AFM topographic image of pGC1 plasmid DNA. (A) 5x5 µm image and (B) a close-up of a 1x1 µm area. To remove outliers, a root mean squared (RMS) value of 4.00 was used.

Upon plasmid incubation with GL, small circle-shaped structures were visible, mainly concentrated in regions of higher DNA supercoiling (Figure 3.11-A). These structures most probably correspond to GL protein since they were very similar to the structures identified in an image of free GL protein that was performed as a control (Figure 3.12). The GL protein concentration used was the same as for the GL-plasmid DNA image. Low amount of protein was detected possibly due to the low affinity of the protein to the surface and subsequent wash step, performed before imaging. The structure of TATA-box binding protein (Tbp, 38 kDa) which has a molecular mass similar to the GL protein, was previously studied by AFM[140]. The images obtained for Tbp protein reflect a circle-shaped structure of a similar size to what was observed for the GL protein. In the close-up image of the GL-DNA interaction (Figure 3.11-B), the signal from the GL protein had a much higher intensity than in the image obtained with the free GL protein (Figure

3.12), possibly caused by the position of the protein molecules above the plasmid DNA molecules, as this image is topographic and brighter signals correspond to more elevated structures.

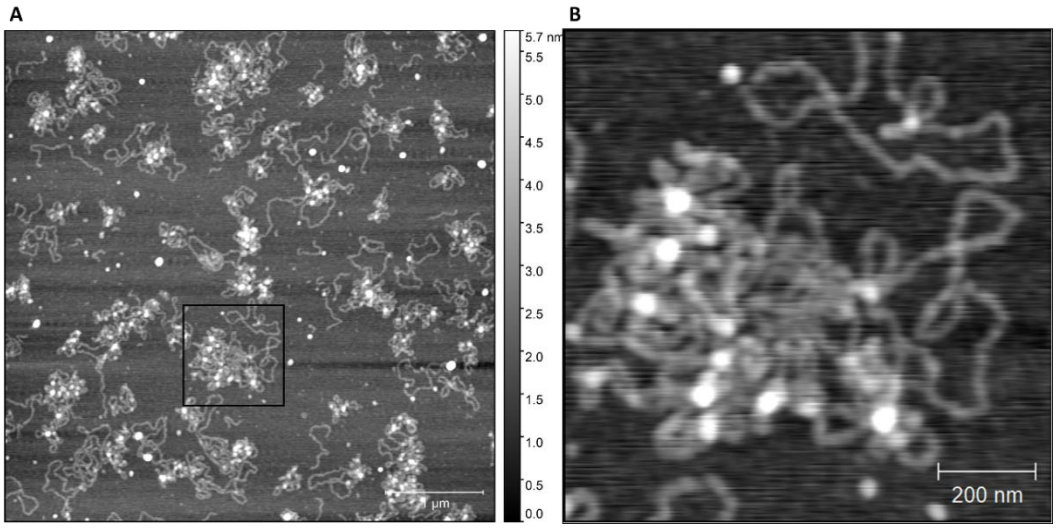

Figure 3.11: AFM topographic image of pGC1 plasmid DNA and recombinant GL protein. (A) 5x5 µm image and (B) a close-up of a 1x1 µm to a detail of one of the aggregates between the two molecules are shown. To remove outliers, a RMS value of 4.00 was used in all images.

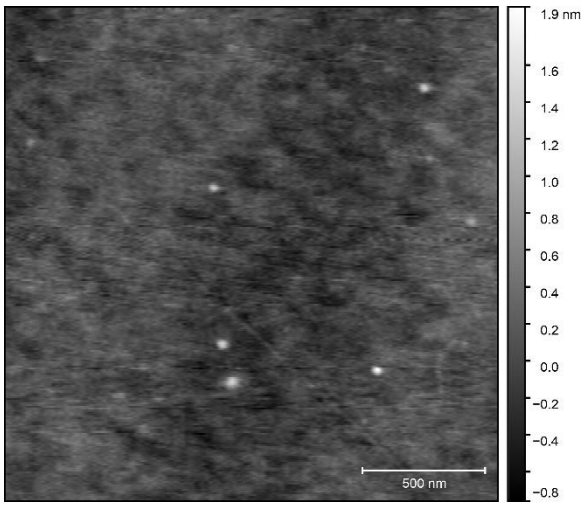

Figure 3.12: Topographic image of recombinant GL protein. 2x2 µm image. To remove outliers, a root mean squared (RMS) value of 4.00 was used.

In the case of the assay of pGC1 plasmid DNA with the AM domain, the resulting image was similar to the image of free plasmid DNA (Figure 3.13). The supercoiled DNA topology was visible, but the circle-shaped structures were not present, which indicates the absence of the AM-DNA association, as AM protein must have been removed during the wash step of the procedure. Some rare brighter areas could be seen but, as in the free DNA image, these should correspond to other proteins that naturally are associated to DNA or to non-biological material contamination.

Taken together, AFM technology allowed to visualize the structure of the complex formed by GL protein and plasmid DNA, as well as the spatial arrangement of both molecules upon association.

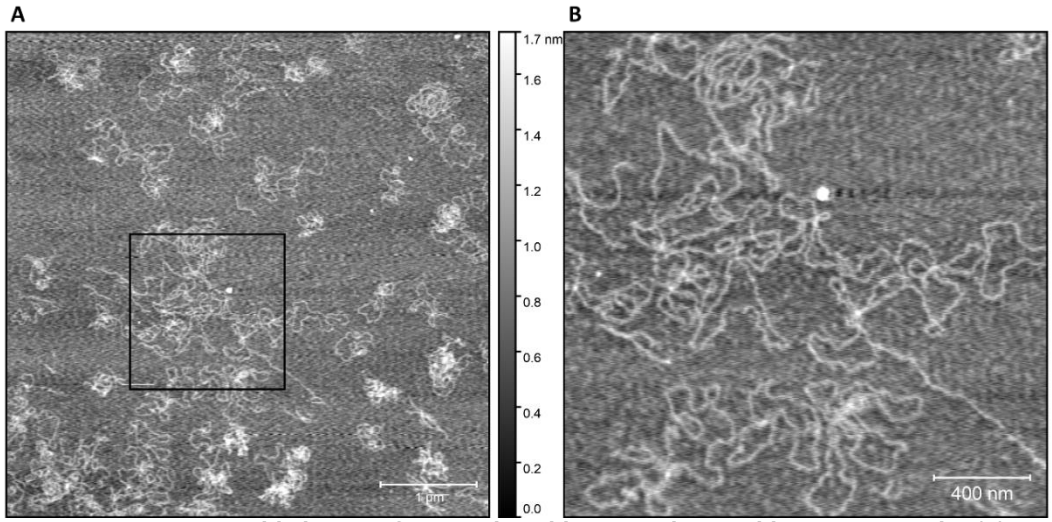

Figure 3.13: AFM topographic image of pGC1 plasmid DNA and recombinant AM protein. (A) 5x5 µm image and (B) a close-up of a 2x2 µm to a detail of one of the aggregates between the two molecules are shown. To remove outliers, a RMS value of 4.00 was used in all images.

3.1.6 – Hydrolytic activity of GL and R_3GL proteins

Atl protein is the major *S. aureus* autolysin and therefore it is important to determine if the peptidoglycan hydrolytic activity of GL is affected by its interaction with DNA. The recombinant proteins GL and R_3GL were used to perform hydrolytic assays against heat-inactivated cells from different microorganisms. The heat inactivated cells integrity was verified through optical microscopy (data not shown). The optimum pH for GL hydrolytic activity was determined beforehand with *M. luteus* heat-inactivated cells, since the capacity of GL to hydrolyse the cell wall of this microorganism was already described[90].

For both GL and R_3GL, lower pH values were found to enhance the hydrolytic activity, increasing the percentage of hydrolysed cells in approximately 20%, comparing the highest (8.07) and the lowest (5.85) pH values (Figure 3.14). Sodium phosphate buffer (50 mM), pH 6.08 was chosen for the subsequent hydrolytic activity assays due to a higher activity of the GL protein.

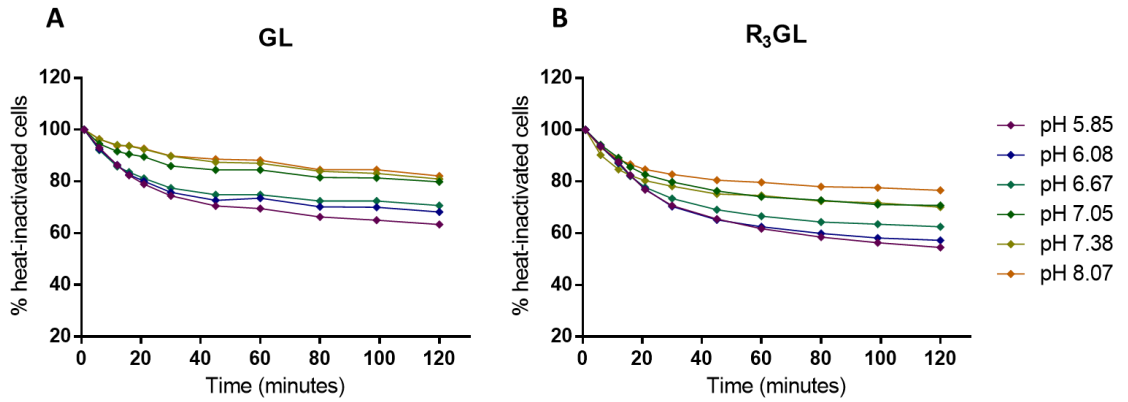

Figure 3.14: Hydrolytic activity of GL and R_3GL recombinant proteins at different pH values. 10 µg/ml of each protein was added to heat inactivated M. luteus cells and hydrolysis was followed by measuring the decrease in OD_{600nm} for 120 minutes. Sodium phosphate buffer 50 mM was used at different pH values from 5.85 up to 8.07.

Nine different microorganisms were used to test the GL hydrolytic activity in the presence of added low molecular salmon sperm DNA (ssDNA). Mulcahy *et al*. 2008, had shown that 1% (w/v) of extracellular DNA inhibits the bacterial growth in *S. aureus* and lower concentrations can be consider as physiological[141]. Following that evidence, the ssDNA concentrations were used up until this value (10 mg/ml corresponds to 1% (w/v)).

The hydrolytic activity of both GL and R_3GL proteins was monitored for 120 minutes, and the final results at 120 minutes are represented for comparison (Figures 3.15 to 3.23). In these assays, the effect of ssDNA added to heat-inactivated cells of the different microorganisms was also tested. These results are also summarized in Annex 2 (Tables A.1, A.2 and A.3).

As previously described [90], *M. luteus* cell wall is susceptible to hydrolysis by either GL or R_3GL proteins (Figure 3.15-A and B). GL and R_3GL proteins hydrolysed approximately 34% and 40% of the heat-inactivated cells available, after 120 min of incubation, respectively. As ssDNA was added, the hydrolytic capacity decreased to less than 15%, for both proteins, for the lowest ssDNA concentration used (0.5 mg/ml). This inhibitory trend continued with the increase of ssDNA concentration, and when 10 mg/ml of ssDNA was added the hydrolytic capacity of the proteins was only around 5%, (Figure 3.15-C).

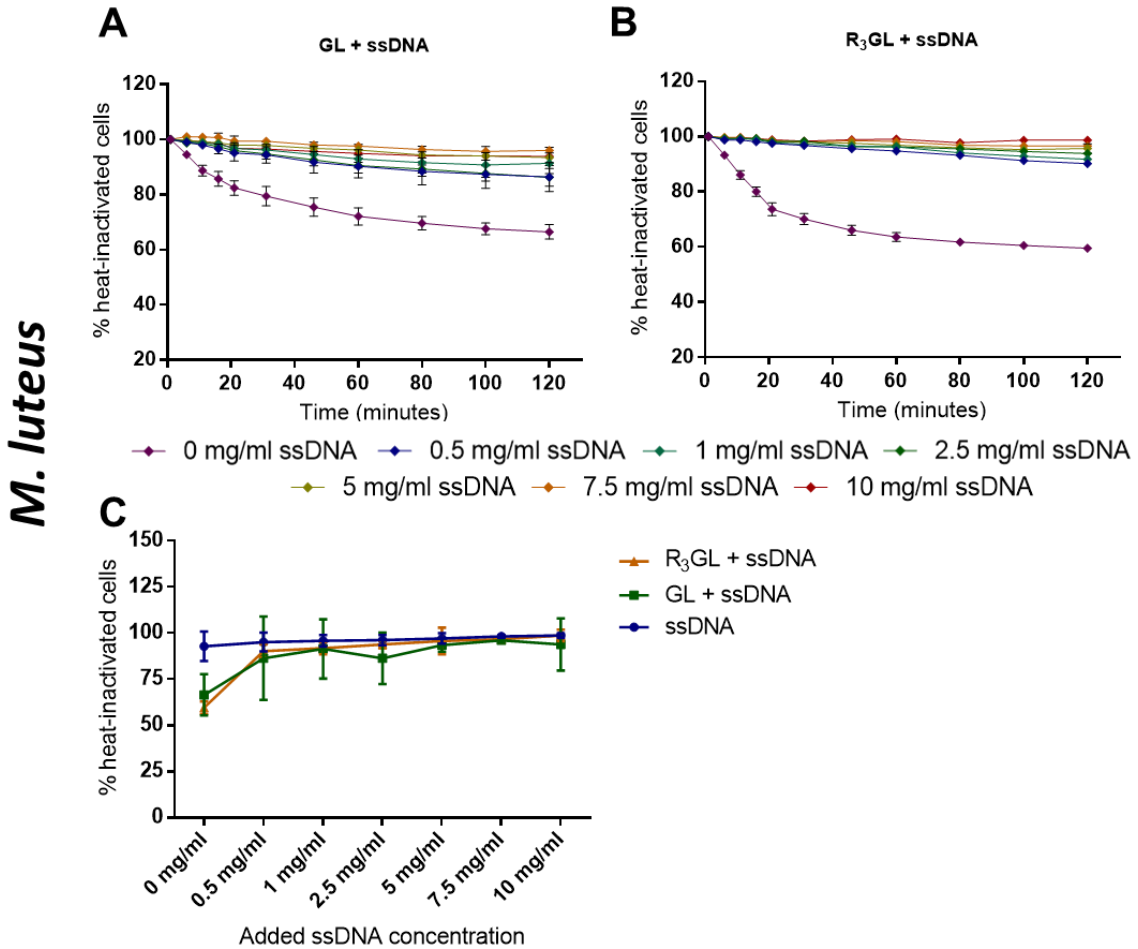

Figure 3.15: Hydrolytic activity of recombinant GL and R_3GL proteins with *M. luteus* heat-inactivated cells. 10 µg/ml of protein was added to heat-inactivated cells and different concentrations of low molecular salmon sperm DNA (ssDNA) were used. Hydrolytic activity was followed by measuring the decrease in OD_{600nm} for 120 minutes. The results are an average of three biological replicates, shown in percentage, calculated by the difference in OD_{600nm} at each time-point, compared with the initial OD_{600nm}. A: Hydrolytic

activity of recombinant GL (Mean ± the standard error of the mean, SEM). B: Hydrolytic activity of recombinant R_3GL (Mean ± SEM). C: Percentage of heat-inactivated cells at the end of the assay (120 minutes) (Mean ± CI 95%). Blue: heat inactivated cells and ssDNA, Green: heat inactivated cells and GL+ssDNA, and Orange: heat inactivated cells and R_3GL+ssDNA.

Oshida *et al.* showed that the GL domain did not have the capacity to hydrolyse *S. aureus* heat-inactivated cells[90], and the same was verified in this assay, at pH 6.08 (Figure 3.16). The presence of ssDNA, did not improve the hydrolytic activity of GL, but in the case of R_3GL, the addition of ssDNA at low concentrations (0.5 mg/ml to 2.5 mg/ml) seemed to slightly enhance its hydrolytic activity against *S. aureus* cells, but without statistical significance (Figure 3.16-C).

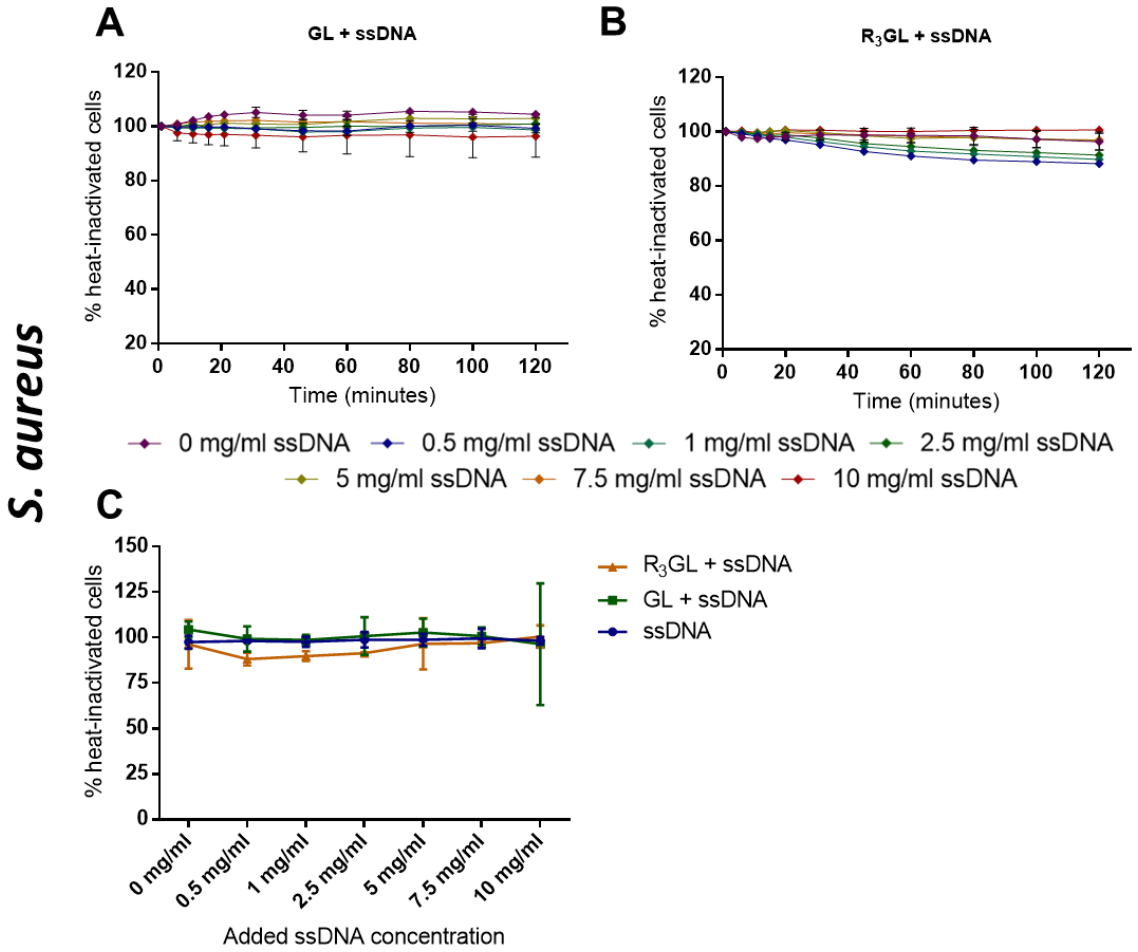

Figure 3.16: Hydrolytic activity of recombinant GL and R_3GL proteins with *S. aureus* heat-inactivated cells. 10 µg/ml of protein was added to heat-inactivated cells and different concentrations of low molecular salmon sperm DNA (ssDNA) were used. Hydrolysis activity was followed by measuring the decrease in OD_{600nm} for 120 minutes. The results are an average of three biological replicates, shown in percentage, calculated by the difference in OD_{600nm} at each timepoint, compared with the initial OD_{600nm}. A: Hydrolytic activity of recombinant GL (Mean ± the standard error of the mean, SEM). B: Hydrolytic activity of recombinant R^3GL (Mean ± SEM). C: Percentage of heat-inactivated cells at the end of the assay (120 minutes) (Mean ± CI 95%). Blue: heat inactivated cells and ssDNA, Green: heat inactivated cells and GL+ssDNA, and Orange: heat inactivated cells and R_3GL+ssDNA.

S. epidermidis heat-inactivated cells were also tested and in this case the GL protein showed low hydrolytic activity, as it reduced the cell percentage by only 10% (Figure 3.17-A). Upon addition of ssDNA, no major alterations were visualized; the percentage of hydrolysed heat-

inactivated cells oscillated between 11% and 4%. In the case of R_3GL, the hydrolytic activity was slightly higher, reaching 18% of heat-inactivated cells at the end of 120 minutes, while the percentage of hydrolysed heat-inactivated cells remained between 16% and 10% with the addition of ssDNA (Figure 3.17-B). All reported differences did not show statistical significance (Figure 3.17-C).

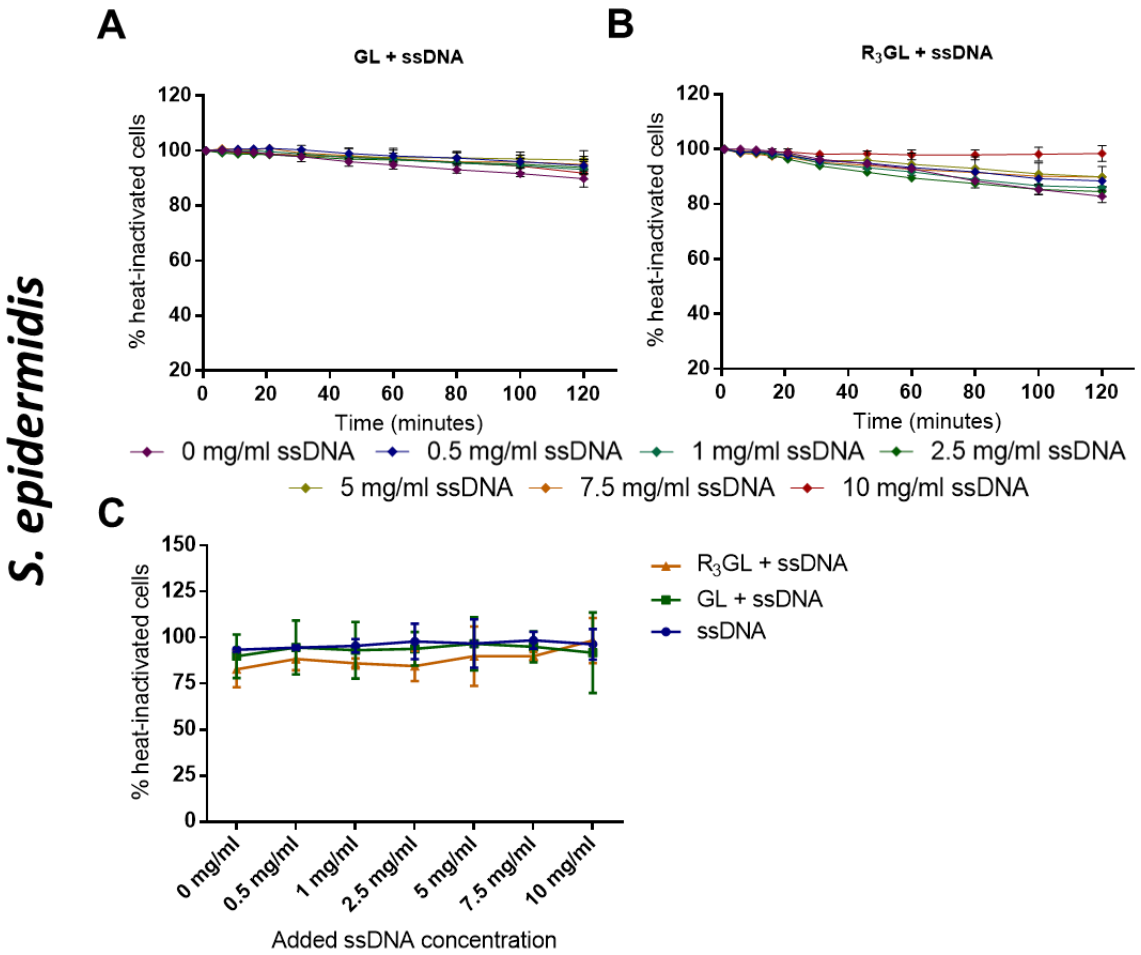

Figure 3.17: Hydrolytic activity of recombinant GL and R_3GL proteins with *S. epidermidis* heat-inactivated cells. 10 µg/ml of protein was added to heat-inactivated cells and different concentrations of low molecular salmon sperm DNA (ssDNA) were used. Hydrolysis activity was followed by measuring the decrease in OD_{600nm} for 120 minutes. The results are an average of three biological replicates, shown in percentage, calculated by the difference in OD_{600nm} at each timepoint, compared with the initial OD_{600nm}. A: Hydrolytic activity of recombinant GL (Mean ± the standard error of the mean, SEM). B: Hydrolytic activity of recombinant R_3GL (Mean ± SEM). C: Percentage of heat-inactivated cells at the end of the assay (120 minutes) (Mean ± CI 95%). Blue: heat inactivated cells and ssDNA, Green: heat inactivated cells and GL+ssDNA, and Orange: heat inactivated cells and R_3GL+ssDNA.

S. agalactiae was one of the less susceptible species to GL and R_3GL hydrolytic activity. For both proteins, the percentage of heat-inactivated cells remained close to the initial value, as well as in the presence of different ssDNA concentrations (Figure 3.18-A and B). No statistical differences were detected between the results of all conditions tested (Figure 3.18-C)

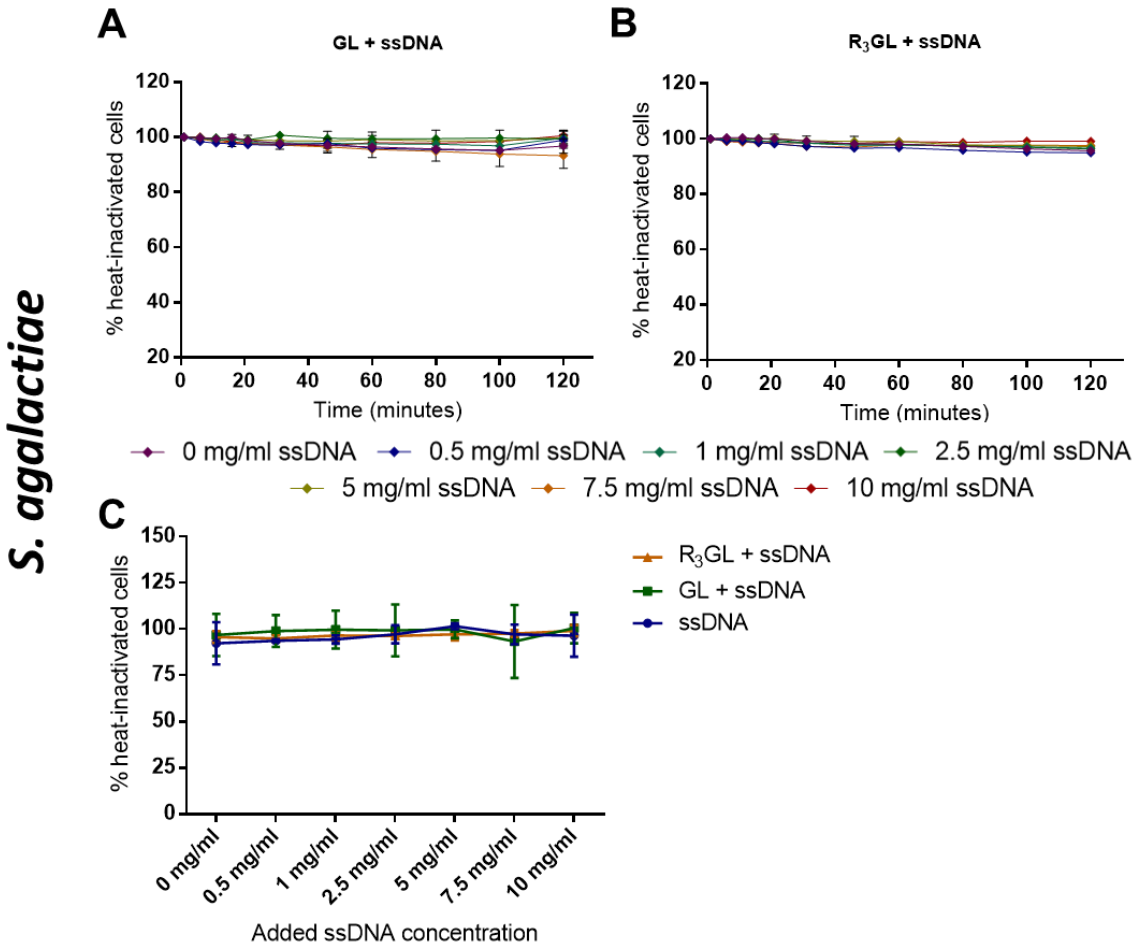

Figure 3.18: Hydrolytic activity of recombinant GL and R$_3$GL proteins with *S. agalactiae* heat-inactivated cells. 10 µg/ml of protein was added to heat-inactivated cells and different concentrations of low molecular salmon sperm DNA (ssDNA) were used. Hydrolysis activity was followed by measuring the decrease in OD_{600nm} for 120 minutes. The results are an average of three biological replicates, shown in percentage, calculated by the difference in OD_{600nm} at each timepoint, compared with the initial OD_{600nm}. A: Hydrolytic activity of recombinant GL (Mean ± the standard error of the mean, SEM). B: Hydrolytic activity of recombinant R$_3$GL (Mean ± SEM). C: Percentage of heat-inactivated cells at the end of the assay (120 minutes) (Mean ± CI 95%). Blue: heat inactivated cells and ssDNA, Green: heat inactivated cells and GL+ssDNA, and Orange: heat inactivated cells and R$_3$GL+ssDNA.

The addition of GL or R$_3$GL proteins led to hydrolysis of heat-inactivated cells of *S. pyogenes* (Figure 3.19). In particular, the R$_3$GL protein led to a 12% decrease of heat-inactivated cells (Figure 3.19-B). Upon addition of ssDNA, both proteins partially lost their hydrolytic activity, for all concentrations tested. Despite the differences between the percentages obtained for all the conditions tested, those did not present statistical significance (Figure 3.19-C).

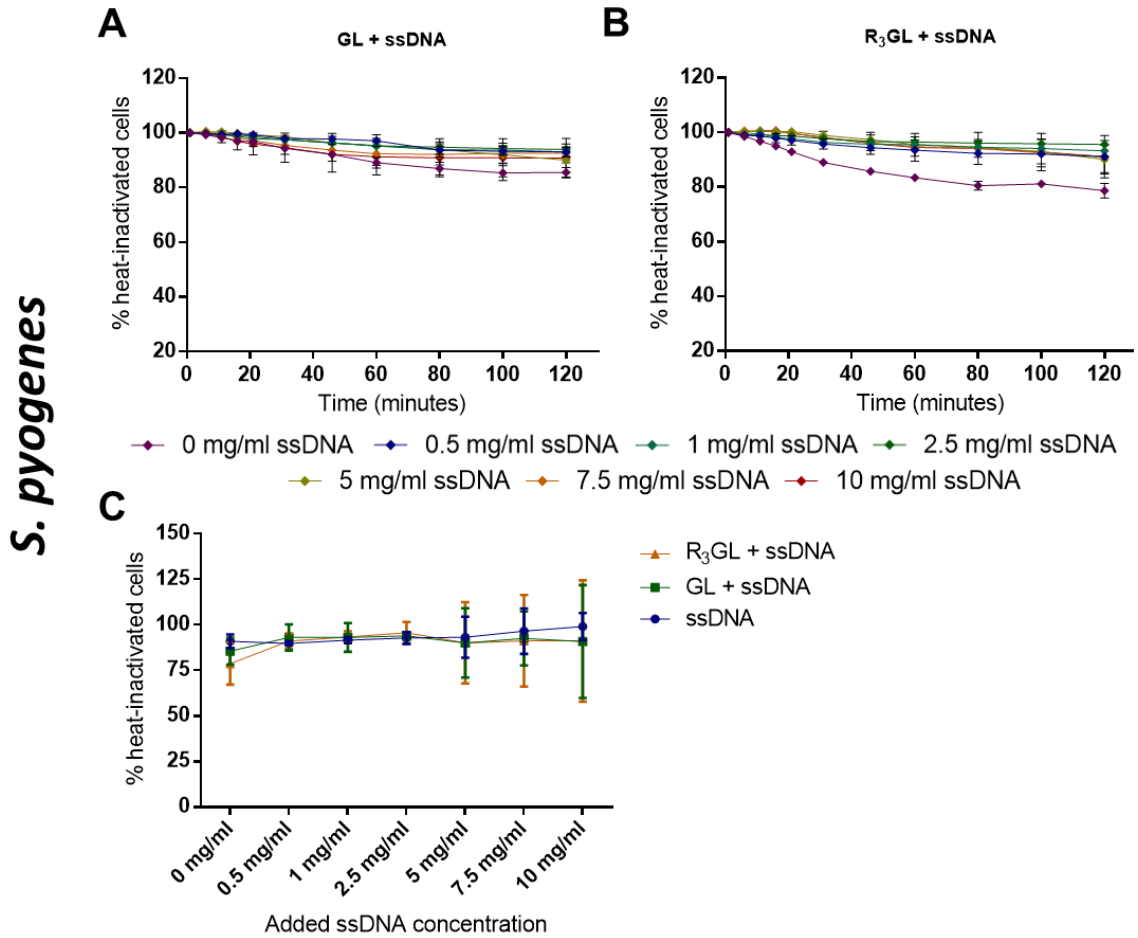

Figure 3.19: Hydrolytic activity of recombinant GL and R_3GL proteins with *S. pyogenes* heat-inactivated cells. 10 µg/ml of protein was added to heat-inactivated cells and different concentrations of low molecular salmon sperm DNA (ssDNA) were used. Hydrolysis activity was followed by measuring the decrease in OD_{600nm} for 120 minutes. The results are an average of three biological replicates, shown in percentage, calculated by the difference in OD_{600nm} at each timepoint, compared with the initial OD_{600nm}. A: Hydrolytic activity of recombinant GL (Mean ± the standard error of the mean, SEM). B: Hydrolytic activity of recombinant R_3GL (Mean ± SEM). C: Percentage of heat-inactivated cells at the end of the assay (120 minutes) (Mean ± CI 95%). Blue: heat inactivated cells and ssDNA, Green: heat inactivated cells and GL+ssDNA, and Orange: heat inactivated cells and R_3GL+ssDNA.

E. faecalis heat-inactivated cells were not hydrolysed by either GL or R_3GL (Figure 3.20-A and B). Upon addition of ssDNA, no major differences could be seen in any concentration tested for both GL and R_3GL proteins. This species seemed to be one of the less affected by the presence of the GL and R_3GL proteins or ssDNA.

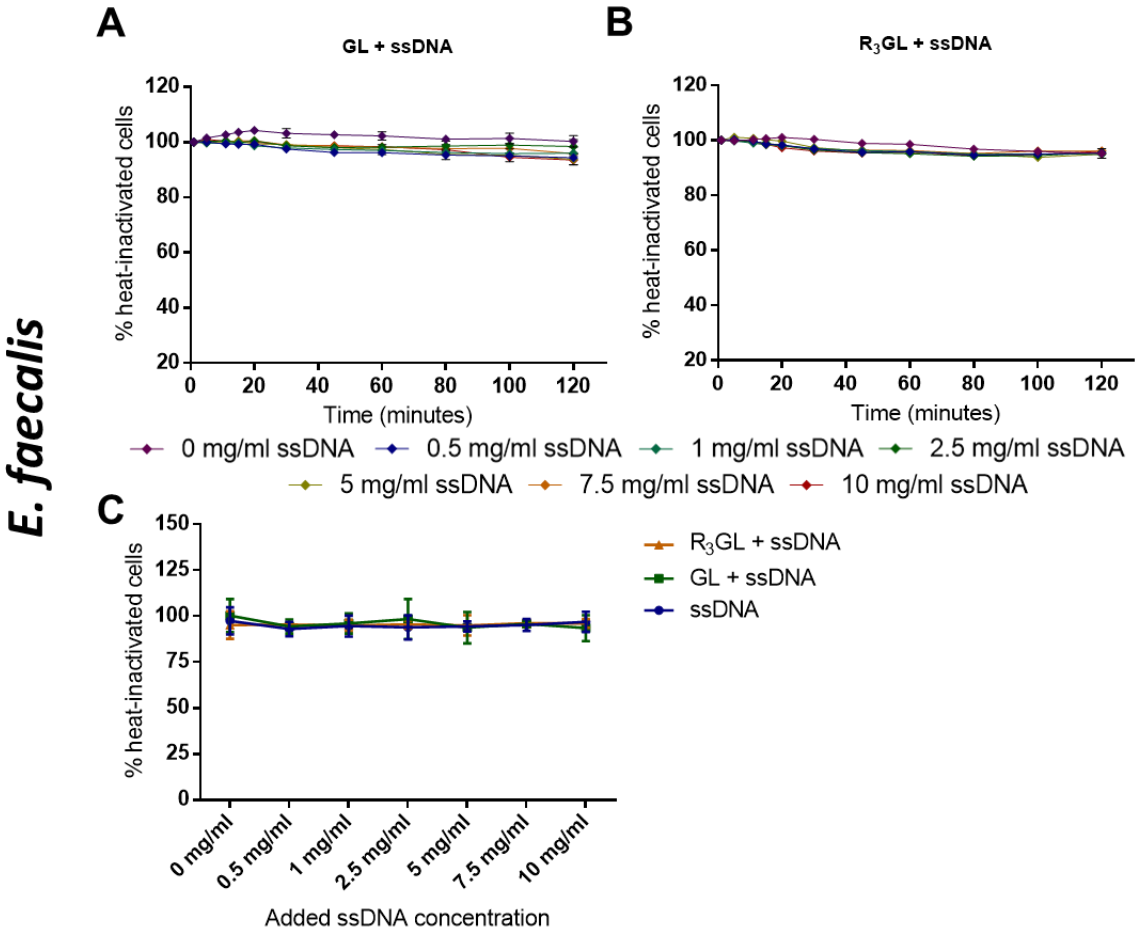

Figure 3.20: Hydrolytic activity of recombinant GL and R_3GL proteins with *E. faecalis* heat-inactivated cells. 10 µg/ml of protein was added to heat-inactivated cells and different concentrations of low molecular salmon sperm DNA (ssDNA) were used. Hydrolysis activity was followed by measuring the decrease in OD_{600nm} for 120 minutes. The results are an average of three biological replicates, shown in percentage, calculated by the difference in OD_{600nm} at each timepoint, compared with the initial OD_{600nm}. A: Hydrolytic activity of recombinant GL (Mean ± the standard error of the mean, SEM). B: Hydrolytic activity of recombinant R_3GL (Mean ± SEM). C: Percentage of heat-inactivated cells at the end of the assay (120 minutes) (Mean ± CI 95%). Blue: heat inactivated cells and ssDNA, Green: heat inactivated cells and GL+ssDNA, and Orange: heat inactivated cells and R_3GL+ssDNA.

Gram-negative bacteria were also tested. These species' heat-inactivated cells were most susceptible to hydrolysis by both proteins tested than Gram-positive species. For *E. coli*, the presence of GL or R_3GL reduced the percentage of heat-inactivated cells by approximately 53% (Figure 3.21-C). Upon addition of ssDNA, the hydrolytic activity of both proteins was severely decreased, as for the lowest DNA concentration (0.5 mg/ml), only 12% of heat inactivated cells were hydrolysed and this percentage continued to decrease with the increase of ssDNA concentration (Figure 3.21-A and B).

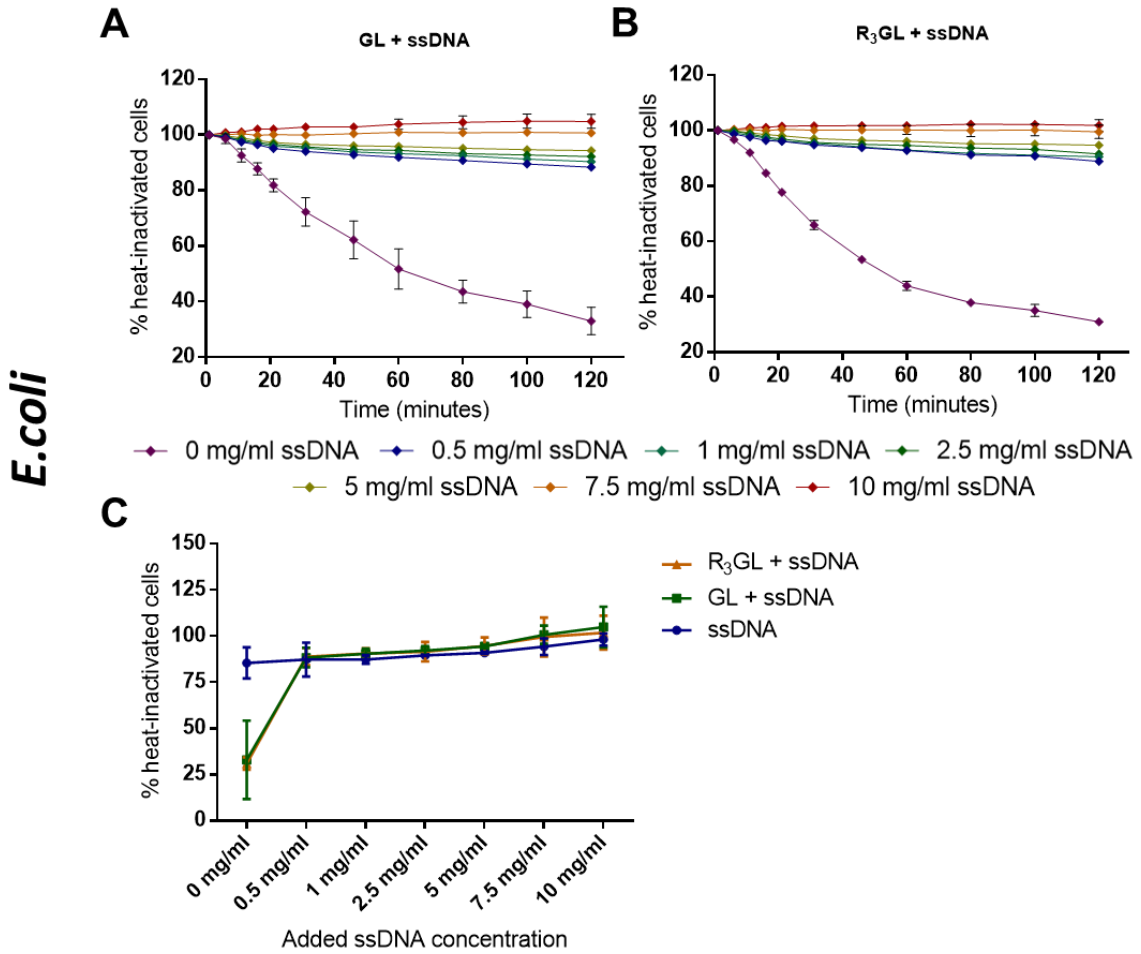

Figure 3.21: Hydrolytic activity of recombinant GL and R_3GL proteins with *E. coli* heat-inactivated cells. 10 µg/ml of protein was added to heat-inactivated cells and different concentrations of low molecular salmon sperm DNA (ssDNA) were used. Hydrolysis activity was followed by measuring the decrease in OD_{600nm} for 120 minutes. The results are an average of three biological replicates, shown in percentage, calculated by the difference in OD_{600nm} at each timepoint, compared with the initial OD_{600nm}. A: Hydrolytic activity of recombinant GL (Mean ± the standard error of the mean, SEM). B: Hydrolytic activity of recombinant R_3GL (Mean ± SEM). C: Percentage of heat-inactivated cells at the end of the assay (120 minutes) (Mean ± CI 95%). Blue: heat inactivated cells and ssDNA, Green: heat inactivated cells and GL+ssDNA, and Orange: heat inactivated cells and R_3GL+ssDNA.

In the presence of GL or R_3GL, the percentage of hydrolysed heat-inactivated cells from *C. marina* was very high, reaching 59% and 65%, respectively (Figure 3.22-A and B). The major decrease in the percentage of heat-inactivated cells started only after 20 minutes of incubation for both proteins. The addition of ssDNA contributed to a decrease in the GL and R_3GL hydrolytic activity, leading to a percentage of heat-inactivated cells of approximately 14% at the end of the assay in the presence of 0.5 mg/ml ssDNA. As the ssDNA concentration increased, so did the inhibition of hydrolytic activity of GL and R_3GL.

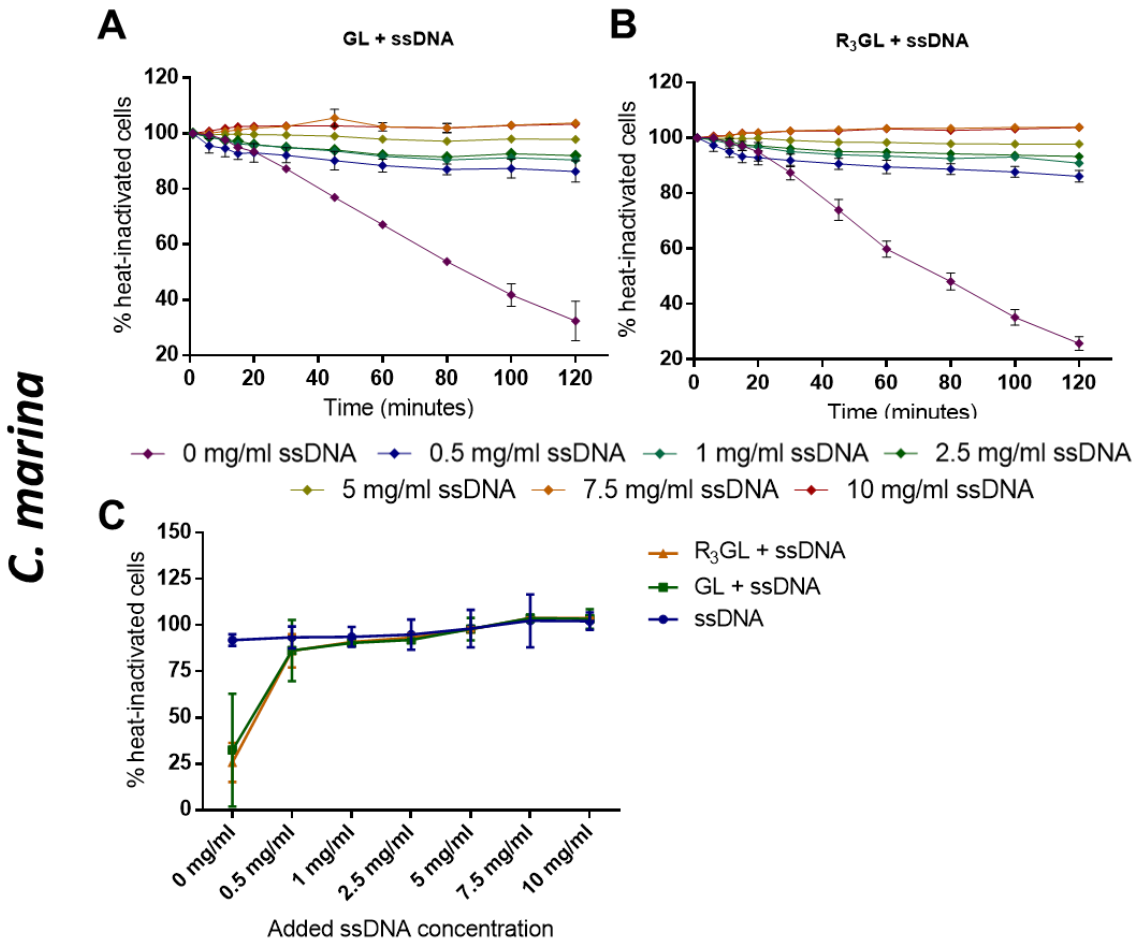

Figure 3.22: Hydrolytic activity of recombinant GL and R_3GL proteins with *C. marina* heat-inactivated cells. 10 µg/ml of protein was added to heat-inactivated cells and different concentrations of low molecular salmon sperm DNA (ssDNA) were used. Hydrolysis activity was followed by measuring the decrease in OD_{600nm} for 120 minutes. The results are an average of three biological replicates, shown in percentage, calculated by the difference in OD_{600nm} at each timepoint, compared with the initial OD_{600nm}. A: Hydrolytic activity of recombinant GL (Mean ± the standard error of the mean, SEM). B: Hydrolytic activity of recombinant R_3GL (Mean ± SEM). C: Percentage of heat-inactivated cells at the end of the assay (120 minutes) (Mean ± CI 95%). Blue: heat inactivated cells and ssDNA, Green: heat inactivated cells and GL+ssDNA, and Orange: heat inactivated cells and R_3GL+ssDNA.

M. hydrocarbonoclasticus heat-inactivated cells could be hydrolysed by both the GL protein and by the R_3GL protein, with a reduction of 30% and 42% of the heat-inactivated cells, respectively (Figure 3.23-C). In contrast to what occurred with *C. marina* cells, the major decrease in percentage of heat-inactivated cells occurred during the first 20 minutes of the assay. With the addition of ssDNA, the hydrolytic activity dropped to values below 10% of hydrolysed heat-inactivated cells and continued with the increase of ssDNA concentration as occurred with *E. coli* and *C. marina* heat-inactivated cells (Figure 3.23-A and B).

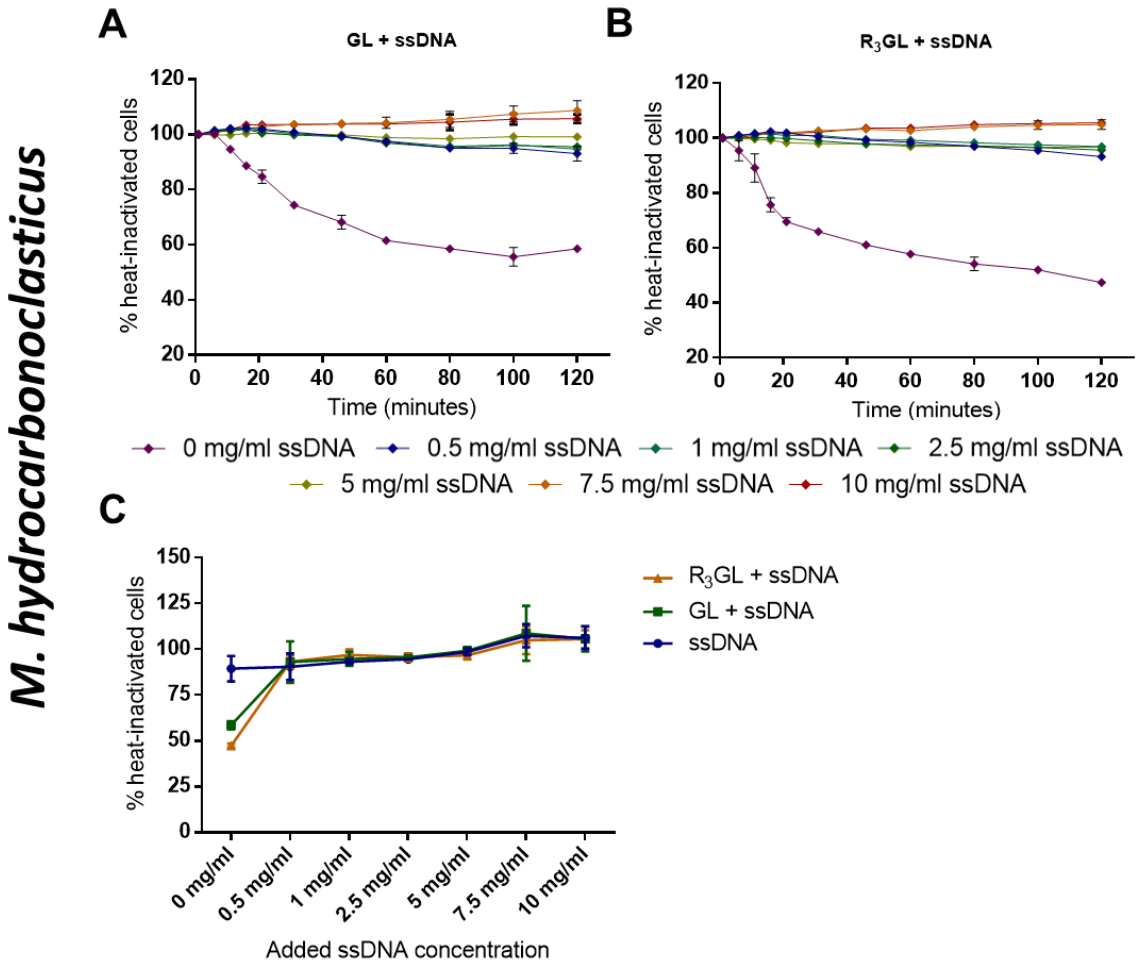

Figure 3.23: Hydrolytic activity of recombinant GL and R_3GL proteins with *M. hydrocarbonoclasticus* heat-inactivated cells. 10 µg/ml of protein was added to heat-inactivated cells and different concentrations of low molecular salmon sperm DNA (ssDNA) were used. Hydrolysis activity was followed by measuring the decrease in OD_{600nm} for 120 minutes. The results are an average of three biological replicates, shown in percentage, calculated by the difference in OD_{600nm} at each timepoint, compared with the initial OD_{600nm}. A: Hydrolytic activity of recombinant GL (Mean ± the standard error of the mean, SEM). B: Hydrolytic activity of recombinant R_3GL (Mean ± SEM). C: Percentage of heat-inactivated cells at the end of the assay (120 minutes) (Mean ± CI 95%). Blue: heat inactivated cells and ssDNA, Green: heat inactivated cells and GL+ssDNA, and Orange: heat inactivated cells and R_3GL+ssDNA.

Overall, the heat-inactivated cells most affected by the presence of GL and R_3GL proteins were *C. marina*, *E. coli*, *M. hydrocarbonoclasticus* and *M. luteus* and the least affected were *S. agalactiae*, *S. pyogenes* and *E. faecalis* (Table 3.2).

Table 3.2: Summarized activity of GL and R_3GL proteins against heat inactivated cells of different species. Symbols represent the hydrolytic activity in presence of ssDNA comparing with the activity of the protein: ↑ - increase in the hydrolytic activity; ↓- decrease in the hydrolytic activity; = - hydrolytic activity not affected.

Bacterial species	Protein	Without ssDNA	With 0.5 mg/ml ssDNA	With 10 mg/ml ssDNA
M. luteus	GL	Yes	↑	↑
	R_3GL	Yes	↑	↑
S. aureus	GL	No	=	=
	R_3GL	No	↓	↑
S. epidermidis	GL	No	=	=
	R_3GL	Yes	=	=
S. agalactiae	GL	No	=	=
	R_3GL	No	=	=
S. pyogenes	GL	No	=	=
	R_3GL	No	=	=
E. faecalis	GL	No	=	=
	R_3GL	No	=	=
E. coli	GL	Yes	↑	↑
	R_3GL	Yes	↑	↑
C. marina	GL	Yes	↑	↑
	R_3GL	Yes	↑	↑
M. hydrocarbonoclasticus	GL	Yes	↑	↑
	R_3GL	Yes	↑	↑

The different hydrolytic activities of GL and R_3GL proteins towards gram-positive bacteria revealed different scenarios between the microorganisms. The GL protein showed hydrolytic activity, against the heat inactivated cells of *M. luteus*, but the hydrolytic activity was lost when ssDNA was added. In case of the other species, GL protein did not show hydrolytic activity and it continued to be unaffected in the presence of ssDNA. The R_3GL protein showed similar hydrolytic activity compared with GL protein towards all gram-positive heat inactivated cells, differing only on the percentage of hydrolyzed cells but without alterations on the activity pattern towards all the species.

Gram-positive bacteria have a greater variation in the composition and structure of peptidoglycan[79], a fact that may help to understand the differences in the hydrolytic activity of the GL and R_3GL proteins towards the different heat-inactivated cells. According to the literature[113], the lower degree of cross-linking in *M. luteus* peptidoglycan (around 20%[142]) facilitates the hydrolytic activity of the GL domain, compared with *S. aureus* peptidoglycan that has a higher cross-linking degree (up to 90%[143]). This may indicate that the GL domain hydrolyses the β-1,4-glycosidic bond between GlcNAc and MurNAc only if the peptidoglycan was already pre-digested by AM domain, since AM has hydrolytic activity against *S. aureus* heat inactivated cells, contrarily to GL[90,96]. The cross-linking degree of the peptidoglycan of the bacteria used in this study and its peptidoglycan types are presented in the Table A.4 of Annex 2. Despite the differences between strains of the same species, in general, most of the gram-positive bacteria have a high degree of peptidoglycan cross-linking, being *M. luteus* the more evident exception. The degree of peptidoglycan cross-linking can influence the hydrolytic capacity of peptidoglycan hydrolases, but this activity is also influenced by the length and composition of the cross-bridge and the other components of the cell wall[79].

All gram-negative bacteria tested were hydrolyzed by GL or R_3GL. Along with the heat inactivated cells of *M. luteus*, the heat inactivated cells of *E. coli* and the other gram-negative bacteria tested were hydrolysed to a higher degree by GL and R_3GL (above 30% for *M. hydrocarbonoclasticus* and above 60% for *E. coli* and *C. marina*). In the presence of ssDNA the hydrolytic activity against heat inactivated cells from all gram-negative bacteria was gradually lost, as happened with the heat inactivated cells from gram-positive bacteria. Contrarily to the gram-positive bacteria, the peptidoglycan of gram-negative bacteria shows a low degree of cross-linking[79,112], which could indicate that a higher degree of cross-linking can hinder the peptidoglycan hydrolytic activity of GL, by for example, not allowing the protein to reach its substrate. The *E. coli* peptidoglycan is structurally different when compared with gram-positive bacteria[112], and has a low cross-linking degree, approximately 20%[144].

The overall loss of hydrolytic activity of GL and R_3GL proteins against the studied heat inactivated cells in the presence of ssDNA can be caused by the interaction of the protein with the DNA molecules, inhibiting the hydrolytic action of the GL domain against the heat-inactivated cells. Only two exceptions were obtained: the increase of R_3GL hydrolytic activity against *S. epidermidis* without ssDNA; and the increase of R_3GL hydrolytic activity against *S. aureus* with ssDNA below 2.5 mg/ml concentration. In both cases, the differences in the percentage of the respective heat inactivated cells did not have statistical significance. These slight differences can be explained by a possible higher affinity of the R_3 to the staphylococcal lipoteichoic acids than to the DNA molecules, anchoring the GL protein to the cell wall in a way that is more available to the reach the β-1,4- glycosidic bond, than in the absence of the repeat region. Is important to retain that the repeat regions do not have lytic activity[39] so it does not contribute directly to a higher hydrolytic activity.

3.2 - Impact of GL-DNA association in *S. aureus* physiology

3.2.1 – Effect of Atl on *S. aureus* growth profile

Since the Atl protein is essential for cell growth and separation, we aimed to determine the impact of the GL-DNA association on the growth profile of *S. aureus*. For this purpose, the growth of the *atl* mutant strain, WISΔ*atl* and the respective parental strain WIS, were monitored under several conditions.

3.2.1.1 – Growth profiles at different temperatures

The optimal growth temperature of *S. aureus* is 37ºC, but it can grow at a temperature range from 15ºC to 45ºC[145]. Therefore, four different growth temperatures within this range were tested: 25ºC, the typical room temperature; 30ºC, the temperature at which the AtlR transcriptional repressor has been shown to influence *atl* expression[97]; 37ºC, the optimal bacterial growth temperature for *S. aureus*; and 42ºC, for a higher temperature in the temperature range of *S. aureus* growth. The bacterial growth of *S. aureus* strains WIS and WISΔ*atl* was monitored hourly up to 10 hours and at 24 hours.

The growth curves of the two strains were virtually identical, indicating that the absence of the *atl* gene did not alter the growth profile at any temperature (Figure 3.24). The growth rate at the exponential phase of WIS and WIS∆*atl* was 0.01 min^{-1} at higher temperatures (37ºC and 42ºC), and 0.004 min^{-1} for lower temperatures (25ºC and 30ºC), reflecting a lower rate of growth at lower temperatures.

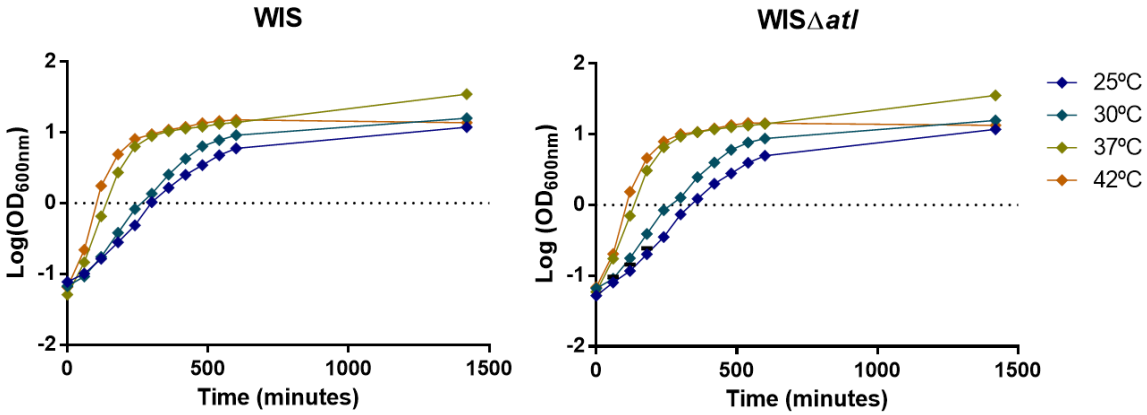

Figure 3.24: Growth monitoring of *S. aureus* parental and mutant strain, WIS and WIS∆*atl*, at different temperatures. Optical density (OD_{600nm}) was monitored hourly until 10 hours, and then at 24 hours. Growth assays were performed three times and a representative curve is shown.

3.2.1.2. – Growth profiles in presence of ssDNA using non-buffered media

The effect of the presence of eDNA in the growth media on bacterial growth was assayed, since the hydrolytic activity of the GL protein towards heat inactivated cells was affected by its interaction with DNA, as described above. Different ssDNA concentrations were tested, and their effects were compared with the growth at 37ºC, without added DNA (Figure 3.25). *S. aureus* strain WIS and its *atl* mutant WIS∆*atl* were tested. For both strains, the presence of ssDNA at low concentrations (0.1 and 0.5 mg/ml, corresponding to 0.1% and 0.5%) had a negligible effect on the bacterial growth, being the growth curves very similar to the control growth curve, at 37ºC without added ssDNA (Figure 3.24). For the highest tested ssDNA concentration (1 mg/ml corresponding to 1%), the effects on growth were very evident for both strains. The fact that this behaviour happened either in WIS or in WIS∆*atl*, indicates that the absence of the Atl protein did not affect bacterial growth. The pH of the media was measured at 24 hours, showing that the addition of 1% of ssDNA led to a pH decrease to a value of approximately 4-5, contrary to what occurred in the media enriched with 0.5% ssDNA, in which the pH remained approximately 7-8 (Annex 3). This could mean that the low pH values, induced by the presence of 1% ssDNA, were detrimental to bacterial growth, and the cells could not overcome this condition.

The growth rate at the exponential phase of WIS and WIS∆*atl* was around 0.01 min^{-1} at 0, 0.1 and 0.5 % of ssDNA, and 0.004 min^{-1} for 1% of ssDNA, reflecting a lower rate of growth at this ssDNA concentration.

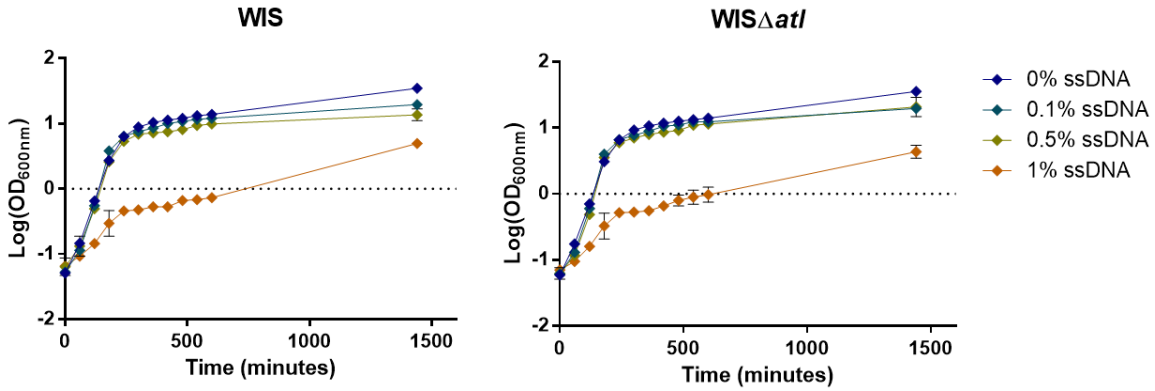

Figure 3.25: Growth monitoring of *S. aureus* parental and mutant strains, WIS and WIS*Δatl*, in the presence of ssDNA in non-buffered media. 0.1%, 0.5% and 1% (w/v) of low molecular weight salmon sperm DNA (ssDNA) were added separately to TSB non-buffered media. Optical density (OD_{600nm}) was monitored hourly until 10 hours, and then at 24 hours. Growth assays were performed three times and a representative curve is shown.

3.2.1.3 – Bacterial growth in presence of ssDNA using buffered media

To prevent the alteration of the pH of the media due to added ssDNA, the media was buffered at 7.4 to ensure that the pH was not altered during bacterial growth. As a result of media buffering, no differences were observed in growth. Both WIS and WIS*Δatl* presented a similar growth rate of approximately 0.0117 min^{-1}, and the different ssDNA concentrations did not affect growth, indicating that the low pH of the media was the factor that had more impact rather than the presence/absence ssDNA (Figure 3.26).

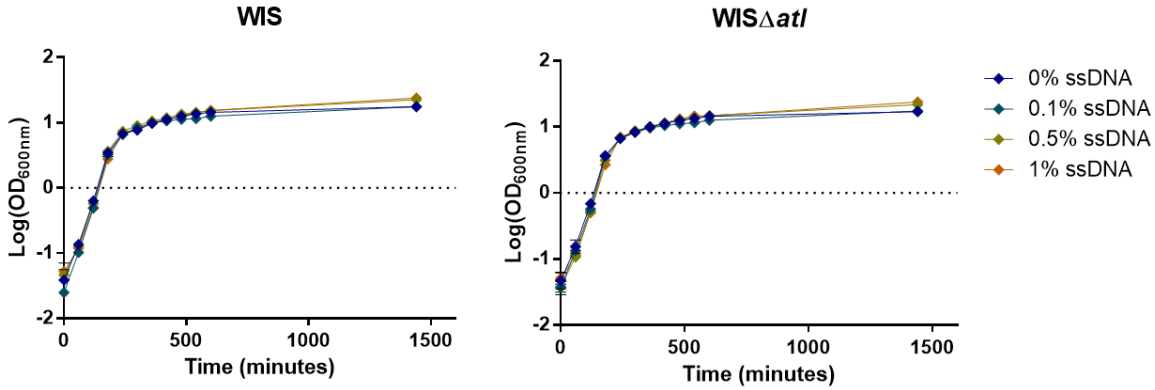

Figure 3.26: Growth monitoring of *S. aureus* parental and mutant strains, WIS and WIS-Δ*atl*, in the presence of ssDNA in buffered media. 0.1%, 0.5% and 1% (w/v) of low molecular weight salmon sperm DNA (ssDNA) were added separately to TSB buffered media at pH 7.4. Optical density (OD_{600nm}) was monitored hourly until 10 hours, and then at 24 hours. Growth assays were performed three times and a representative curve is shown.

3.2.2 – *atl* promoter activity for different conditions

atl promoter activity was monitored during the bacterial growth, as gene expression can change along time to respond to the bacterial needs at the different growth phases. To monitor *atl* promoter activity, the pIG4 plasmid, carrying the GFP gene under the control of *atl* promoter was used (Table 2.1). At different time points, fluorescence was measured, corresponding to the

level of *atl* promoter activity. Different factors such as temperature and the presence of ssDNA were tested, in the same conditions and concentrations previously used for growth monitoring.

3.2.2.1 – *atl* promoter activity at different temperatures

Both WIS and WIS∆*atl* strains showed high fluorescence values at the beginning of the assay, around 200 A.U. This value continuously decreased at 25ºC until 360 minutes to a minimum value of 20 A.U (Figure 3.27-A and B), and at 37ºC until 180 minutes to a minimum value of 30 A.U (Figure 3.27-C and D). The temperature effect on *atl* expression was more pronounced in the WIS strain, as fluorescence decreased more rapidly at 37ºC (124 A.U. in the first 60 minutes of the assay), but more slowly at the 25ºC (36 A.U. in the first 60 minutes of the assay). At 37ºC, the fluorescence started to increase again at 240 minutes, while at 25ºC, this occurred at 420 minutes. After these time-points, the activity of *atl* promoter increased until 600 minutes, at both temperatures for the two strains to values above 70 A.U. The last time point at 1440 minutes showed a decrease of the fluorescence to values below 35 A.U.

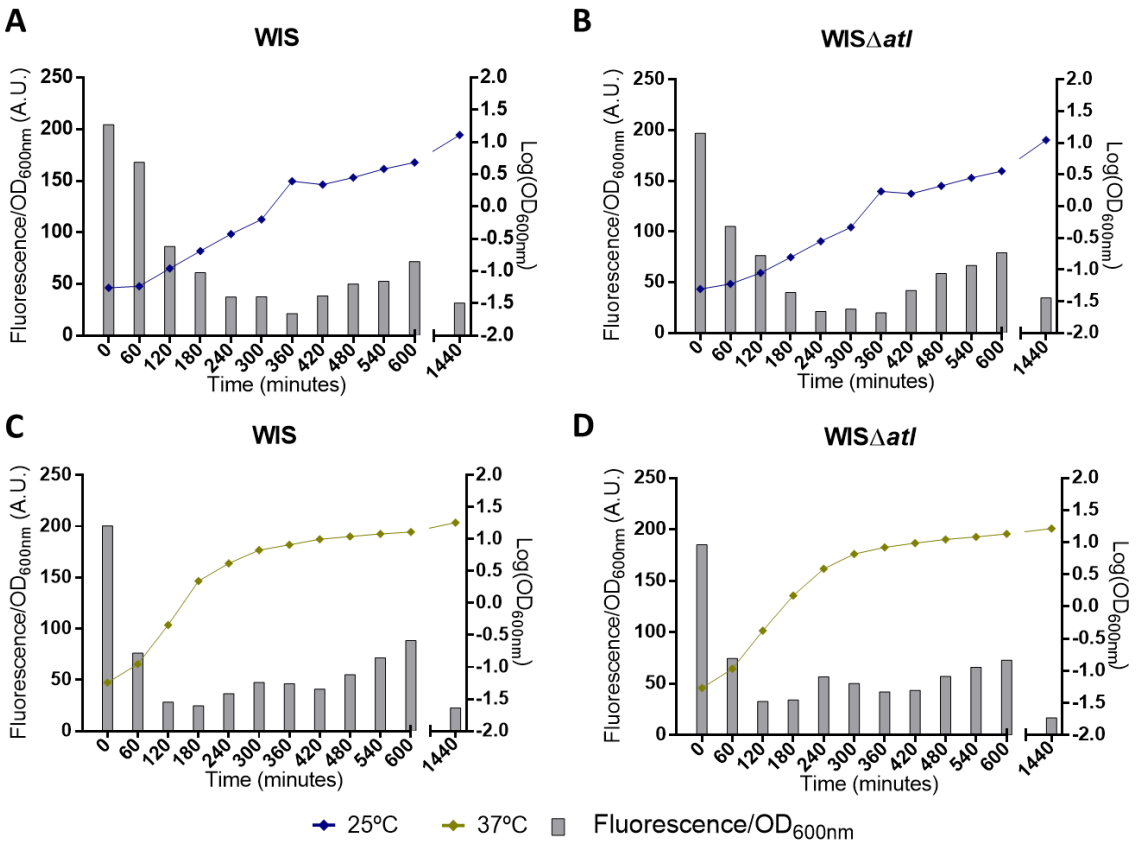

Figure 3.27: GFP expression under the control of the *atl* promoter of *S. aureus* parental strain WIS and mutant strain WIS∆*atl*, at different temperatures. Each strain was grown at 25ºC and 37ºC and the fluorescence was monitored hourly until 10 hours, and then at 24 hours. Fluorescence values were normalized by the respective optical density value for comparison. Fluorescence/OD_{600nm} is shown in bars (grey) at each time point and the respective OD_{600nm} is represented by a line.

Comparing these results with the respective growth curves, the increase of *atl* promoter activity started at the beginning of the stationary phase at both temperatures and for both strains. The differences in the expression of atl along time can be explained by the delay in bacterial

growth induced by the lower growth temperature. Comparing *atl* expression along the growth curve, the expression of this gene seems similar for both strains, at both temperatures. The decrease in fluorescence at the beginning of the assay was less steep at 25ºC, compared with the obtained values at 37ºC, which can be a result of the different progression of the growth curve. Despite that, the overall values of fluorescence do not present evident variations at any growth phase, regardless of the different temperatures or strains.

3.2.3.2 - *atl* promoter activity in presence of eDNA

The presence of eDNA could be a major factor for the expression of the *atl* gene, since the GL domain has the capacity to bind DNA. As before, assays with non-buffered TSB and buffered TSB media were performed to verify the influence of the pH of the media during the assay. To compare the impact of different ssDNA concentrations and the absence of ssDNA in non-buffered media, the previous results at 37ºC were used. Only the *S. aureus* parental WIS strain was monitored.

Using non-buffered media, the *S. aureus* WIS strain showed similar fluorescence values regardless of the ssDNA concentration, presenting a high *atl* promoter activity at the beginning of the growth curve (Figure 3.28-A, C and E). After the initial values, the expression of the *atl* promoter gene in the presence of 0% and 0.1% ssDNA, suffered a decrease in fluorescence in the first 180 minutes to very similar values, 24 and 33 A.U. respectively. From that time-point on, these bacterial cultures had an increase in the fluorescence values until 600 minutes. In the presence of 0.5% ssDNA, the decrease in fluorescence values continued until the 600 minutes, with some fluctuations between 25 and 50 A.U. (Figure 3.28-E). All assays showed a decrease of the fluorescence values in the last time-point at 1440 minutes as happened with all *atl* promoter gene expression assays performed.

Nonetheless, the fluorescence values of buffered media were more diverse at the beginning of the assay than in the non-buffered media (Figure 3.28-B, C and F). When 0.1% of ssDNA was added, the fluorescence value was 378 A.U., 77% higher than in the absence of ssDNA, 214 A.U., indicating a high *atl* promoter gene expression (Figure 3.28-D). At 0.5% ssDNA concentration, the fluorescence values decreased to 146 A.U, indicating a lower *atl* promoter gene expression at the beginning of the assay (Figure 3.28-F). After 240 minutes, the fluorescence values start to slightly increase for all ssDNA concentrations tested, with some fluctuations, until 600 minutes reaching 84 A.U. in the absence of ssDNA, 53 A.U. with 0.1% ssDNA and 65 A.U. with 0.5% ssDNA. The last time-point at 1440 minutes showed a decrease in the fluorescence to values of approximately 27 A.U. for all ssDNA concentrations.

Taken together, the *atl* promoter seems more active at the beginning of the bacterial growth curve corresponding to the growth phase immediately before the exponential phase, when the cell division machinery is more required. The bacteria used to initiate the assay were at a more advanced growth stage in the moment of inoculation to the culture, around 16-18 hours of overnight inoculation. This can be an explanation to the higher fluorescence values in the initial time-point, a phenomenon related with the methodology of the assay. This can also be an explanation for the differences between the different ssDNA concentrations, since each inoculum

could be at different growth phases. It can only be assured after performing more replicates of the assay.

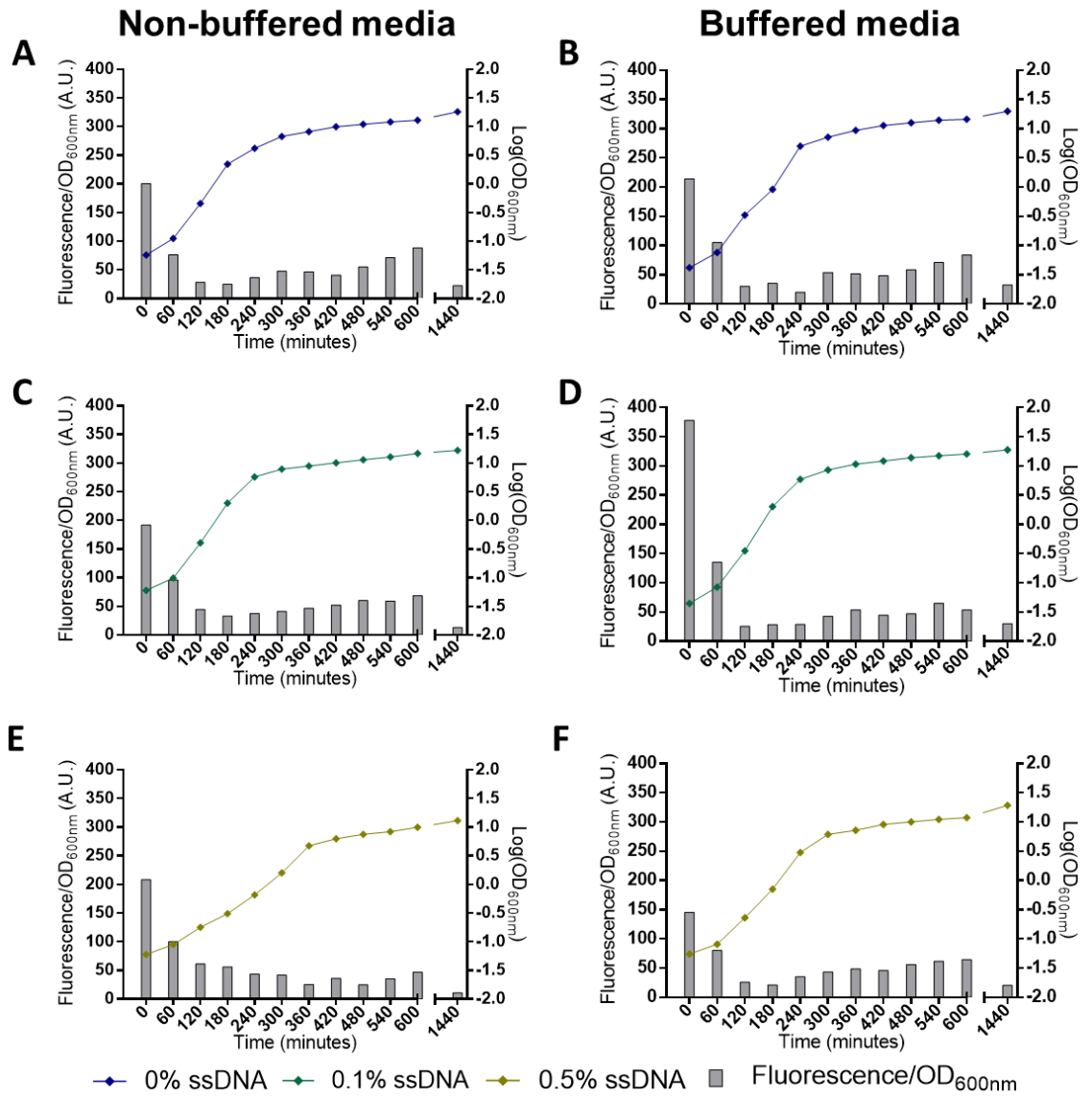

Figure 3.28: GFP expression under the control of the *atl* promoter of *S. aureus* parental strain, WIS in presence of eDNA. Concentrations of 0%, 0.1 % and 0.5% (w/v) of low molecular weight salmon sperm DNA (ssDNA) were used to enrich TSB media, non-buffered or buffered at pH 7.4. Fluorescence was monitored hourly until 10 hours, and then at 24 hours. Fluorescence values were normalized by the respective optical density value for comparison. Fluorescence/OD_{600nm} is shown in bars (grey) at each time point and the respective OD_{600nm} is depicted in a line.

4 – Conclusions

This work aimed to study the molecular interaction between the glucosaminidase domain (GL) of the major *S. aureus* autolysin Atl and DNA, and the roles of this interaction on the activity of this protein. The DNA-binding capacity of the GL catalytic domain of Atl had been reported[96], and a wide range of new features were hypothesized for this protein.

This work allowed to uncover the hydrolytic activity of GL in the presence of extracellular DNA and also the dynamics of the interaction between the two molecules.

The GL-DNA interaction has an electrostatic component and is affected by specific cations

Since the GL-DNA interaction did not show sequence specificity[96], it was hypothesized to be of electrostatic nature. EMSAs performed at different pH values showed that the surrounding pH influences the DNA-binding capacity of GL protein. The binding affinity of the GL-DNA interaction was increased in acidic environments, as a lower GL protein concentration was required to interact with the same amount of DNA, 100 nM of GL protein was required at pH 5 and 500 nM of GL protein at pH 7.4. The binding affinity decreased gradually with the pH increase, which can be visualized in the EMSA images, despite the impossibility to calculate the dissociation constant of the interaction, reaching a pH value for which the protein no longer had the capacity to bind DNA molecules. Such pH value was above the estimated pI of GL domain (9.58), for which the net charge of the protein is negative. Despite the evidences, the interaction between the two molecules is not totally dependent of the electrostatic forces, since the DNA pI value is approximately 5[129], the molecule has nearly a neutral net charge at this pH value. This higher interaction between GL and DNA can be explained by conformational changes of the DNA molecule at these conditions. For low pH values it has been reported that DNA molecules have the capacity to condensate[131]. It is possible that a more condensed conformation facilitates the protein binding capacity due to a lower surface area of DNA molecule available to interaction. It is interesting to note that the pH of the human skin is approximately 5 and that it was reported that an acid skin pH (4-4.5) keeps the resident bacterial flora attached to the skin. On the other hand, *S. aureus* is a typical example of the potentially pathogenic transient flora that can colonize the human skin being more successful at pH ≥ 5[146]. Several *S. aureus* adhesins have the capacity to bind collagen[31], the main structural protein of the human skin. The balance between the surrounding pH, the apparent higher affinity of GL-DNA interaction at pH 5 can be important to a proper attachment to the skin and consequently a better colonization of the host, since the skin's pH never rises to much higher values[146].

Another feature tested was the behaviour of the GL-DNA interaction in the presence of different cations. Cations are known to interact with DNA molecules through electrostatic forces correlated with their different charges[133,134], a fact that was confirmed for Na^+, K^+, Ca^{2+}, Cd^{2+}, Co^{2+}, Cu^{2+}, Mg^{2+}, Mn^{2+}, Ni^{2+} and Zn^{2+} from the studied cations. None of the tested cations was able to enhance the association between the GL protein and DNA. However, two divalent cations, Fe^{2+} and Mg^{2+}, showed the capacity to disturb the GL-DNA binding, probably due to the interaction

of these cations with the GL protein, since the DNA molecules were not influenced by Fe^{2+} and Mg^{2+} at the used concentrations. The structural changes that can occur in the GL protein due to the presence of these cations that hinder its DNA-binding capacity were not investigated and should be tested in subsequent studies.

S. aureus can grow in a varied type of conditions, at pH values from 4.8 up to 9.4 and at NaCl concentrations as high as 10%[5]. *S. aureus* bacteria is prepared to tolerate low pH values, as it can occur in biofilm formations, where the eDNA can act as an electrostatic net, interconnecting cells surrounded by positively charged matrix proteins at a low pH[62]. These are the conditions mimicked by the EMSA at pH 5, for which the highly positive protein, GL, and DNA showed higher biding affinity. This result suggests a role for GL-DNA binding in the establishment of cell-cell interactions during biofilm development.

All the studied cations are essential elements for the normal function of the human body[147]. *S. aureus* tolerates high concentrations of Na^+ and K^+ as well (10% NaCl and 700 mM in medium, respectively)[5,148]. In the case of Ca^{2+} and Mg^{2+} the survival rate of *S. aureus* diminishes to about 50% when the cation concentrations are around 40 mM[149]. In the case of some of the transient metal cations used, as Cd^{2+}, Cu^{2+} and Zn^{2+}, these demonstrate antibacterial activity against *S. aureus* (Cu^{2+}: 150 ng/ml[150]; Cd^{2+} and Zn^{2+}: 6.25 µg/ml[151]). These cations are also present in the human blood at low concentrations (in the order of µg/l)[152]. Despite the importance of all these electrolytes, they have to be present at very low concentrations to not be harmful to the cells. This can be the cause to the high interference of DNA molecules with transition metal divalent cations, as the case of ferrous cation through the Fenton reaction and the creation of reactive oxygen species that are known to damage DNA[153].

These results indicate that the DNA-binding capacity of GL is not exclusively due to electrostatic forces or the overall ionic strength of the solution, but the components of the surrounding environment can also influence the interaction. Thus, despite the influence of the pH on the GL-DNA interaction, the surrounding net charge is not the only factor that influences GL-DNA interaction, as the presence of Fe^{2+} and Mg^{2+} also affects the interaction, in contrast to the other ions tested, suggesting a specific effect. One hypothesis is that these cations interact with the acidic amino acids of the protein, altering GL tertiary structure as happens with other proteins[135]. This protein-cation interaction can unable a proper interaction between GL protein and DNA molecules, by conformational change or by occupying interaction spots.

GL binds to different nucleic acid molecules

Besides binding to linear DNA fragments of different sizes, the GL protein showed the capacity to bind plasmid DNA, either extracted from *S. aureus* or *E. coli*, regardless of the restriction-modification systems differences that exist between the two species[136]. This assay suggested that GL protein can have a slightly higher affinity for *E. coli* plasmid DNA. However, more repetitions must be performed to ensure that the small difference of 50 nM of GL concentration needed to retain all plasmid DNA of *E. coli* and *S. aureus* consistently occurs. Nevertheless, the assays showed that the GL protein can bind plasmid DNA, and the fact that this interaction can occur with DNA molecules extracted from different bacterial species

strengthens the premise that GL protein can be involved in the process of natural competence for DNA genetic transformation of *S. aureus*[116]. To acquire natural competence for DNA genetic transformation, eDNA has to be in the surrounding environment to bind, non-covalently, to sites present on the cell surface in order to be uptaken by the cells through a sequence-independent mechanism[154]. GL binds to eDNA without sequence specificity and at the cell surface (Grilo, I.R, unpublished), meaning that it is possible that GL protein can have a function in the DNA uptake process.

Thus, the GL protein has the capacity to bind DNA fragments without length or sequence specificity, and plasmid DNA, showing that GL can bind DNA in different conformations, although, the spatial conformation of the different molecules may result in different a GL association with the DNA molecule, parallel with the effect of the pH on the GL-DNA binding, already described (Section 3.1.1). If the alterations in spatial arrangement of DNA, creating a more condensed structure, can enhance the DNA-binding capacity of GL protein, the same possibly happens with the different conformations that plasmid DNA can adopt.

The interaction of GL with RNA molecules remains to be tested.

GL binding to different DNA molecules

Other features of the GL-DNA interaction, as the DNA capacity to promote oligomerization of the GL protein were also assessed. β-toxin (pI above 10[46,155]), an *S. aureus* protein involved in biofilm development, oligomerizes in the presence of DNA molecules [46]. The assays performed with GL demonstrated that DNA did not promote covalent binding between different GL protein molecules, since no additional bands of higher molecular mass were visible in the SDS-PAGE performed for the GL-DNA complex. Also, EMSA performed in acidic native-PAGE, showed that DNA did not promote GL oligomerization of non-covalent nature either. Instead, this assay elucidated about the GL-DNA interaction, confirming results already obtained with the EMSA performed in agarose electrophoresis: As the DNA concentration increased, the capacity of the protein to migrate on the native-PAGE decreased, as for a GL:DNA ratio below 573:1 no protein bands were detected, suggesting that all protein molecules are interacting with the available DNA. This molar ratio represents the number of protein molecules that can interact with one plasmid DNA molecule and is in agreement with the molar ratio obtained for the EMSA performed with plasmid DNA by agarose gel electrophoresis, which was 500 for *S. aureus* plasmid and 545 for *E. coli* plasmid. The molar ratio for the GL:DNA interaction obtained for the DNA fragment was 31.25:1, indicating that it is possible to accommodate one molecule of GL protein for each 8 base pairs of fragment DNA. In the case of plasmid DNA, the results indicate that one molecule of GL associates with 13 DNA base, suggesting that the binding capacity of GL is similar for both nucleic acid molecules and that GL may have slight higher affinity for linear molecules than for supercoiled conformations. It was not possible to determine with certainty if GL had different affinities for the plasmid conformations, although it appeared that GL could bind to all plasmid conformations equally.

AFM imaging of the GL-DNA interaction revealed information that the EMSA could not provide, as how the interaction occurs in terms of spatial rearrangement. The AFM images of

DNA alone showed high amounts of supercoiled plasmid DNA molecules, as visualized in the EMSAs performed with plasmid DNA. After imaging of the DNA molecules, the GL protein was added onto the mica, allowed to interact with the immobilized DNA, and excess protein was washed. The obtained images revealed that the GL protein co-localizes with the plasmid DNA molecules into an intricate agglomeration. The image of GL protein without DNA helped in the identification of the GL molecules in the GL-DNA image, as another protein, Tbp, with a similar molecular weight, was previously studied by AFM[140]. The images obtained for Tbp protein reflect a circle-shaped structure of a similar size to what was observed for the GL protein. It remains unknown if the GL protein promoted a higher condensation degree of the DNA molecules, since the co-localization of the two molecules seemed to create a more intricate conformation of DNA, already imaged in a supercoiled topology. The image between AM and DNA confirms the evidence of AM domain being unable to interact with DNA molecules, since no interaction was detected. All these generated images, suggested that with Atomic Force Microscopy it is possible the identify DNA interactions with specific proteins as well as the spatial arrangement of the molecules, allowing the study of other interactions within the scope of Atl-DNA interactions. Other recombinant Atl proteins can be tested, as the repeat regions of both GL and AM domains, since they have strong adhesive properties and bind to DNA[39,96]. Lower DNA concentrations and different nucleic acid molecules, as smaller DNA fragments, should also be used to obtain a better individual visualization of the interactions. If the imaging could be optimized, it would likely be possible to confirm the protein:DNA molar ratio calculated from the EMSAs, since it could make it easier to visualize the interactions of GL molecules with each individual DNA molecule.

The presence of extracellular DNA affects the hydrolytic activity of the GL domain

The GL domain is able to hydrolyse heat-inactivated cells of *M. luteus* but is unable to hydrolyse *S. aureus* heat-inactivated cells[90,96]. Also, the hydrolytic activity of R_3GL protein against *M. luteus* heat-inactivated cells in the presence of ssDNA had been reported to have no significant effect[96]. In this work, the hydrolytic activity of both R_3GL and GL was more thoroughly studied, using a wider range of ssDNA concentrations and a larger group of bacterial species as source of heat inactivated cells. Some of the bacterial species tested, such as *M. luteus*, *S. epidermidis* and *S. pyogenes* can co-colonize the same site of the host as *S. aureus* and compete for nutrients and space[156,157].

Both GL and R_3GL independently show the ability to hydrolyse a significant percentage of heat-inactivated cells from different species such as *M. luteus*, *E. coli*, *C. marina* and *M. hydrocarbonoclasticus*. The hydrolytic activity of both proteins towards all heat inactivated cells had a similar pattern. The small differences in the hydrolytic activity of both proteins against the heat-inactivated cells used are related with the different cell walls and diversity of peptidoglycan types present in these species[79], as the different peptidoglycan types reflect different compositions and cross-linking degrees, which can interfere with the hydrolytic activity.

The presence of ssDNA altered the hydrolytic activity of GL and R_3GL proteins under the conditions tested, revealing that the presence of extracellular DNA inhibits the peptidoglycan hydrolytic activity of the GL domain against the majority of the bacteria tested. This can be caused

by the interaction of the proteins with the DNA molecules, that prevent the protein from reaching the β-1,4- glycosidic bond between GlcNAc and MurNAc of peptidoglycan. The only two cases that showed different results were the increase of R_3GL hydrolytic activity against *S. epidermidis* in the absence of ssDNA and the increase of R_3GL hydrolytic activity against *S. aureus* for ssDNA concentrations below 2.5 mg/ml concentration. Since the repeat regions do not have lytic activity[39] they do not contribute directly to a higher hydrolytic activity. Despite the lack of statistical significance, this slight increase of activity can be explained by a possible higher affinity of the R_3 domain to the *S. aureus* lipoteichoic acids than to the DNA molecules, anchoring the GL protein to the cell wall in such a way that the protein reaches the β-1,4- glycosidic bond more easily than in the absence of the repeat region. This hypothesis could be tested with competition assays between lipoteichoic acids and DNA to know if R_3GL protein actually has a higher affinity to teichoic acids than to DNA.

The fact that the GL hydrolytic activity is impaired in the presence of DNA is especially important with microorganisms that share the same ecological niche as *S. aureus*, being commonly a part of the normal human microbiota like *M. luteus*, *S. epidermidis* and *S. pyogenes* which are part of the normal skin flora and *E. coli* and *E. faecalis* that belong to the normal intestinal and urogenital flora[157]. The ability of *S. aureus* to hydrolyse other bacteria can be essential to a better survival in a multi-species environment, or to uptake DNA from other species, as in case of blaZ gene responsible for the *S. aureus* penicillin resistance[13,14].

Also, the fact that DNA is one of the components of the extracellular matrix (ECM) of biofilms, the effect of its interaction with GL domain can interfere in the biofilm development. Since both GL and eDNA have adhesive roles in the ECM[38,61,62], the interaction of the two molecules could be related with the adhesion process to surfaces or to maintain the intracellular cohesion.

The absence of *atl* gene does not affect the bacterial growth rate

The Atl protein is only required for normal cellular separation of *S. aureus*, and due to that, the absence of *atl* gene showed no alterations on the growth rate, since the parental and mutant strains WIS and WIS*Δatl* showed virtually no differences in their growth profiles. This behaviour had already been described[39], and this result was not unexpected.

However, the study of the influence of Atl at different growth temperatures and in the presence of DNA had not been tested. Overall, WIS and WIS*Δatl* responded to temperature changes in the same manner, regarding their growth rate. At higher temperatures (37ºC and 42ºC), the strains reached the stationary phase more rapidly than at lower temperatures (25ºC and 30ºC). When the presence of extracellular DNA was tested, only the highest ssDNA concentration tested (1% w/v) showed an effect on the growth rate in both strains. This concentration of extracellular DNA had been previously shown to inhibit the bacterial growth of *S. aureus*[141]. However, the inhibition of bacterial growth was not caused by the presence of DNA in the media but to the resultant decrease in the pH of the media, due to the addition of DNA. The differences between the pH values of the TSB media with the addition of 0.5 % and 1% of ssDNA at the end of the assay were very high; TSB with 0.5% ssDNA had a pH value of 8, while TSB with 1% ssDNA had an acidic pH of approximately 4. The pH of the media had more relevance

than the presence of ssDNA, as was confirmed by performing the same assay with TSB medium buffered at pH 7.4, for which no differences on growth rate between ssDNA concentrations were detected. Another condition that could be tested would be using growth media with different pH values.

The effect of the presence of eDNA on the activity of the *atl* promoter was monitored under the same conditions as the growth assays. The results showed that the *atl* promoter seems more active at the beginning of the bacterial growth curve. The activity of the *atl* promoter of *S. aureus* strains WIS and WISΔ*atl* was always similar, regardless of the concentration of DNA added. At different temperatures, the evolution of the activity of the *atl* promoter along time was consistent with the progression of the growth curve and no major differences between temperatures were detected. In the presence of eDNA, the 0.1% (w/v) ssDNA concentration enhanced the expression of the *atl* promoter gene at the beginning of the growth curve, when compared with the absence of ssDNA. On the other hand, the addition of 0.5% (w/v) ssDNA seemed to inhibit the activity of the *atl* promoter at the same time points. Despite that initial difference, the overall effect of the ssDNA concentration did not affect the activity of the *atl* promoter during the rest of the bacterial growth, being similar for all the tested conditions. This higher *atl* promoter expression at the beginning of the bacterial growth curve can be caused by fact that the bacteria used to initiate the assay were at a later growth stage upon inoculation to the culture, around 16-18 hours of overnight inoculation. The higher fluorescence values in the initial time-point can be a phenomenon related with the methodology of the assay and not an *atl* promoter expression feature. This can also be an explanation for the differences between the different ssDNA concentrations, since each inoculum could be at different growth phases. It can only be assured after performing more replicates of the assay.

All the assays that included growth curves at different temperatures and in the presence of different ssDNA concentrations, were performed only once, and therefore the results may not be conclusive regarding the activity of the *atl* promoter, and replicates should be performed so that a proper interpretation can be made. The temperatures of 30ºC and 42ºC and the 1% (w/v) ssDNA concentrations must be tested as well. The *atl* promoter gene expression at 30ºC is especially relevant since this temperature is optimum for the expression of AtlR transcriptional repressor that has been shown to influence *atl* expression[96].

This study revealed important molecular features of the GL-DNA interaction and also insights into the importance of this association for the physiology of the bacteria and its interactions with the host environment and other bacterial species. The new data obtained should be complemented with the proposed assays, but also with other experiments.

With all the new information obtained in this work, several different growing assays should be performed, namely inter-species competition. Co-cultures of *S. aureus* growing together with another species, a species that is hydrolyzed by GL (*E. coli* or *M. luteus*) and a species that is not affected by GL (*S. pyogenes* or *E. faecalis*), would be monitored to determine which species, *S.*

aureus or the competing species, prevails. These assays would then be repeated for the DNA concentrations already tested to determine if eDNA has an impact in species competition. Then, the same experiments would be repeated for *atl* mutant strains of *S. aureus*. The integration of all these results will provide evidence on whether the GL-DNA interaction plays a role on species competition.

Performing static biofilm assays with GL domain in the presence of different ssDNA concentrations must be performed, since both Atl protein catalytic domains[38,97] and eDNA[32,58,59] are essential for a proper biofilm assembly in *S. aureus*. Biofilm assays using *atl* mutants and enriching the media with ssDNA and several recombinant Atl proteins were already performed and showed that the addition of DNA together with Atl proteins, resulted in the reestablishment of biofilm, compared with the parental strain, meaning that both molecules are essential for proper biofilm formation (Grilo, I.R., unpublished). Static biofilms were only monitored for recombinant Atl protein with repeats. Performing these assays with the GL domain, without repeats, could give important information about the dynamic of the GL-DNA interaction and how it interferes with the biofilm development.

5 – References

(1) **Ogston, A.** Report upon Micro-Organisms in Surgical Diseases. *Br. Med. J.* **1881**, *1* (1054), 369–377.

(2) **Ogston, A.** On Abscesses. *Rev. Infect. Dis.* **1984**, *6* (1), 122–128.

(3) Wertheim, H. F. L.; Melles, D. C.; Vos, M. C.; van Leeuwen, W.; van Belkum, A.; Verbrugh, H. A.; Nouwen, J. L. The Role of Nasal Carriage in Staphylococcus Aureus Infections. *Lancet Infect. Dis.* **2005**, *5* (12), 751–762.

(4) **Pelz, A.; Wieland, K. P.; Putzbach, K.; Hentschel, P.; Albert, K.; Götz, F.** Structure and Biosynthesis of Staphyloxanthin from *Staphylococcus aureus*. *J. Biol. Chem.* **2005**, *280* (37), 32493–32498.

(5) **Somerville, G. A.; Proctor, R. A**. The Biology of Staphylococci. In *Staphylococci in Human Disease: Second Edition*; **2009**; pp 3–18.

(6) **Kenneth, J. R.** Staphylococci. In *Medical Microbiology*; Kenneth, J. R., Ray, C. G., Eds.; **2004**; pp 261–271.

(7) **Pancholi, V.** Staphylococcal Extracellular/ Surface Enzymatic Activity. In *Staphylococcus aureus infection and disease*; Honeyman, A. L., Friedman, H., Bendinelli, M., Eds.; Kluwer Academic, **2002**; pp 137–153.

(8) **Gorwitz, R. J.; Kruszon-Moran, D.; McAllister, S. K.; McQuillan, G.; McDougal, L. K.; Fosheim, G. E.; Jensen, B. J.; Killgore, G.; Tenover, F. C.; Kuehnert, M. J.** Changes in the Prevalence of Nasal Colonization with *Staphylococcus aureus* in the United States, 2001–2004. *J. Infect. Dis.* **2008**, *197* (9), 1226–1234.

(9) **Williams, R. E.** Healthy Carriage of *Staphylococcus aureus*: Its Prevalence and Importance. *Bacteriol. Rev.* **1963**, *27* (96), 56–71.

(10) **Knox, J.; Uhlemann, A.; Lowy, F. D.; Biology, C.** *Staphylococcus aureus* Infections: Transmission within Households and the Community. *Trends Microbiol.* **2015**, *23* (7), 437–444.

(11) **Paterson, G. K.; Harrison, E. M.; Holmes, M. A.** The Emergence of MecC Methicillin-Resistant *Staphylococcus aureus*. *Trends Microbiol.* **2014**, *22* (1), 42–47.

(12) **Pinho, M. G.; de Lencastre, H.; Tomasz, A.** An Acquired and a Native Penicillin-Binding Protein Cooperate in Building the Cell Wall of Drug-Resistant Staphylococci. *Proc. Natl. Acad. Sci.* **2001**, *98* (19), 10886–10891.

(13) **Lowy, F.** Antimicrobial Resistance: The Example of *Staphylococcus aureus*. *J. Clin. Invest.* **2003**, *111* (9), 1265–1273.

(14) **Musser, J. M.; Kapur, V.** Clonal Analysis of Methicillin-Resistant *Staphylococcus aureus* Strains from Intercontinental Sources: Association of the Mec Gene with Divergent Phylogenetic Lineages Implies Dissemination by Horizontal Transfer and Recombination. *J. Clin. Microbiol.* **1992**, *30* (8), 2058–2063.

(15) **Hartman, B. J.; Tomasz, A.** Low-Affinity Penicillin-Binding Protein Associated with r-Lactam Resistance in *Staphylococcus aureus*. *J. Bacteriol.* **1984**, *158* (2), 513–516.

(16) **Hiramatsu, K.; Katayama, Y.; Yuzawa, H.; Ito, T.** Molecular Genetics of Methicillin-Resistant *Staphylococcus aureus*. *Int.J.Med.Microbiol.* **2002**, *292* (2), 67–74.

(17) **de Lencastre, H.; Tomasz, A.** Reassessment of the Number of Auxiliary Genes Essential for Expression of High-Level Methicillin Resistance in *Staphylococcus aureus*. *Antimicrob. Agents Chemother.* **1994**, *38* (11), 2590–2598.

(18) **Berger-Bächi, B.; Rohrer, S.** Factors Influencing Methicillin Resistance in Staphylococci. *Arch. Microbiol.* **2002**, *178* (3), 165–171.

(19) **Van Bambeke, F.; Glupczynski, Y.; Mingeot-Leclerq, M.-P.; Tulkens, P. M.** Mechanisms of Action. In *Infectious Diseases*; **2010**; pp 1288–1307.

(20) **Lindsay, J. A.** Hospital-Associated MRSA and Antibiotic Resistance-What Have We Learned from Genomics? *Int. J. Med. Microbiol.* **2013**, *303* (6–7), 318–323.

(21) **DeLeo, F. R., Otto, M., Kreiswirth, B. N., Chambers, H. F.** Community-Associated Methicillin-Resistant *Staphylococcus aureus*. *Lancet.* **2010**, *375* (9725), 1557–1568.

(22) **Naimi, T. S.; Ledell, K. H.; Como-sabetti, K.; Borchardt, S. M.; Boxrud, D. J.; Johnson, S. K.; Fridkin, S.; Boyle, C. O.; Danila, R. N.** Comparison of Community- and Health Care–Associated Methicillin-Resistant *Staphylococcus aureus* Infection. *Am. Med. Assoc.* **2003**, *290* (22).

(23) **Rudkin, J. K.; Edwards, A. M.; Bowden, M. G.; Brown, E. L.; Pozzi, C.; Waters, E. M.; Chan, W. C.; Williams, P.; Gara, J. P. O.; Massey, R. C.** Methicillin Resistance Reduces the Virulence of *Staphylococcus aureus* by Interfering With the Agr Quorum Sensing System. *J. Infect. Dis.* **2012**, *205*, 798–806.

(24) **Khan, A.; Wilson, B.; Gould, I. M.** Current and Future Treatment Options for Community-Associated MRSA Infection. *Expert Opin. Pharmacother.* **2018**, 1–14.

(25) **Bonar, E.; Wojcik, I.; Jankowska, U.; Kedracka-Krok, S.; Bukowski, M.; Polakowska, K.; Lis, M. W.; Kosecka-Strojek, M.; Sabat, A. J.; Dubin, G.; et al.** Identification of Secreted Exoproteome Fingerprints of Highly-Virulent and Non-Virulent *Staphylococcus aureus* Strains. *Front. Cell. Infect. Microbiol.* **2016**, *6* (51), 1–15.

(26) **Bramley, A. J.; Patel, A. H.; Oreilly, M.; Foster, R.; Foster, T. J.** Roles of Alpha-Toxin and Beta-Toxin in Virulence of *Staphylococcus aureus* for the Mouse Mammary-Gland. *Infect. Immun.* **1989**, *57* (8), 2489–2494.

(27) **Neill, E. O.; Pozzi, C.; Houston, P.; Humphreys, H.; Robinson, D. A.; Loughman, A.; Foster, T. J.; Gara, J. P. O.** A Novel *Staphylococcus aureus* Biofilm Phenotype Mediated by the Fibronectin-Binding Proteins , FnBPA and FnBPB. *Am. Soc. Microbiol.* **2008**, *190* (11), 3835–3850.

(28) **Geoghegan, J. A.; Corrigan, R. M.; Gruszka, D. T.; Speziale, P.; O'Gara, J. P.; Potts, J. R.; Foster, T. J.** Role of Surface Protein SasG in Biofilm Formation by *Staphylococcus aureus*. *J. Bacteriol.* **2010**, *192* (21), 5663–5673.

(29) **Mack, D.** The Intercellular Adhesion Involved in Biofilm Accumulation of *Staphylococcus epidermidis* Is a Linear [Beta]-1,6-Linked Glycosaminoglycan: Purification and Structural Analysis. *J. Bacteriol.* **1996**, *178* (1), 175–183.

(30) **Wanner, S.; Schade, J.; Keinhörster, D.; Weller, N.; George, S. E.; Kull, L.; Bauer, J.; Grau, T.; Winstel, V.; Stoy, H.; et al.** Wall Teichoic Acids Mediate Increased Virulence in *Staphylococcus aureus*. *Nat. Microbiol.* **2017**, *2* (16257), 1–11.

(31) **Timothy J. Foster; Geoghegan, J. A.; Ganesh, V. K.; Höök, M.** Adhesion, Invasion and Evasion: The Many Functions of the Surface Proteins of *Staphylococcus aureus*. *Nat Rev Microbiol* **2016**, *16* (1), 49–62.

(32) **Montanaro, L.; Poggi, A.; Visai, L.; Ravaioli, S.; Campoccia, D.; Speziale, P.; Arciola, C. R.** Extracellular DNA in Biofilms. *Int. J. Artif. Organs* **2011**, *34* (9), 824–831.

(33) **Flemming, H. C.; Wingender, J.** The Biofilm Matrix. *Nat. Rev. Microbiol.* **2010**, *8* (9), 623–633.

(34) **Moormeier, D. E.; Bayles, K. W.** *Staphylococcus aureus* Biofilm: A Complex Developmental Organism. *Mol. Microbiol.* **2017**, *104* (3), 365–376.

(35) **Otto, M.** Staphylococcal Biofilms. *Curr. Top. Microbiol. Immunol.* **2008**, *322*, 207–228.

(36) **Cucarella, C.; Solano, C.; Valle, J.** Bap, a *Staphylococcus aureus* Surface Protein Involved in Biofilm Formation. *J. …* **2001**, *183* (9), 2888–2896.

(37) **Merino, N.; Toledo-Arana, A.; Vergara-Irigaray, M.; Valle, J.; Solano, C.; Calvo, E.; Lopez, J. A.; Foster, T. J.; Penadés, J. R.; Lasa, I.** Protein A-Mediated Multicellular Behavior in *Staphylococcus aureus*. *J. Bacteriol.* **2009**, *191* (3), 832–843.

(38) **Bose, J. L.; Lehman, M. K.; Fey, P. D.; Bayles, K. W.** Contribution of the *Staphylococcus aureus* Atl AM and GL Murein Hydrolase Activities in Cell Division, Autolysis, and Biofilm Formation. *PLoS One* **2012**, *7* (7), e42244.

(39) **Biswas, R.; Voggu, L.; Simon, U. K.; Hentschel, P.; Thumm, G.; Götz, F**. Activity of the Major Staphylococcal Autolysin Atl. *FEMS Microbiol. Lett.* **2006**, *259* (2), 260–268.

(40) **Lister, J. L.; Horswill, A. R.** *Staphylococcus aureus* Biofilms: Recent Developments in Biofilm Dispersal. *Front. Cell. Infect. Microbiol.* **2014**, *4* (178), 1–9.

(41) **Herman-Bausier, P.; El-Kirat-Chatel, S.; Foster, T. J.; Geoghegan, J. A.; Dufrêne, Y. F.**

Staphylococcus aureus Fibronectin-Binding Protein A Mediates Cell-Cell Adhesion through Low-Affinity Homophilic Bonds. *MBio* **2015**, *6* (3), e00413-15.

(42) **Vergara-Irigaray, M.; Valle, J.; Merino, N.; Latasa, C.; García, B.; De Los Mozos, I. R.; Solano, C.; Toledo-Arana, A.; Penadés, J. R.; Lasa, I.** Relevant Role of Fibronectin-Binding Proteins in *Staphylococcus aureus* Biofilm-Associated Foreign-Body Infections. *Infect. Immun.* **2009**, *77* (9), 3978–3991.

(43) **Yang, Y. H.; Jiang, Y. L.; Zhang, J.; Wang, L.; Bai, X. H.; Zhang, S. J.; Ren, Y. M.; Li, N.; Zhang, Y. H.; Zhang, Z.; et al.** Structural Insights into SraP-Mediated *Staphylococcus aureus* Adhesion to Host Cells. *PLoS Pathog.* **2014**, *10* (6), e1004169.

(44) **Sanchez, C. J.; Shivshankar, P.; Stol, K.; Trakhtenbroit, S.; Sullam, P. M.; Sauer, K.; Hermans, P. W. M.; Orihuela, C. J.** The Pneumococcal Serine-Rich Repeat Protein Is an Intraspecies Bacterial Adhesin That Promotes Bacterial Aggregation in Vivo and in Biofilms. *PLoS Pathog.* **2010**, *6* (8), e1001044.

(45) **Siboo, I.; Chambers, H.; Sullam, P. M.** Role of SraP, a Serine-Rich Surface Protein of *Staphylococcus aureus*, in Binding to Human Platelets. *Infect. Immun.* **2005**, *73* (4), 2273–2280.

(46) **Huseby, M. J.; Kruse, A. C.; Digre, J.; Kohler, P. L.; Vocke, J. A.; Mann, E. E.; Bayles, K. W.; Bohach, G. A.; Schlievert, P. M.; Ohlendorf, D. H.; et al.** Beta Toxin Catalyzes Formation of Nucleoprotein Matrix in Staphylococcal Biofilms. *Proc. Natl. Acad. Sci.* **2010**, *107* (32), 14407–14412.

(47) **Pasztor, L.; Ziebandt, A.; Nega, M.; Schlag, M.; Haase, S.; Franz-wachtel, M.; Madlung, J.; Nordheim, A.; Heinrichs, D. E.; Go, F.; et al.** Staphylococcal Major Autolysin (Atl) Is Involved in Excretion of Cytoplasmic Proteins. *J. Biol. Chem.* **2010**, *285* (47), 36794–36803.

(48) **Ebner, P.; Rinker, J.; Nguyen, T.; Popella, P.; Nega, M.; Luqman, A.; Schittek, B.; Marco, M. Di; Stevanovic, S.** Excreted Cytoplasmic Proteins Contribute to Pathogenicity in *Staphylococcus aureus*. **2016**, *84* (6), 1672–1682.

(49) **Ebner, P.; Rinker, J.; Götz, F.** Excretion of Cytoplasmic Proteins in Staphylococcus Is Most Likely Not Due to Cell Lysis. *Curr. Genet.* **2016**, *62* (1), 19–23.

(50) **Wang, G.; Chen, H.; Xia, Y.; Cui, J.; Gu, Z.; Song, Y.; Chen, Y. Q.; Zhang, H.; Chen, W.** How Are the Non-Classically Secreted Bacterial Proteins Released into the Extracellular Milieu? *Curr. Microbiol.* **2013**, *67* (6), 688–695.

(51) **Foulston L., Elsholz, A. K. W. , DeFrancesco A. S., L. R.** The Extracellular Matrix of *Staphylococcus aureus* Biofilms Comprises Cytoplasmic Proteins That Associate with the Cell Surface in Response to Decreasing pH. *Mbio.Asm.Org* **2014**, *5* (5), 1–9.

(52) **Leibig, M.; Liebeke, M.; Mader, D.; Lalk, M.; Peschel, A.; Götz, F.** Pyruvate Formate Lyase Acts as a Formate Supplier for Metabolic Processes during Anaerobiosis in *Staphylococcus aureus*. *J. Bacteriol.* **2011**, *193* (4), 952–962.

(53) **O'Gara, J. P.** Ica and beyond: Biofilm Mechanisms and Regulation in *Staphylococcus epidermidis* and *Staphylococcus aureus*. *FEMS Microbiol. Lett.* **2007**, *270* (2), 179–188.

(54) **Cramton, S. E.; Gerke, C.; Schnell, N. F.; Nichols, W. W.; Götz, F.** The Intercellular Adhesion (Ica) Locus Is Present in *Staphylococcus aureus* and Is Required for Biofilm Formation. *Infect. Immun.* **1999**, *67* (10), 5427–5433.

(55) **Gross, M.; Cramton, S. E.; Götz, F.; Peschel, A.** Key Role of Teichoic Acid Net Charge in *Staphylococcus aureus* Colonization of Artificial Surfaces. *Infect. Immun.* **2001**, *69* (5), 3423–2426.

(56) **Boles, B. R.; Thoende, M.; Roth, A. J.; Horswill, A. R.** Identification of Genes Involved in Polysaccharide- Independent *Staphylococcus aureus* Biofilm Formation. *PLoS One* **2010**, *5* (4), e10146.

(57) **Toledo-Arana, A.; Merino, N.; Débarbouillé, M.; Penadés, J. R.; Lasa, I.; Vergara-irigaray, M.; De, M**. *Staphylococcus aureus* Develops an Alternative , Ica- Independent Biofilm in the Absence of the ArlRS Two-Component System. *J. Bacteriol.* **2005**, *187* (15), 5318–5329.

(58) **Okshevsky, M.; Meyer, R. L.** The Role of Extracellular DNA in the Establishment, Maintenance and Perpetuation of Bacterial Biofilms. *Crit. Rev. Microbiol.* **2015**, *41* (3), 341–352.

(59) **Gloag, E. S.; Turnbull, L.; Huang, A.; Vallotton, P.; Wang, H.; Nolan, L. M.; Mililli, L.; Hunt, C.; Lu, J.; Osvath, S. R.; et al.** Self-Organization of Bacterial Biofilms Is Facilitated by Extracellular

DNA. *Proc. Natl. Acad. Sci.* **2013**, *110* (28), 11541–11546.

(60) **Izano, E. A.; Amarante, M. A.; Kher, W. B.; Kaplan, J. B.** Differential Roles of Poly-N-Acetylglucosamine Surface Polysaccharide and Extracellular DNA in *Staphylococcus aureus* and *Staphylococcus epidermidis* Biofilms. *Appl. Environ. Microbiol.* **2008**, *74* (2), 470–476.

(61) **Mann, E. E.; Rice, K. C.; Boles, B. R.; Endres, J. L.; Ranjit, D.; Chandramohan, L.; Tsang, L. H.; Smeltzer, M. S.; Horswill, A. R.; Bayles, K. W.** Modulation of eDNA Release and Degradation Affects *Staphylococcus aureus* Biofilm Maturation. *PLoS One* **2009**, *4* (6), e5822.

(62) **Dengler, V.; Foulston, L.; Defrancesco, A. S.; Losick, R.** An Electrostatic Net Model for the Role of Extracellular DNA in Biofilm Formation by *Staphylococcus aureus*. *J Bacteriol* **2015**, *197* (24), 3779–3787.

(63) **McCarthy, H.; Rudkin, J. K.; Black, N. S.; Gallagher, L.; O'Neill, E.; O'Gara, J. P.** Methicillin Resistance and the Biofilm Phenotype in *Staphylococcus aureus*. *Front. Cell. Infect. Microbiol.* **2015**, *5* (January), 1–9.

(64) **Chaignon, P.; Sadovskaya, I.; Ragunah, C.; Ramasubbu, N.; Kaplan, J. B.; Jabbouri, S.** Susceptibility of Staphylococcal Biofilms to Enzymatic Treatments Depends on Their Chemical Composition. *Appl. Microbiol. Biotechnol.* **2007**, *75*, 125–132.

(65) **Peschel, A.; Otto, M.** Phenol-Soluble Modulins and Staphylococcal Infection. *Nat. Rev. Microbiol.* **2013**, *11* (10), 667–673.

(66) **Periasamy, S.; Joo, H.-S.; Duong, A. C.; Bach, T.-H. L.; Tan, V. Y.; Chatterjee, S. S.; Cheung, G. Y. C.; Otto, M.** How *Staphylococcus aureus* Biofilms Develop Their Characteristic Structure. *Proc. Natl. Acad. Sci.* **2012**, *109* (4), 1281–1286.

(67) **Schwartz, K.; Ganesan, M.; Payne, D. E.; Solomon, M. J.; Blaise, R.; Arbor, A.; Arbor, A.; Roy, J.; City, I.** Extracellular DNA Facilitates the Formation of Functional Amyloids in *Staphylococcus aureus* Biofilms. *Mol. Microbiol.* **2016**, *99* (1), 123–134.

(68) **Schwartz, K.; Syed, A. K.; Stephenson, R. E.; Rickard, A. H.; Boles, B. R.** Functional Amyloids Composed of Phenol Soluble Modulins Stabilize *Staphylococcus aureus* Biofilms. *PLoS Pathog.* **2012**, *8* (6), e1002744.

(69) **Neuhaus, F. C.; Baddiley, J.** A Continuum of Anionic Charge: Structures and Functions of D-Alanyl- Teichoic Acids in Gram- Positive Bacteria. *Microbiol. Mol. Biol. Rev.* **2003**, *67* (4), 686–723.

(70) **Dramsi, S.; Magnet, S.; Davison, S.; Arthur, M.** Covalent Attachment of Proteins to Peptidoglycan. *FEMS Microbiol. Rev.* **2008**, *32* (2), 307–320.

(71) **Mengin-Lecreulx, D.; Lemaitre, B.** Structure and Metabolism of Peptidoglycan and Molecular Requirements Allowing Its Detection by the Drosophila Innate Immune System. *J. Endotoxin Res.* **2005**, *11* (2), 105–111.

(72) **Xia, G.; Kohler, T.; Peschel, A.** The Wall Teichoic Acid and Lipoteichoic Acid Polymers of *Staphylococcus aureus*. *Int. Jl Med. Microbiol.* **2010**, *300* (2–3), 148–154.

(73) **Peschel, A.; Otto, M.; Jack, R. W.; Kalbacher, H.; Jung, G.; Götz, F.** Inactivation of the *Dlt* Operon in *Staphylococcus aureus* Confers Sensitivity to Defensins, Protegrins, and Other Antimicrobial Peptides. *J. Biol. Chem.* **1999**, *274* (13), 8405–8410.

(74) **Schlag, M.; Biswas, R.; Krismer, B.; Kohler, T.; Zoll, S.; Yu, W.; Schwarz, H.; Peschel, A.; Götz, F.** Role of Staphylococcal Wall Teichoic Acid in Targeting the Major Autolysin Atl. *Mol. Microbiol.* **2010**, *75* (4), 864–873.

(75) **Rohde, H.; Frankenberger, S.; Zähringer, U.; Mack, D.** Structure, Function and Contribution of Polysaccharide Intercellular Adhesin (PIA) to *Staphylococcus epidermidis* Biofilm Formation and Pathogenesis of Biomaterial-Associated Infections. *Eur. J. Cell Biol.* **2010**, *89* (1), 103–111.

(76) **Tjalsma, H.; Antelmann, H.; Jongbloed, J. D. H.; Braun, P. G.; Darmon, E.; Dorenbos, R.; Dubois, F.; Westers, H.; Zanen, G.; Quax, W. J.; et al.** Proteomics of Protein Secretion by *Bacillus subtilis*: Separating the "'Secrets'" of the Secretome. *Microbiol. Mol. Biol. Rev.* **2004**, *68* (2), 207–233.

(77) **Van Roosmalen, M. L.; Geukens, N.; Jongbloed, J. D. H.; Tjalsma, H.; Dubois, J. Y. F.; Bron, S.; Van Dijl, J. M.; Anné, J.** Type I Signal Peptidases of Gram-Positive Bacteria. *Biochim. Biophys. Acta - Mol. Cell Res.* **2004**, *1694*, 279–297.

(78) **Lowy, F.** *Staphylococcus aureus* Infections. *N. Engl. J. Med.* **1998**, *339*, 520–532.

(79) **Schleifer, K. H.; Kandler, O.** Peptidoglycan Types of Bacterial Cell Walls and Their Taxonomic Implications. *Bacteriol. Rev.* **1972**, *36* (4), 407–477.

(80) **Snowden, M. A.; Perkins, H. R.** Peptidoglycan Cross-linking in *Staphylococcus aureus* An Apparent Random Polymerisation Process. *Eur. J. Biochem.* **1990**, *191* (2), 373–377.

(81) **Smith, C. A.** Structure, Function and Dynamics in the Mur Family of Bacterial Cell Wall Ligases. *J. Mol. Biol.* **2006**, *362* (4), 640–655.

(82) **Schneider, T.; Senn, M. M.; Berger-Bächi, B.; Tossi, A.; Sahl, H. G.; Wiedemann, I.** In Vitro Assembly of a Complete, Pentaglycine Interpeptide Bridge Containing Cell Wall Precursor (Lipid II-Gly5) of *Staphylococcus aureus*. *Mol. Microbiol.* **2004**, *53* (2), 675–685.

(83) **Monteiro, J. M.; Pereira, A. R.; Reichmann, N. T.; Saraiva, B. M.; Fernandes, P. B.; Veiga, H.; Tavares, A. C.; Santos, M.; Ferreira, M. T.; Macário, V.; et al.** Peptidoglycan Synthesis Drives an FtsZ-Treadmilling- Independent Step of Cytokinesis. *Nat. Publ. Gr.* **2018**, *554*, 528–532.

(84) **Goffin, C.; Ghuysen, J.-M.** Multimodular Penicillin-Binding Proteins: An Enigmatic Family of Orthologs and Paralogs. *Microbiol. Mol. Biol. Rev.* **1998**, *62* (4), 1079–1093.

(85) **Vollmer, W.** Structural Variation in the Glycan Strands of Bacterial Peptidoglycan. *FEMS Microbiol. Rev.* **2008**, *32* (2), 287–306.

(86) **Wilkinson, B. J.; Muthaiyan, A.; Jayaswal, R. K.** The Cell Wall Stress Stimulon of *Staphylococcus aureus* and Other Gram- Positive Bacteria. *Curr. Med. Chem. Anti-Infective Agents* **2005**, *4*, 259–276.

(87) **Vollmer, W.; Joris, B.; Charlier, P.; Foster, S.** Bacterial Peptidoglycan (Murein) Hydrolases. *FEMS Microbiol. Rev.* **2008**, *32* (2), 259–286.

(88) **Sugai, M.; Komatsuzawa, H.; Akiyama, T.; Hong, Y. M.; Oshida, T.; Miyake, Y.; Yamaguchi, T.; Suginaka, H.** Identification of Endo-Beta-N-Acetylglucosaminidase and N-Acetylmuramyl-L-Alanine Amidase as Cluster-Dispersing Enzymes in *Staphylococcus aureus*. *J. Bacteriol.* **1995**, *177* (6), 1491–1496.

(89) **Yamada, S.; Sugai, M.; Komatsuzawa, H.; Nakashima, S.; Oshida, T.; Matsumoto, A.; Suginaka, H.** An Autolysin Ring Associated with Cell Separation of *Staphylococcus aureus*. *J. Bacteriol.* **1996**, *178* (6), 1565–1571.

(90) **Oshida, T.; Sugai, M.; Komatsuzawa, H.; Hong, Y. M.; Suginaka, H.; Tomasz, A.** A *Staphylococcus aureus* Autolysin That Has an N-Acetylmuramoyl-L-Alanine Amidase Domain and an Endo-Beta-N-Acetylglucosaminidase Domain: Cloning, Sequence Analysis, and Characterization. *Proc. Natl. Acad. Sci. U. S. A.* **1995**, *92* (1), 285–289.

(91) **Baba, T.; Schneewind, O.** Targeting of Muralytic Enzymes to the Cell Division Site of Gram-Positive Bacteria: Repeat Domains Direct Autolysin to the Equatorial Surface Ring of *Staphylococcus aureus*. *EMBO J.* **1998**, *17* (16), 4639–4646.

(92) **Zoll, S.; Schlag, M.; Shkumatov, A. V; Rautenberg, M.; Svergun, D. I.; Götz, F.** Ligand-Binding Properties and Conformational Dynamics of Autolysin Repeat Domains in Staphylococcal Cell Wall Recognition. *Am. Soc. Microbiol.* **2012**, *194* (15), 3789–3802.

(93) **Marino, M.; Banerjee, M.; Jonquières, R.; Cossart, P.; Ghosh, P.** GW Domains of the *Listeria monocytogenes* Invasion Protein InlB Are SH3-like and Mediate Binding to Host Ligands. *EMBO J.* **2002**, *21* (21), 5623–5634.

(94) **Heilmann, C.; Hussain, M.** Evidence for Autolysin-Mediated Primary Attachment of *Staphylococcus epidermidis* to a Polystyrene Surface. *Mol. Microbiol.* **1997**, *24* (5), 1013–1024.

(95) **Sugai, M.; Yamada, S.; Nakashima, S.; Komatsuzawa, H.; Matsumoto, A.; Oshida, T.; Suginaka, H.** Localized Perforation of the Cell Wall by a Major Autolysin: *J. Bacteriol.* **1997**, *179* (9), 2958–2962.

(96) **Grilo, I. R.; Ludovice, A. M.; Tomasz, A.; de Lencastre, H.; Sobral, R. G.** The Glucosaminidase Domain of Atl - the Major *Staphylococcus aureus* Autolysin - Has DNA-Binding Activity. *Microbiologyopen* **2014**, *3* (2), 247–256.

(97) **Houston, P.; Rowe, S. E.; Pozzi, C.; Waters, E. M.; O'Gara, J. P.** Essential Role for the Major Autolysin in the Fibronectin-Binding Protein-Mediated *Staphylococcus aureus* Biofilm Phenotype.

Infect. Immun. **2011**, *79* (3), 1153–1165.

(98) **Delauné, A.; Dubrac, S.; Blanchet, C.; Poupel, O.; Mäder, U.; Hiron, A.; Leduc, A.** The WalKR System Controls Major Staphylococcal Virulence Genes and Is Involved in Triggering the Host Inflammatory Response. *Am. Soc. Microbiol.* **2012**, *80* (10), 3438–3453.

(99) **Falord, M., Mäder, U., Hiron, A., Debarbouillé, M., Msadek, T.** Investigation of the *Staphylococcus aureus* GraSR Regulon Reveals Novel Links to Virulence, Stress Response and Cell Wall Signal Transduction Pathways. *PLoS One* **2011**, *6* (7), e21323.

(100) **Dubrac, S.; Boneca, I. G.; Poupel, O.; Msadek, T.** New Insights into the WalK/WalR (YycG/YycF) Essential Signal Transduction Pathway Reveal a Major Role in Controlling Cell Wall Metabolism and Biofilm Formation in *Staphylococcus aureus*. *J. Bacteriol.* **2007**, *189* (22), 8257–8269.

(101) **Rice, K. C.; Firek, B. a; Nelson, J. B.; Patton, T. G.; Bayles, K. W.; Yang, S.** The *Staphylococcus aureus* CidAB Operon : Evaluation of Its Role in Regulation of Murein Hydrolase Activity and Penicillin Tolerance. *J. Bacteriol.* **2003**, *185* (8), 2635–2643.

(102) **Bayles, K. W.** Identification of LytSR-Regulated Genes from *Staphylococcus aureus*. **1996**, *178* (19), 5810–5812.

(103) **Rice, K. C.; Nelson, J. B.; Patton, T. G.; Bayles, K. W.; Yang, S.** Acetic Acid Induces Expression of the *Staphylococcus aureus* CidABC and LrgAB Murein Hydrolase Regulator Operons. *J. Bacteriol.* **2005**, *187* (3), 813–821.

(104) **Groicher, K. H.; Firek, B. A.; Fujimoto, D. F.; Bayles, K. W.** The *Staphylococcus aureus* LrgAB Operon Modulates Murein Hydrolase Activity and Penicillin Tolerance. *J. Bacteriol.* **2000**, *182* (7), 1794–1801.

(105) **Patton, T. G.; Yang, S.-J.; Bayles, K. W.** The Role of Proton Motive Force in Expression of the *Staphylococcus aureus Cid* and *Lrg* Operons. *Mol. Microbiol.* **2006**, *59* (5), 1395–1404.

(106) **Sharma-Kuinkel, B. K.; Mann, E. E.; Ahn, J. S.; Kuechenmeister, L. J.; Dunman, P. M.; Bayles, K. W.** The *Staphylococcus aureus* LytSR Two-Component Regulatory System Affects Biofilm Formation. *J. Bacteriol.* **2009**, *191* (15), 4767–4775.

(107) **Rice, K. C.; Mann, E. E.; Endres, J. L.; Weiss, E. C.; Cassat, J. E.; Smeltzer, M. S.; Bayles, K. W.** The CidA Murein Hydrolase Regulator Contributes to DNA Release and Biofilm Development in *Staphylococcus aureus*. *Proc. Natl. Acad. Sci.* **2007**, *104* (19), 8113–8118.

(108) **Vergara-irigaray, M.; Maira-litrán, T.; Merino, N.; Pier, G. B.; José, R.; Lasa, I.** Wall Teichoic Acids Are Dispensable for Anchoring the PNAG Exopolysaccharide to the *Staphylococcus aureus* Cell Surface. *Microbiology* **2008**, *154* (3), 865–877.

(109) **Albrecht, T.; Raue, S.; Rosenstein, R.; Nieselt, K.; Götz, F.** Phylogeny of the Staphylococcal Major Autolysin and Its Use in Genus and Species Typing. *J. Bacteriol.* **2012**, *194* (10), 2630–2636.

(110) **Zoll, S.; Pätzold, B.; Schlag, M.; Götz, F.; Kalbacher, H.; Stehle, T.** Structural Basis of Cell Wall Cleavage by a Staphylococcal Autolysin. *PLoS Pathog.* **2010**, *6* (3).

(111) **Hirschhausen, N.; Schlesier, T.; Schmidt, M. A.; Götz, F.; Peters, G.; Heilmann, C.** A Novel Staphylococcal Internalization Mechanism Involves the Major Autolysin Atl and Heat Shock Cognate Protein Hsc70 as Host Cell Receptor. *Cell. Microbiol.* **2010**, *12* (12), 1746–1764.

(112) **Strominger, J. L.; Ghuysen, J. M.** Mechanisms of Enzymatic Bacteriolysis. *Science (80-.).* **1967**, *156* (3772), 213–221.

(113) **Götz, F.; Heilmann, C.; Stehle, T.** Functional and Structural Analysis of the Major Amidase (Atl) in Staphylococcus. *Int. J. Med. Microbiol.* **2014**, *304* (2), 156–163.

(114) **Lorenz, M. G.; Wackernagel, W.** Bacterial Gene Transfer by Natural Genetic Transformation in the Environment. *Microbiol. Rev.* **1994**, *58* (3), 563–602.

(115) **Kishan, K.; Agrawal, V.** SH3-like Fold Proteins Are Structurally Conserved and Functionally Divergent. *Curr. Protein Pept. Sci.* **2005**, *6*, 143–150.

(116) **Morikawa, K.; Takemura, A. J.; Inose, Y.; Tsai, M.; Nguyen Thi, L. T.; Ohta, T.; Msadek, T**. Expression of a Cryptic Secondary Sigma Factor Gene Unveils Natural Competence for DNA Transformation in *Staphylococcus aureus*. *PLoS Pathog.* **2012**, *8* (11), e1003003.

(117) **Domenech, M.; García, E.; Prieto, A.; Moscoso, M.** Insight into the Composition of the Intercellular Matrix of *Streptococcus pneumoniae* Biofilms. *Environ. Microbiol.* **2013**, *15* (2), 502–516.

(118) **O'Brien, F. G.; Pearman, J. W.; Gracey, M.; Riley, T. V.; Grubb, W. B.** Community Strain of Methicillin-Resistant *Staphylococcus aureus* Involved in a Hospital Outbreak. *J. Clin. Microbiol.* **1999**, *37* (9), 2858–2862.

(119) **Blattner, F. R.; Plunkett, G.; Bloch, C.; Perna, N. T.; Burland, V.; Riley, M.; Collado-Vides, J.; Glasner, J. D.; Rode, C. K.; Mayhew, G. F.; et al.** The Complete Genome Sequence of *Escherichia coli* K-12. *Science (80).* **1997**, *277* (5331), 1453–1462.

(120) **Gill, S. R.; Fouts, D. E.; Archer, G. L.; Mongodin, E. F.; Deboy, R. T.; Ravel, J.; Paulsen, I. T.; Kolonay, J. F.; Brinkac, L.; Beanan, M.; et al.** Insights on Evolution of Virulence and Resistance from the Complete Genome Analysis of an Early Methicillin-Resistant *Staphylococcus aureus* Strain and a Biofilm-Producing Methicillin-Resistant *Staphylococcus epidermidis* Strain. *J. Bacteriol.* **2005**, *187* (7), 2426–2438.

(121) **Herbert, M. A.; Beveridge, C. J. E.; McCormick, D.; Aten, E.; Jones, N.; Snyder, L. A. S.; Saunders, N. J.** Genetic Islands of *Streptococcus agalactiae* Strains NEM316 and 2603VR and Their Presence in Other Group B Streptococcal Strains. *BMC Microbiol.* **2005**, *5* (31).

(122) **Pires, R.; Rolo, D.; Morais, A.; Brito-Avô, A.; Johansson, C.; Henriques-Normark, B.; Goṇalo-Marques, J.; Santos-Sanches, I.** Description of Macrolide-Resistant and Potential Virulent Clones of *Streptococcus pyogenes* Causing Asymptomatic Colonization during 2000-2006 in the Lisbon Area. *Eur. J. Clin. Microbiol. Infect. Dis.* **2012**, *31* (5), 849–857.

(123) **Atilano, M. L.; Pereira, P. M.; Vaz, F.; Catalão, M. J.; Reed, P.; Grilo, I. R.; Sobral, R. G.; Ligoxygakis, P.; Pinho, M. G.; Filipe, S. R.** Bacterial Autolysins Trim Cell Surface Peptidoglycan to Prevent Detection by the Drosophila Innate Immune System. *Elife* **2014**, No. 3, e02277.

(124) **Studier, F. W.** Protein Production by Auto-Induction in High Density Shaking Cultures. *Protein Expr. Purif.* **2005**, *41* (1), 207–234.

(125) **McLellan, T**. Electrophoresis Buffers for Polyacrylamide Gels at Various PH. *Anal. Biochem.* **1982**, *126*, 94–99.

(126) **Yokoi, K. J.; Kawasaki, K. I.; Taketo, A.; Kodaira, K. I.** Characterization of Lytic Enzyme Activities of *Lactobacillus gasseri* with Special Reference to Autolysis. *Int. J. Food Microbiol.* **2004**, *96* (3), 273–279.

(127) **Arnaud, M.; Chastanet, A.; De, M.** New Vector for Efficient Allelic Replacement in Naturally Gram-Positive Bacteria New Vector for Efficient Allelic Replacement in Naturally Gram-Positive Bacteria. *Appl. Enviromental Microbiol.* **2004**, *70* (11), 6887–6891.

(128) **Novick, R.** Properties of a Cryptic High-Frequency Transducing Phage in *Staphylococcus aureus*. *Virology* **1967**, *33*, 155–166.

(129) **Sherbet, G. V.; Lakshmi, M. S.; Cajone, F.** Isoelectric Characteristics and the Secondary Structure of Some Nucleic Acids. *Biophys. Struct. Mech.* **1983**, *10* (3), 121–128.

(130) **Mathieson, A. R.; Matty, S.** Influence of pH and Ionic Strength on Size, Shape, and Electric Charge of the Deoxyribonucleic Acid Molecule. *J. Polym. Sci.* **1957**, *23*, 747–764.

(131) **Guo, Z.; Wang, Y.; Yang, A.; Yang, G.** The Effect of pH on Charge Inversion and Condensation of DNA. *Soft Matter* **2016**, *12* (31), 6669–6674.

(132) **Heffler, M. A.; Walters, R. D.; Kugel, J. F.** Using Electrophoretic Mobility Shift Assays to Measure Equilibrium Dissociation Constants: GAL4-P53 Binding DNA as a Model System. *Biochem. Mol. Biol. Educ.* **2012**, *40* (6), 383–387.

(133) **Burda, J. V.; Šponer, J.; Hobza, P.** Ab Initio Study of the Interaction of Guanine and Adenine with Various Mono- and Bivalent Metal Cations (Li^+, Na^+, K^+, Rb^+, Cs^+; Cu^+, Ag^+, Au^+; Mg^{2+}, Ca^{2+}, Sr^{2+}, Ba^{2+}; Zn^{2+}, Cd^{2+}, and Hg^{2+}). *J. Phys. Chem.* **1996**, *100* (17), 7250–7255.

(134) **Duguid, J.; Bloomfield, V. A.; Benevides, J.; Thomas, G. J.** Raman Spectroscopy of DNA-Metal Complexes. I. Interactions and Conformational Effects of the Divalent Cations: Mg, Ca, Sr, Ba, Mn, Co, Ni, Cu, Pd, and Cd. *Biophys. J.* **1993**, *65* (5), 1916–1928.

(135) **Arias-Moreno, X.; Abian, O.; Vega, S.; Sancho, J.; Velazquez-Campoy, A.** Protein-Cation Interactions: Structural and Thermodynamic Aspects. *Curr. Protein Pept. Sci.* **2011**, *12* (4), 325–338.

(136) **Oliveira, P. H.; Touchon, M.; Rocha, E. P. C.** The Interplay of Restriction-Modification Systems with Mobile Genetic Elements and Their Prokaryotic Hosts. *Nucleic Acids Res.* **2014**, *42* (16),

10618–10631.

(137) **Jalili, N.; Laxminarayana, K.** A Review of Atomic Force Microscopy Imaging Systems: Application to Molecular Metrology and Biological Sciences. *Mechatronics* **2004**, *14* (8), 907–945.

(138) **Lyubchenko, Y. L.; Shlyakhtenko, L. S.** Visualization of Supercoiled DNA with Atomic Force Microscopy *in Situ*. *Proc. Natl. Acad. Sci.* **1997**, *94* (2), 496–501.

(139) **Shlyakhtenko, Luda S., Gal, Alexander A., Lyubchenko, Y. L.** Mica Functionalization for Imaging of DNA and Protein-DNA Complexes with Atomic Force Microscopy. *methods Mol. Biol.* **2013**, *931* (11), 1–20.

(140) **Schneider, S. W.; Lärmer, J.; Henderson, R. M.; Oberleithner, H.** Molecular Weights of Individual Proteins Correlate with Molecular Volumes Measured by Atomic Force Microscopy. *Pflugers Arch. Eur. J. Physiol.* **1998**, *435* (3), 362–367.

(141) **Mulcahy, H.; Charron-Mazenod, L.; Lewenza, S.** Extracellular DNA Chelates Cations and Induces Antibiotic Resistance in *Pseudomonas aeruginosa* Biofilms. *PLoS Pathog.* **2008**, *4* (11), e1000213.

(142) **Shockman, G. D.; Barrett, J. F.** Structure, Function, and Assembly of Call Walls of Gram-Positive Bacteria. *Ann. Rev. Microbiol.* **1983**, *37*, 501–527.

(143) **Vollmer, W.; Seligman, S. J.** Architecture of Peptidoglycan: More Data and More Models. *Trends Microbiol.* **2010**, *18* (2), 59–66.

(144) **Vollmer, W.; Blanot, D.; De Pedro, M. A.** Peptidoglycan Structure and Architecture. *FEMS Microbiol. Rev.* **2008**, *32* (2), 149–167.

(145) **Mathema B., Mediavilla J.R., Chen L, K. B. N.** Evolution and Taxonomy of Staphylococci. In *Staphylococci in Human Disease*; Crossley, Kent B., Kimberly K. Jefferson, Gordon L. Archer, V. G. F. J., Ed.; **2009**; Vol. 53, pp 31–64.

(146) **Lambers, H.; Piessens, S.; Bloem, A.; Pronk, H.; Finkel, P.** Natural Skin Surface pH Is on Average below 5, Which Is Beneficial for Its Resident Flora. *Int. J. Cosmet. Sci.* **2006**, *28* (5), 359–370.

(147) **Fraga, C. G.** Relevance, Essentiality and Toxicity of Trace Elements in Human Health. *Mol. Aspects Med.* **2005**, *26*, 235–244.

(148) **Price-Whelan, A.; Poon, C. K.; Benson, M. a.; Eidem, T. T.; Roux, C. M.; Boyd, J. M.; Dunman, P. M.; Torres, V. J.; Krulwich, T. a.** Transcriptional Profiling of *Staphylococcus aureus* during Growth in 2 M NaCl Leads to Clarification of Physiological Roles for Kdp and Ktr K^+ Uptake Systems. *MBio* **2013**, *4* (4), e00407-13.

(149) **Xie, Y.; Yang, L.** Calcium and Magnesium Ions Are Membrane-Active against Stationary-Phase *Staphylococcus aureus* with High Specificity. *Sci. Rep.* **2016**, *6* (20628).

(150) **Saracino, I.; Zaccaro, C.; Re, G.; Vaira, D.; Holton, J.** The Effects of Two Novel Copper-Based Formulations on *Helicobacter pylori*. *Antibiotics* **2013**, *2*, 265–273.

(151) **Aghatabay, N. M.; Neshat, A.; Karabiyik, T.; Somer, M.; Haciu, D.; Dülger, B.** Synthesis, Characterization and Antimicrobial Activity of Fe(II), Zn(II), Cd(II) and Hg(II) Complexes with 2,6-Bis(Benzimidazol-2-Yl) Pyridine Ligand. *Eur. J. Med. Chem.* **2007**, *42* (2), 205–213.

(152) **Nisse, C.; Tagne-Fotso, R.; Howsam, M.; Richeval, C.; Labat, L.; Leroyer, A.** Blood and Urinary Levels of Metals and Metalloids in the General Adult Population of Northern France: The IMEPOGE Study, 2008–2010. *Int. J. Hyg. Environ. Health* **2016**, *220* (2), 341–363.

(153) **Imlay, J. A.** Pathways of Oxidative Damage. *Annu. Rev. Microbiol.* **2003**, *57* (1), 395–418.

(154) **Thomas, C. M.; Nielsen, K. M.** Mechanisms of, and Barriers to, Horizontal Gene Transfer between Bacteria. *Nat. Rev. Microbiol.* **2005**, *3* (9), 711–721.

(155) **Gaskin, D. K.; Bohach, G. a; Schlievert, P. M.; Hovde, C. J.** Purification of *Staphylococcus aureus* Beta-Toxin: Comparison of Three Isoelectric Focusing Methods. *Protein Expr. Purif.* **1996**, *9* (1), 76–82.

(156) **Sanford, J. A.; Gallo, R. L.** Functions of the Skin Microbiota in Health and Disease. *Semin Immunol.* **2013**, *25* (5), 370–377.

(157) **Kenneth, J. R.** Normal Microbial Flora. In Medical Microbiology; Kenneth, J. R., Ray, C. G., Eds.; **2004**; pp 261–271.

(158) **Tipper, D. J.; Berman, M. F.** Structures of the Cell Wall Peptidoglycans of *Staphylococcus epidermidis* Texas 26 and *Staphylococcus aureus* Copenhagen. I. Chain Length and Average Sequence of Cross-Bridge Peptides. *Biochemistry* **1969**, *8* (5), 2183–2192.

(159) **Caliot, É.; Dramsi, S.; Chapot-Chartier, M.-P.; Courtin, P.; Kulakauskas, S.; Péchoux, C.; Trieu-Cuot, P.; Mistou, M.-Y.** Role of the Group B Antigen of *Streptococcus agalactiae*: A Peptidoglycan-Anchored Polysaccharide Involved in Cell Wall Biogenesis. *PLoS Pathog.* **2012**, *8* (6), e1002756.

(160) **Mainardi, J.-L.; Billot-Klein, D.; Coutrot, A.; Legrand, R.; Schoot, B.; Gutmann, L.** Resistance to Cefotaxime and Peptidoglycan Composition in *Enterococcus faecalis* Are Influenced by Exogenous Sodium Chloride. *Microbiology* **1998**, *144*, 2679–2685.

(161) **Glauner, B.; Holtje, J. V.; Schwarz, U.** The Composition of the Murein of *Escherichia coli*. *J. Biol. Chem.* **1988**, *263* (21), 10088–10095.

(162) **Gumbart, J. C.; Beeby, M.; Jensen, G. J.; Roux, B**. *Escherichia coli* Peptidoglycan Structure and Mechanics as Predicted by Atomic-Scale Simulations. *PLoS Comput. Biol.* **2014**, *10* (2), e1003475.

Annexes

Annex 1

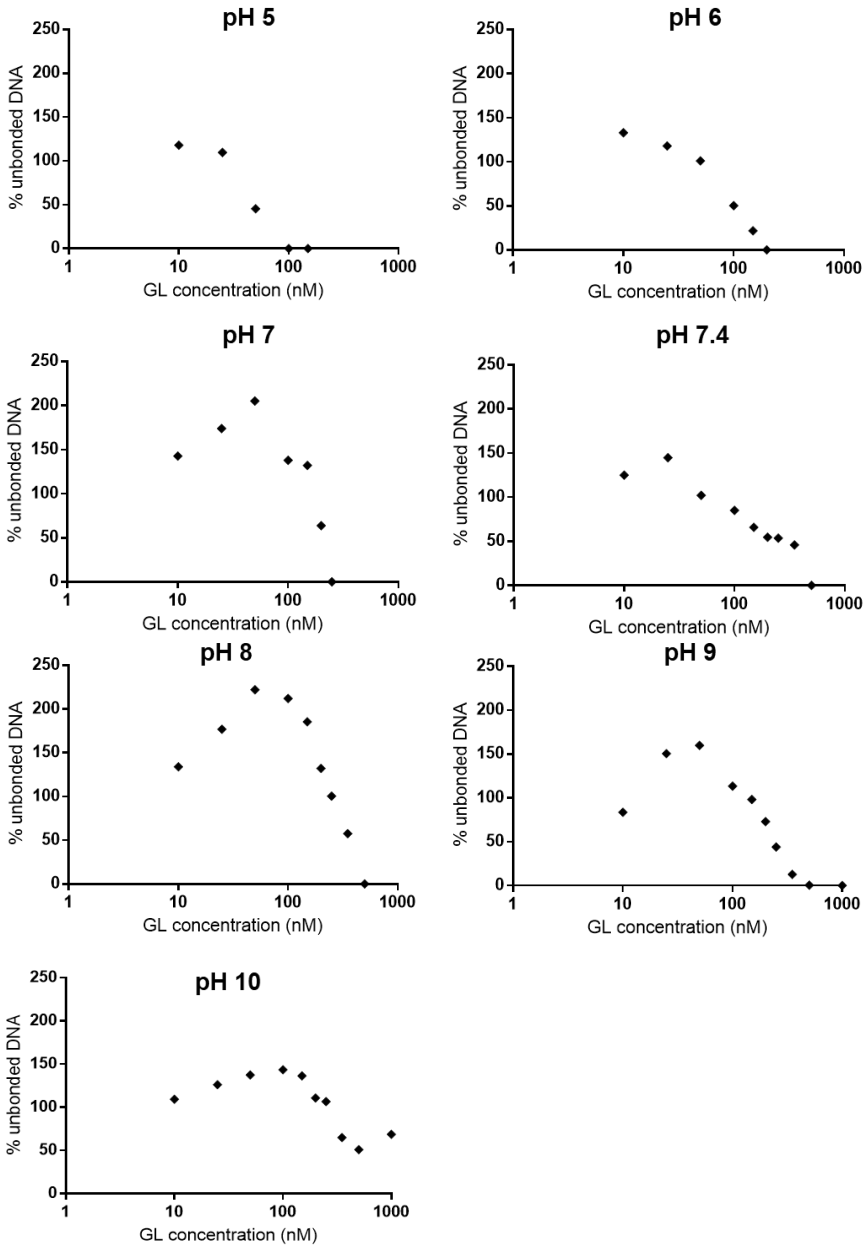

Figure A.1: Percentage of unbound DNA as GL protein concentrations increased at different pH values. Shown is the data after adjusting to a non-linear regression curve fit, plotted with a logarithmic X-axis.

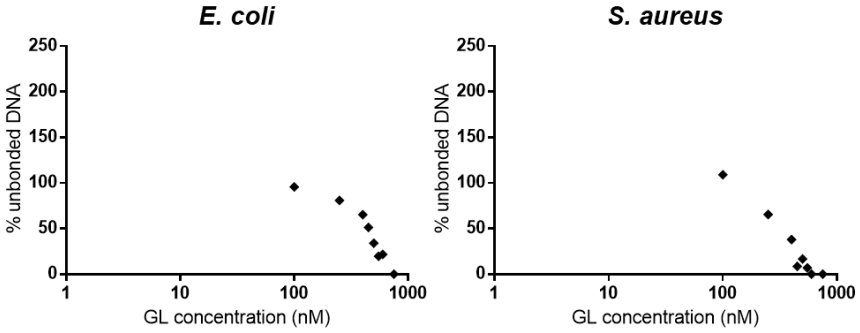

Figure A.2: Percentage of unbonded plasmid DNA, extracted from *E. coli* or *S. aureus*, as GL protein concentration increased. Shown is the data after adjusting to a non-linear regression curve fit using GraphPad, plotted with a logarithmic X-axis.

Annex 2

Table A.1 - Percentage of heat-inactivated cells of the different microorganisms at the end of the assay (120 min) by addition of ssDNA. Shown is the average of the three biological replicates and the standard error of the mean (SEM).

	Heat-inactivated cells (%)						
ssDNA concentration (mg/ml)	0.0	0.5	1	2.5	5.0	7.5	10.0
M. luteus	92.8 ±1.9	95.1 ±1.2	95.8 ±0.7	96.2 ±0.6	97.1 ±0.7	98.2 ±0.2	98.7 ±0.3
S. aureus	97.5 ±0.8	98.1 ±0.1	97.7 ±0.6	98.8 ±0.9	98.8 ±0.8	99.5 ±1.2	98.3 ±0.5
S. epidermidis	93.4 ±0.2	94.6 ±0.3	95.5 ±0.8	97.9 ±2.2	96.8 ±3.0	98.6 ±1.1	96.4 ±1.9
S. agalactiae	92.3 ±2.6	93.7 ±0.2	94.4 ±0.5	97.2 ±1.1	101.6 ±0.4	97.2 ±1.2	96.5 ±2.6
S. pyogenes	90.9 ±0.9	89.9 ±0.2	91.5 ±0.4	92.8 ±0.7	93.2 ±2.6	96.5 ±2.9	99.0 ±1.7
E. faecalis	97.4 ±1.7	93.0 ±0.9	94.6 ±1.3	93.9 ±1.5	94.4 ±0.6	95.2 ±0.8	96.9 ±1.3
E. coli	85.4 ±1.9	87.3 ±2.1	87.4 ±0.6	89.5 ±0.1	90.9 ±0.1	94.3 ±1.0	98.1 ±0.8
C. marina	91.1 ±0.7	93.4 ±1.4	93.7 ±1.2	94.9 ±1.9	98.2 ±2.4	102.4 ±3.3.	102.2 ±1.1
M. hydrocarbonoclasticus	89.4 ±1.6	90.4 ±1.7	93.1 ±0.3	94.5 ±0.1	98.5 ±0.4	107.4 ±1.5	106.2 ±1.4

Table A.2 - Summary of the % of heat-inactivated cells of different microorganisms at the end of the assay by addiction of GL + ssDNA. Shown is the average of the three biological replicates and the standard error of the mean (SEM).

	Heat-inactivated cells (%)						
ssDNA concentration (mg/ml)	0.0	0.5	1	2.5	5.0	7.5	10.0
M. luteus	66.5 % ±2.6	86.4 % ±5.2	91.4 % ±3.7	86.3 % ±3.2	93.5 % ±0.8	96.0 % ±0.3	93.8 % ±3.4
S. aureus	104.5 % ±1.0	99.3 % ±1.6	98.7 % ±0.7	100.9 % ±2.4	102.9 % ±1.8	100.8 % ±1.1.	96.4 % ±7.7
S. epidermidis	89.8 % ±2.8	94.7 % ±3.4	93.2 % ±3.6	93.9 % ±2.1	96.7 % ±3.3	95.0 % ±1.9	91.8 % ±5.1
S. agalactiae	96.8 % ±2.6	98.9 % ±2.0	99.7 % ±2.4	99.3 % ±3.3	99.9 % ±1.1	93.3 % ±4.6	100.6 % ±1.9
S. pyogenes	85.6 % ±1.7	93.1 % ±1.7	93.1 % ±1.8	93.9 % ±0.5	90.1 % ±4.4	92.5 % ±3.5	90.8 % ±7.2
E. faecalis	100.3 % ±2.1	94.4 % ±0.9	96.1 % ±1.3	98.4 % ±2.5	93.8 % ±2.0	95.8 % ±0.4	93.5 % ±1.7
E. coli	32.9 % ±4.9	88.4 % ±1.2	90.4 % ±0.7	92.2 % ±0.6	94.4 % ±0.2	100.7 % ±1.1	104.9 % ±2.6
C. marina	32.4 % ±7.1	86.3 % ±3.9	90.4 % ±0.1	92.0 % ±0.2	97.9 % ±1.4	103.7 % ±0.5	103.4 % ±1.2
M. hydrocarbonoclasticus	58.5 % ±0.5	93.0 % ±2.6	94.6 % ±0.9	95.5 % ±0.3	99.1 % ±0.5	108.7 % ±3.5	105.7 % ±1.6

Table A.3 - Summary of the % of heat-inactivated cells of different microorganisms at the end of the assay by addiction of R_3GL + ssDNA. Shown is the average of the three biological replicates and the standard error of the mean (SEM).

	Heat-inactivated cells (%)						
ssDNA concentration (mg/ml)	0.0	0.5	1	2.5	5.0	7.5	10.0
M. luteus	59.6 ±0.8	90.2 ±0.8	91.8 ±0.8	93.4 ±0.5	95.7 ±1.7	96.6 ±0.4	98.7 ±0.7
S. aureus	96.3 ±3.1	88.2 ±0.8	89.8 ±0.6	91.4 ±0.1	96.6 ±3.3.	96.9 ±0.2	100.6 ±1.4
S. epidermidis	82.8 ±2.3	88.4 ±1.4	86.0 ±0.6	84.6 ±1.9	89.9 ±3.7	89.9 ±0.5	98.4 ±2.8
S. agalactiae	95.7 ±0.7	94.9 ±0.4	96.6 ±0.6	96.4 ±0.3	97.2 ±0.8	97.6 ±0.4	99.1 ±0.7
S. pyogenes	78.7 ±2.7	91.1 ±0.9	93.3 ±0.7	95.7 ±1.4	90.1 ±5.2	91.2 ±5.8	91.1 ±7.7
E. faecalis	95.2 ±1.7	95.4 ±1.9	94.9 ±0.7	95.5 ±0.5	94.9 ±1.3	96.1 ±0.4	96.0 ±0.6
E. coli	30.9 ±0.8	88.9 ±1.1	90.5 ±0.7	91.6 ±1.2	94.7 ±1.1	99.5 ±2.5	101.9 ±2.1
C. marina	25.8 ±2.5	86.2 ±2.1	90.9 ±0.1	93.3 ±0.4	97.8 ±0.2	103.9 ±0.1	103.8 ±0.1
M. hydrocarbonoclasticus	47.4 ±0.2	93.2 ±0.8	96.9 ±0.7	95.6 ±0.5	96.6 ±0.5	104.9 ±1.8	105.6 ±1.1

Table A.4: Cross-linking degree and peptidoglycan type of the bacterial species used in the hydrolytic activity assays. ND: not determined

Bacterial species	**Cross-linking degree**	**Peptidoglycan type** [79]
M. luteus	20 % [142]	L-Lys-peptide subunit
S. aureus	90 % [143]	L-Lys-$Gly_{5,6}$
S. epidermidis	85 % [158]	L-Lys-L-Ala-$Gly_{4.}$, L-Lys-Gly_4, L-Ser $_{0.5\text{-}1.5}$
S. agalactiae	63 % [159]	L-Lys-L-Ala_2 (L-Ser)
S. pyogenes	ND	L-Lys-L-$Ala_{2\text{-}3}$
E. faecalis	73 % [160]	L-LyS-L-$Ala_{2\text{-}3}$
E. coli	50 % [161,162]	direct cross-linkage position 3 → position 4.
C. marina	ND	Data unavailable
M. hydrocarbonoclasticus	ND	Data unavailable

Annex 3

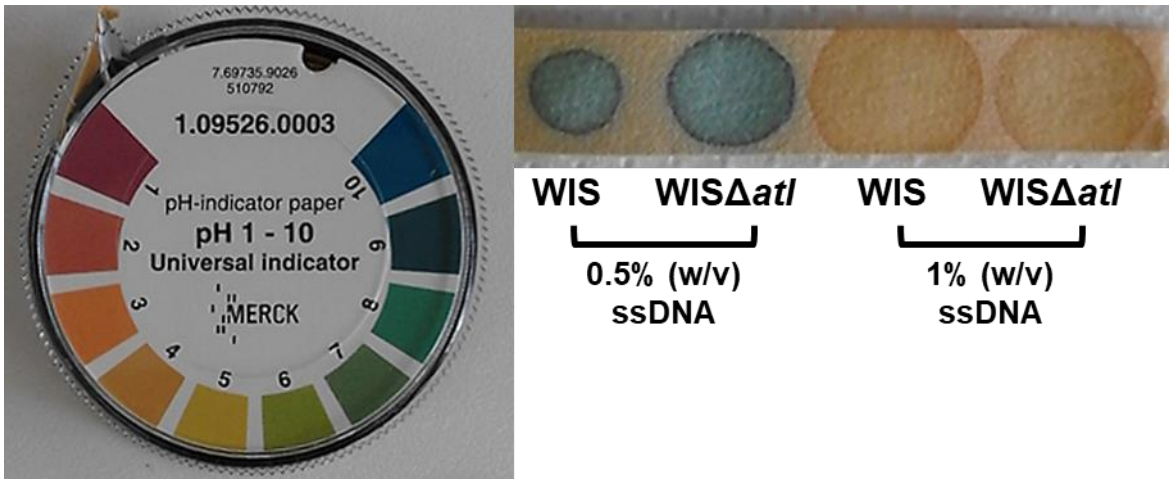

Figure A.3: pH at the end of the bacterial growth in presence of ssDNA using non-buffered media. The pH of TSB media enriched with 0.5% and 1% of ssDNA from both *S. aureus* WIS and WISΔ*atl* strains was measured using pH-indicator paper (Merck) at 24 hours of bacterial growth.